

This is to certify that the

thesis entitled

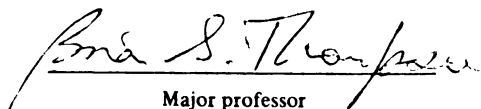
AN ANALYTICAL AND EXPERIMENTAL INVESTIGATION OF THE
DYNAMIC RESPONSE OF A FOUR BAR MECHANISM CONSTRUCTED
FROM A VISCOELASTIC COMPOSITE MATERIAL

presented by

Wang Chun-hwa

has been accepted towards fulfillment
of the requirements for

M. S. degree in Mechanical Eng.


Major professor

Date 2 April 1984



RETURNING MATERIALS:
Place in book drop to
remove this checkout from
your record. FINES will
be charged if book is
returned after the date
stamped below.

WVNDIC 2

FEB 12 1999

LIBRARY

**AN ANALYTICAL AND EXPERIMENTAL
INVESTIGATION OF THE DYNAMIC RESPONSE
OF A FOUR BAR MECHANISM CONSTRUCTED FROM
A VISCOELASTIC COMPOSITE MATERIAL**

By

Wang Chun-hwa

Thesis

Submitted to

Michigan State University

in partial fulfilment of the requirement

for the degree of

MASTER OF SCIENCE

Department of Mechanical Engineering

1984

ABSTRACT

AN ANALYTICAL AND EXPERIMENTAL

INVESTIGATION OF THE DYNAMIC RESPONSE

OF A FOUR BAR MECHANISM CONSTRUCTED FROM

A VISCOELASTIC COMPOSITE MATERIAL

By

Wang Chun-hwa

The intense competition in the international marketplace for mechanism systems which operate at higher speeds, are less noisy and more energy efficient than previous designs has imposed considerable pressures upon the machinery designer. This is because classical rigid-body analyses are unable to predict the elastodynamic phenomena associated with these new modes of operation. In order to respond to these commercial stimuli, mechanical systems need to incorporate members with high stiffness to weight ratios and also high strength to weight ratios.

The work presented here develops appropriate finite element models for four-bar mechanisms constructed in elastic and viscoelastic materials. Experimental investigations into the effects of different link materials upon the dynamic flexural response of four bar mechanisms are also described. The correlations between the analytical and experimen-

tal results for the midspan transverse deflections of the coupler and rocker links are good, thereby suggesting that these models may be used with confidence in the computer aided design of high-speed machine systems fabricated in the commercial materials and also composite laminates.

Acknowledgment

The author wish to express his sincere thanks to Dr. B.S.Thompson for his continual suggestions and guidance during the investigation. Sincere appreciation is extended to Dr. G.E.Mase of the Department of Metallurgy, Mechanics and Material Science and Dr. B.Fallahi of the Department of Mechanical Engineering for serving on the guidance committee for their helpful suggestions.

The efforts and assistance of Mr. C.K.Sung and other friends in Michigan State University are sincerely appreciated.

Special credit must be given to every member of author's family for their encouragement and financial support that help to complete this work.

TABLE OF CONTENTS

List of figures	vii
Chapter 1. Introduction	1
Chapter 2. Variational Theorem	5
2-1. Theoretical development	5
2-2. Finite element formulation	17
Chapter 3. Mathematical Model of a Flexible Linkage	28
3-1. Planar beam element	28
3-2. Shape functions of beam element	33
3-3. Element mass and stiffness matrices	36
3-4. Assembling the mass and stiffness matrices of the mechanism system	39
3-5. Linkage model	41
3-6. Construction of the system matrices for the finite element model	42
3-7. Modeling the viscoelastic constitutive equations	44
Chapter 4. Experimental Investigation	49
4-1. Material characterization studies	49
4-2. Experimental apparatus	59
4-3. Instrumentation	61
Chapter 5. Experimental and Computational Results	65
Chapter 6. Discussion of Results	77
Chapter 7. Conclusions	80
References	81

LIST OF FIGURES

Figure 2-1.1	Definition of Axis Systems and Position Vectors.-----	6
Figure 2-2.1	Deformations of the beam element-----	17
Figure 2-2.2	Finite difference representation-----	22
Figure 3-1.1	A General Beam Element.-----	29
Figure 3-2.1	The Deformations of a Beam Element.-----	34
Figure 3-4.1	The Relation between Global and Local Coordinate.-----	39
Figure 3-5.1	Four Bar Linkage Model with Flexible Coupler and Rocker.-----	42
Figure 3-6.1	Finite Element Model for the Simulation.-----	43
Figure 3-7.1a	Spring.-----	46
Figure 3-7.1b	Strain-Time Characteristic of Spring.-----	46
Figure 3-7.2a	Dashpot.-----	46
Figure 3-7.2b	Strain-Time Characteristic of Dashpot. -----	46
Figure 3-7.3	Kelvin Model.-----	48
Figure 3-7.4	Standard Linear Solid Model-----	48
Figure 4-1	Result for Material Testing-----	51
Figure 4-2	Result for Creep Testing-----	52
Figure 4-3	Method to Obtain the Relaxation Function-----	54
Figure 4-4	Relxation Function Obtained from Material Testing-----	55
Figure 4-5	Relxation Function Obtained from Curve Fitting-----	56
Figure 4-6	Natural Frequency of the Steel Link-----	58
Figure 4-7	Natural Frequency of the Composite Link-----	58
Figure 4-8	Joint connecting the flexible coupler and rocker-----	60

Figure 4-9	Experimental Four Bar Mechanism-----	60
Figure 4-10	Experimental Appartus Flow Chart-----	62
Figure 5-1	Steel Coupler Response Operated at 342 RPM (Oscilloscope Photograph)-----	67
Figure 5-2	Steel Coupler Response Operated at 342 RPM (Computer plot for Both Results)-----	68
Figure 5-3	45 Composite Coupler Response operated at 280 RPM (Oscilloscope Photograph)-----	67
Figure 5-4	45 Composite Couper Response Operated at 280 RPM (Computer Plot for Both Results)-----	69
Figure 5-5	45 Composite Coupler Response at 205 RPM.-----	71
Figure 5-6	45 Composite Rocker Response at 205 RPM.-----	72
Figure 5-7	45 Composite Coupler Response at 255 RPM.-----	73
Figure 5-8	45 Composite Rocker Response at 255 RPM.-----	74
Figure 5-9	45 Composite Coupler Response at 297 RPM.-----	75
Figure 5-10	45 Composite Rocker Response at 297 RPM.-----	76

Chapter 1

Introduction

For the past decade, the design of machine members have always been based on the rigid body method of analysis, which means designers have traditionally considered all members of a mechanism to be rigid bodies [1-5]. With this rigid body approach, elastodynamic phenomena, such as dynamic stresses and vibrations, associated with link elasticity are neglected. This method can only be considered to be reasonably accurate for those mechanisms which operate at low speeds. The major problem, from designer's point of view is that the traditional rigid-body analysis and synthesis techniques are unable to predict the response of these mechanical systems with flexible members because mathematical models need to incorporate link flexibility.

Recently, machines have been required to operate at higher speeds with more accurate performance characteristics. Because of the higher operating speed creates increased inertial forces, the mechanism must be fabricated as a lightweight form-design to reduce the inertial loading. Unfortunately, mechanism with lighter members develop deformations and vibration due to external and internal forces; therefore, the performance of the mechanism might not be acceptable owing to these inaccuracies. In addition, failure of the mechanism might occur if a vibration analysis has not been undertaken. Owing to this effect, the

analysis of non-rigid mechanisms have become extremely important in the mechanism design area. Research in the field of mechanism design has progressed from studies of systems containing one [1-9], or more, flexible links [10-30] during the past few years as researchers have attempted to develop viable mathematical models for designing high speed mechanism systems with high stiffness weight ratios and lighter weight members because classical techniques based upon rigid-body dynamics are unable to adequately predict the performance characteristics of these flexible systems. These kind of techniques would allow a designer to develop a light weight, flexible mechanism that would meet both requirements. Comprehensive review articles of the early research in the area of the dynamic analysis of elastic mechanism have been presented in [31, 32].

In all of these references, the systems are assumed to be constructed from homogeneous isotropic materials such as carbon steels or aluminum alloys. Some of the more recent work were devoted to developing optimum lightweight form-designs for the members of linkages based on optimizing the stiffness characteristics or focused on the cross-sectional dimensions and shapes of the links [33-37]. Hence links were designed with tapers and complex cross-sectional shapes which directly increases the cost of manufacture, while reducing product marketability.

An alternative philosophy with which to design a mechanism with high strength-to-weight ratio and stiffness-to-weight ratio components

is to fabricate the links from a modern fiber-reinforced composite. As is well known, these materials have much higher strength and stiffness to weight ratios than the commercial materials such as steel or aluminum; furthermore, the composite also have high material damping, and good fatigue life.

Although considerable fundamental research has been undertaken on determining the mechanical properties [38-43] and the response of the composite materials treated as elastic members [44,45], the literature is devoid of reports on the dynamic viscoelastic response of mechanism systems built using these materials. Therefore, the objective here is to establish guidelines for the design of linkage machinery in composite materials. A four bar mechanism was constructed by incorporating these different materials as the coupler and rocker links and treating them as the flexible parts. A finite element code was developed for the nonlinear elastic analysis of flexible four bar linkages based on a variational formulation [46] and presented in [47]. A second code was developed for a four bar linkage fabricated in a ± 45 graphite epoxy laminate.

The material characterization tests show that the ± 45 degree composite was a viscoelastic material. There have been several derivations of variational theorems in linear viscoelasticity [48-56]. The experimental four bar mechanism which was fabricated using a ± 45 degrees composite is analyzed by first developing an appropriate variational principle for a general multi-body system fabricated from a linear

viscoelastic material prior to formulating a model of constitutive equations of the composite laminate and then solving the resulting equations of motion by the finite element method.

This single functional expression with its associated variational equation provides a complete description of this class of mixed boundary value problem and is relevant to the design of all mechanisms. By permitting arbitrary independent variations of the stress, strain, displacement and velocity parameters, this equation yields the governing differential equations as well as the relevant boundary conditions. As an illustrative example, an approximate solution is sought for the response of the flexible four bar linkage by developing a displacement finite element model of the system. This mathematical model incorporates one standard linear solid model to represent the material's constitutive equation. The equation of motion is solved by numerical integration, and the analytical and experimental results are presented.

Chapter 2

Variational Theorem

The objective of this chapter is to develop the equations governing the motion of mechanisms constructed in viscoelastic materials. The approach follows the developments of reference [57].

2-1 Theoretical Development

The volume of a viscoelastic body is taken to be V and the total surface area S is the summation of two prescribed area S_d and S_σ . The dynamic problems of this viscoelastic body V are considered. Let $o-x-y-z$ be a set of Lagrangian coordinates fixed in the body in a reference state with zero deformations, strains and stresses, and furthermore, it is also assumed that these parameters have been zero throughout the previous time t . Employing a Cartesian tensor notation, at time t a general point P in the continuum has the general position vector r_i , which is defined as

$$r_i = r_{0i} + r_{ri} + u_i \quad (2-1.1)$$

where

r_{0i} : the component measured in the $o-x-y-z$ frame with the position

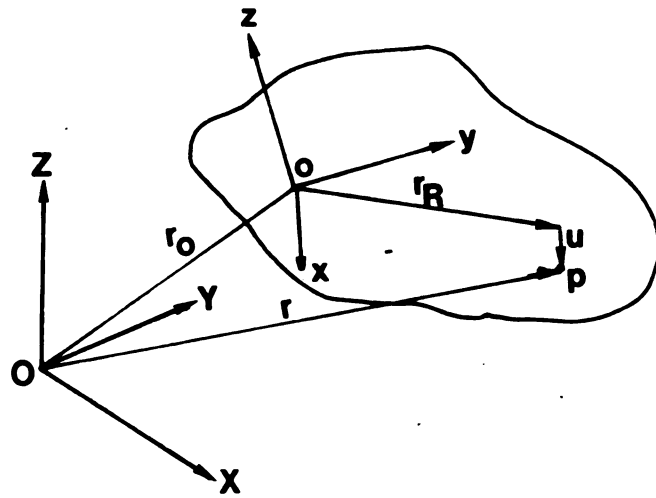


Figure 2-1.1 Definition of Axis Systems and Position Vectors

vector of the origin of the body axes relative to the origin of the inertial frame.

r_{ri} : the position vector of point P in the reference state relative to the origin of the body axes.

u_i : deformation displacement vector.

in Figure 2-1.1, O-X-Y-Z is an inertial reference frame.

The field equations for the linear theory of dynamic viscoelasticity for an body describing a general spatial motion relative to O-X-Y-Z are as follows:

$$(i). \quad p_i = \tilde{r}_{oi} + \tilde{u}_i + e_{ijk} \dot{\theta}_j (r_{ok} + r_{rk} + u_k) \quad (2-1.2)$$

this equation is obtained by differentiate equation (2-1.1), and is the velocity rate of change of position statement; where

p_i : absolute velocity associated with r_i

e_{ijk} : alternating tensor

$\dot{\theta}_j$: angular velocity defining the rotation of the Lagrangian frame

$(\tilde{\quad})$: the time rate of change with respect to the moving coordinate frame

(\quad') : the absolute rate of change with respect to time.

(ii). The boundary conditions for prescribed displacement and tractions are written as

$$\begin{aligned} u_i &= \bar{u}_i \text{ on } S_d \\ \bar{g}_i &= \sigma_{ij} n_j = \tilde{g}_i \text{ on } S_\sigma \end{aligned} \quad (2-1.3)$$

S_d : surface on which the prescribed displacements are imposed

S_σ : surface on which the prescribed tractions are imposed

g_i : surface traction vector

$(\bar{\quad})$: a prescribed quantity

n_i : the outward normal from the surface S_d

(iii). Strain-displacement relation

$$\begin{aligned} \epsilon_{ij} &= (1/2)(u_{i,j} + u_{j,i}) \\ \epsilon_{ij} &: \text{Lagrangian strain tensor} \end{aligned} \quad (2-1.4)$$

(iv). Equation of equilibrium

$$f_i + \sigma_{ij,j} - \rho \dot{p}_i = 0 \quad (2-1.5)$$

f_i : body force per unit volume

$\sigma_{ij,j}$: Lagrangian stress tensor

ρ : mass density of the material

\dot{p}_i : rate-of change of absolute velocity

(v). Strain-stress relation in relaxation form

$$\sigma_{ij} = G_{ijkl} \varepsilon_{kl}(0) + \int_0^t G_{ijkl}(t-\tau) \left[d\varepsilon_{kl}(\tau) / d\tau \right] d\tau \quad (2-1.6)$$

where

G_{ijkl} : Relaxation function

σ_{ij} : stress tensor

the first term in the equation above represents the response at $t=0$, while the second term of the equation is the rate of change during a time interval dt . Equation (2-1.6) can also be written as

$$\sigma_{ij} = G_{ijkl} * d\varepsilon_{kl} \quad (2-1.7)$$

where

* is the convolution form

Equation (2-1.7) is the constitutive equation of the material

In addition, the following energies are defined

kinetic energy: $T = (1/2) \rho p_i \delta_{ij} p_j$

potential energy: $U = (1/2) G_{ijkl} \delta_{kl} \delta_{ij}$

The objective now is to establish a variational theorem which contains equation (2-1.1) to (2-1.7) in the first variation of the functional. When the first variation is set equal to zero, and independent variations are permitted then these governing equations are the stationary conditions of the functional. The task of determining the stationary conditions of this functional expression may be achieved using a the Lagrange multiplier approach to introduce the constraints into the functional and generalise Hamilton's principle [24].

The functional may be written

$$\begin{aligned}
 J = & \int_{t_0}^{t_1} \left\{ \int_V d[T-U] dV + \int_{S_d} \bar{g}_i \delta x_i dS_d \right. \\
 & + \int_V \lambda_{ij}^{(1)} \delta [e_{ij} - (1/2)(u_{i,j} + u_{j,i})] \\
 & + \int_V \lambda_i^{(2)} \delta [p_i - \bar{r}_{oi} - \bar{u}_i - e_{ijk} \phi_i (r_{ok} + r_{rk} + u_k)] dV \\
 & \left. + \int_{S_\sigma} \lambda_i^{(3)} \delta (\bar{u}_i - u_i) dS_\sigma \right\} dt \quad (2-1.8)
 \end{aligned}$$

The first variation may be generated using the standard rules of the variational calculus and this procedure involves utilizing the

divergence theorem and also the symmetric properties of the tensors. On establishing the first variation, this is then set equal to zero, yielding

$$\delta J = 0$$

$$\begin{aligned}
 &= \int_{t_0}^{t_1} \left\{ \int_V d[\delta T - \delta U] dV \right. \\
 &+ \int_{S_d} \bar{g}_i * d(\delta r_{oi} + \delta r_{ri} + \delta u_i) dS_d \\
 &+ \int_V \delta \lambda_{ij}^{(1)} * d[\varepsilon_{ij} - (1/2)(u_{i,j} + u_{j,i})] dV \\
 &+ \int_V \delta \lambda_i^{(2)} * d[p_i - \bar{r}_{oi} - \bar{u}_i - e_{ijk} \delta_j (r_{ok} + r_{rk} + u_k)] dV \\
 &+ \int_{S_\sigma} \delta \lambda_i^{(3)} * d[\bar{u}_i - u_i] dS_\sigma \\
 &+ \int_V \lambda_{ij}^{(1)} * d[\delta \varepsilon_{ij} - (1/2)(\delta u_{i,j} + \delta u_{j,i})] dV \\
 &+ \left. \int_{S_\sigma} \lambda_i^{(3)} * d(-\delta u_i) dS_\sigma \right\} dt \tag{2-1.9}
 \end{aligned}$$

Considering the first term in the equation (2-1.9), the variation of the kinetic energy T may be written as

$$\begin{aligned}
 \delta T &= (\partial T / \partial p_i) \delta p_i \\
 &= (\partial / \partial p_i) [(1/2) \rho p_i * \delta_{ij} p_j] \delta p_i \\
 &= \rho p_i * \delta p_i \tag{2-1.10}
 \end{aligned}$$

Similarly, for the potential energy density,

$$\begin{aligned}
\delta U &= (\partial U / \partial d\varepsilon_{ij}) \delta d\varepsilon_{ij} \\
&= (\partial / \partial d\varepsilon_{ij}) [(1/2) G_{ijkl} * d\varepsilon_{ij} * d\varepsilon_{kl}] \delta d\varepsilon_{ij} \\
&= G_{ijkl} * d\varepsilon_{kl} * \delta d\varepsilon_{ij}
\end{aligned} \tag{2-1.11}$$

Consider the third term in equation (2-1.9), since $\delta u_{i,j} = \delta_{j,i}$, this may be rewritten

$$\begin{aligned}
&\int_V \lambda_{ij}^{(1)} * d[\delta\varepsilon_{ij} - (1/2)(\delta u_{i,j} + \delta u_{j,i})] dV \\
&= \int_V \lambda_{ij}^{(1)} * d[\delta\varepsilon_{ij}] dV - \int_V \lambda_{ij}^{(1)} * d\delta u_{i,j} dV
\end{aligned} \tag{2-1.12}$$

The second term in the equation (2-1.12) can be integrated by parts and upon applying the divergence theorem this leads to

$$\begin{aligned}
\int_V \lambda_{ij}^{(1)} * d\delta u_{i,j} &= \int_S \lambda_{ij}^{(1)} n_j * d\delta u_i dS - \int_V \lambda_{ij,j}^{(1)} * d\delta u_i dV \\
&= \int_{S_d} \lambda_{ij}^{(1)} n_j * d\delta u_i dS_d + \int_{S_\sigma} \lambda_{ij}^{(1)} n_j * d\delta u_i dS_\sigma - \int_V \lambda_{ij,j}^{(1)} * d\delta u_i dV
\end{aligned} \tag{2-1.13}$$

hence, from equation (2-1.12) and (2-1.13), the third term in equation (2-1.9) can be rewritten as

$$\begin{aligned}
&\int_V \lambda_{ij}^{(1)} * d[\delta\varepsilon_{ij} - (1/2)(\delta u_{i,j} + \delta u_{j,i})] dV \\
&= \int_V \lambda_{ij}^{(1)} * d\delta\varepsilon_{ij} dV - \int_S \lambda_{ij}^{(1)} n_j * d\delta u_i dS + \int_V \lambda_{ij,j}^{(1)} * d\delta u_i dV
\end{aligned} \tag{2-1.14}$$

the fourth term in equation (2-1.9) may be written as

$$\begin{aligned} & \int_V \lambda_i^{(2)} * d[\delta p_i - \delta \tilde{r}_{oi} - \delta \tilde{u}_i - e_{ijk} \delta \phi_j * (r_{ok} + r_{rk} + u_k)] dV \\ = & \int_V \lambda_i^{(2)} * d\delta p_i dV - \int_V \lambda_i^{(2)} * d[\delta \tilde{r}_{oi} + \delta \tilde{u}_i + e_{ijk} \delta \phi_j * (r_{ok} + r_{rk} + u_k)] dV \end{aligned} \quad (2-1.15)$$

the second term of equation (2-1.15), may be integrated by parts over time and rewritten as

$$\begin{aligned} & \int_{t_1}^{t_2} \left[\int_V \lambda_i^{(2)} * d[\delta \tilde{r}_{oi} + \delta \tilde{u}_i + e_{ijk} \delta \phi_j * (r_{ok} + r_{rk} + u_k)] dV \right] dt \\ = & \int_{t_1}^{t_2} \int_V \lambda_i^{(2)} * d[\delta \tilde{r}_{oi} + \delta \tilde{u}_i + e_{ijk} \delta \phi_j * (r_{ok} + r_{rk} + u_k)] dV dt \\ - & \left[\int_V \lambda_i^{(2)} * d[\delta \tilde{r}_{oi} + \delta \tilde{u}_i + e_{ijk} \delta \phi_j * (r_{ok} + r_{rk} + u_k)] dV \right]_{t_0}^{t_1} \end{aligned} \quad (2-1.16)$$

the second term in the right hand side of the equation (2-1.16) is zero because variations at the extremes of the time interval are not permitted.

Thus

$$\begin{aligned} & \int_V \lambda_i^{(2)} * d[\delta p_i - \delta \tilde{r}_{oi} - \delta \tilde{u}_i - e_{ijk} \delta \phi_j * (r_{ok} + r_{rk} + u_k)] dV \\ = & \int_V \lambda_i^{(2)} * d\delta p_i dV - \int_V \lambda_i^{(2)} * d[\delta r_{oi} + \delta u_i + e_{ijk} \delta \phi_j * (r_{ok} + r_{rk} + u_k)] dV \end{aligned} \quad (2-1.17)$$

therefore, the first variation of the functional J may be written
as

$\delta J=0$

$$\begin{aligned}
&= \int_{t_0}^{t_1} \left[\int_V \delta p_i * d(\rho p_i + \lambda_i^{(2)}) dV + \int_V \delta \lambda_{ij}^{(1)} * d[\epsilon_{ij} - (1/2)(u_{i,j} + u_{j,i})] dV \right. \\
&+ \int_V \delta \lambda_i^{(2)} * d[p_i - \tilde{r}_{oi} - \tilde{u}_i - e_{ijk} \phi_j * (r_{ok} + r_{rk} + u_k)] dV \\
&+ \int_{S_\sigma} \delta \lambda_i^{(1)} * d(\bar{u}_i - u_i) dS_\sigma + \int_V d\delta \epsilon_{ij} * [\lambda_{ij}^{(1)} - G_{ijkl} * d\epsilon_{kl}] dV \\
&+ \int_V d\delta u_i * [\lambda_{ij,j}^{(1)} + \lambda_i^{(2)}] dV + \delta d r_{oi} * \left[\int_V \lambda_i^{(2)} dV + \int_{S_d} \bar{g}_i dS_d \right] \\
&+ \delta d \phi_j * \left[\int_V e_{ijk} (r_{ok} + r_{rk} + u_k) \lambda_i^{(2)} dV + \int_{S_\sigma} d\delta u_i * (-\lambda_i^{(2)} - \lambda_{ij}^{(1)} n_j) dS_\sigma \right] \\
&- \left. \int_{S_d} (\bar{u}_i - u_i) * d\delta \bar{g}_i dS_d + \int_{S_\sigma} d\delta u_i * (\bar{g}_i - \lambda_{ij}^{(1)} n_j) dS_\sigma \right] dt \tag{2-1.18}
\end{aligned}$$

By permitting independent arbitrary variations in the system
parameters, the Lagrange multipliers may be determined and written
as

$$\lambda_i^{(2)} = -\rho p_i$$

$$\lambda_{ij}^{(1)} = G_{ijkl} * d\epsilon_{kl} = \sigma_{ij}$$

$$\lambda_i^{(s)} = -g_i \quad (2-1.19)$$

So the final form for δJ becomes

$$\delta J = 0$$

$$\begin{aligned} &= \int_{t_0}^{t_1} \left[\int_V \delta \sigma_{ij} * d[\varepsilon_{ij} - (1/2)(u_{i,j} + u_{j,i})] dV \right. \\ &\quad - \int_V \rho \delta p_i * d[p_i - \tilde{r}_{oi} - \tilde{u}_i - e_{ijk} \dot{\phi}_j * (r_{ok} + r_{rk} + u_k)] dV \\ &\quad - \int_{S_\sigma} \delta g_i * d(\bar{u}_i - u_i) dS_\sigma + \int_V d\delta u_i * (\sigma_{ij,j} - \rho \dot{p}_i) dV \\ &\quad + \int_{S_\sigma} d\delta U_i * (\bar{g}_i - \sigma_{ij} n_j) dS_\sigma + \left[\int_{S_\sigma} \bar{g}_i dS_\sigma - \int_V \rho \dot{p}_i dV \right] * d\delta r_{oi} \\ &\quad + \left[\int_{S_d} \bar{g}_i e_{ijk} (r_{ok} + r_{rk} + u_k) dS_d + \int_V \rho \dot{p}_i e_{ijk} (r_{ok} + r_{rk} + u_k) \right] * d\delta \phi_j \\ &\quad \left. + \int_V (\sigma_{ij} - G_{ijkl} * d\varepsilon_{kl}) * d\delta \varepsilon_{ij} dV \right] dt \quad (2-1.20) \end{aligned}$$

Independent arbitrary variations of the deformation displacement, stress, strain, absolute velocity, and the kinematic parameters defining the rigid body equation of motion enable equation (2-1.20) to yield the field equations and boundary conditions for this class of dynamic viscoelastic problem because each integral must be independently equal to zero. The above variational principle represents a generalization to

the theory of viscoelasticity of an elastodynamic variational theorem presented in reference [15].

The characteristic equations obtained from equation (2-1.20) accurately define the dynamic viscoelastic problem for the design of mechanisms fabricated in materials with linear viscoelastic properties. In order to obtain viable solutions, simplifying assumptions must be introduced and in particular the constitutive equation must be modeled. In order to establish an industrially orientated solution methodology, the finite element method was selected as the vehicle for generating approximate solutions. A number of approaches establishing finite element models of viscoelastic media have appeared in the literature, such as references [58, 59, 60].

2-2 Finite Element Formulation

The variational equation of motion may be employed as the basis for a variety of finite element models depending on the geometrical shape of the body being analysed, the type of deformation theory assumed to be appropriate, the information sought from the analysis, the accuracy of the model for the constitutive equations, and the assumption of whether the material is isotropic or orthotropic. A finite element model is developed herein for determining the flexural response of the beam-shaped links of planar linkage mechanisms deforming in the plane of the mechanism. These linkages are assumed to be fabricated from graphite-epoxy laminates with orthotropic properties. The developments are based on publications [61, 62, 63].

The link deformations are governed by the Euler-Bernoulli beam theory, shown as Figure 2-2.1

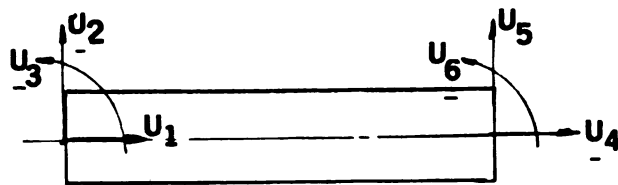


Figure 2-2.1 Nodal Degrees of Freedom Describing the Deformations of The Beam Element

and the transverse deformation may be written as

$$w = [N_w] \{U\} \quad (2-2.1)$$

where

$$\{U\} = \{U_2, U_3, U_4, U_6\}^T$$

Assuming that the member deforms on the axial and flexural modes, then the axial deformations is

$$\begin{aligned} u &= u_0 - z w, \quad x \\ &= [N_u] \{U_u\} - z [N'_w] \{U\} \end{aligned} \quad (2-2.2)$$

where

$$\{U_u\} = \{U_1, U_4\}$$

[N]: the row vector containing the shape functions

z : the spatial variable perpendicular to the beam section in the plane of the mechanism.

, : the spatial derivative with respect to the axial spatial variable. This symbol was also employed to denote the absolute time derivative (see equation 2-1.2) but confusion should not exist because in this section it is confined to operations on the shape functions.

The absolute velocity field $p(x,t)$ is related to the nodal values in the

discretized field by

$$p = [\hat{N}] \{P\} \quad (2-2.3)$$

where

$$\{P\} = \{P_{u_1}, \dots, P_{u_6}\}$$

$$[\hat{N}] = [1-(x/L), 1-(x/L), 1, x/L, x/L, 1]$$

In order that equation (2-1.20) be employed as the basis for a finite element analysis, this tensor expression must be reformulated in linear algebra format

$$\int_V \delta \sigma_{ij} * d[\varepsilon_{ij} - (1/2)(u_{i,j} + u_{j,i})] dv = \int_V d\{\delta \sigma\}^T * [\{\varepsilon\} - [N']\{U\}] dv \quad (2-2.4)$$

$$\begin{aligned} & \int_V \delta p_i * d\rho [p_i - \tilde{r}_{oi} - \tilde{u}_i + e_{ijk} * \delta_j (r_{ok} + r_{rk} + u_k)] dv \\ & = \int_V d\{\delta P\}^T * \rho [\{P\} - [N_R]\{P_R\} - [N]\{\dot{U}\}] dv \end{aligned} \quad (2-2.5)$$

$$\int_{S_\sigma} \delta g_i * d(\bar{u}_i - u_i) dS_\sigma = \int_{S_\sigma} d\{\delta g\}^T * (\{\bar{U}\} - [N]\{U\}) dS_\sigma \quad (2-2.6)$$

$$\int_V d\delta u_i * (\sigma_{ij,j} - \rho \dot{p}_i) dv = \int_V d\{\delta U\}^T * [N]^T * (\{D\}\{\sigma\} - \rho [N]\{\dot{P}\}) dv \quad (2-2.7)$$

$$\int_{S_\sigma} d\delta u_i * (\bar{g} - \sigma_{ij} n_j) dS_\sigma = \int_{S_\sigma} d\{\delta U\}^T * [N]^T * (\{\bar{g}\} - \{g\}) dS_\sigma \quad (2-2.8)$$

$$\left(\int_{S_\sigma} \bar{g}_i dS_\sigma - \int_V \rho \dot{p}_i dv \right) * d\delta r_{oi} = d\{\delta r_o\}^T * \left(\int_{S_\sigma} \{\bar{g}\} dS_\sigma - \int_V \rho [N]\{\dot{P}\} dv \right) \quad (2-2.9)$$

$$\left[\int_{S_d} \bar{g}_i * e_{ijk} (r_{ok} + r_{rk} + u_k) dS_d + \int_V \rho * \dot{p}_i * e_{ijk} * (r_{ok} + r_{rk} + u_k) \right] * d\delta \phi_j$$

$$=d\delta\bar{\theta}_j * [\int_{S_d} (\bar{r}x\bar{g}) dS + \int_v (\bar{r}x\rho\bar{P}) dv] \quad (2-2.10)$$

$$\int_v (\sigma_{ij} - G_{ijkl} * d\epsilon_{kl}) * d\delta\epsilon_{ij} dv = \int_v \{\delta\epsilon_{xx}\}^T * d(\{\sigma_{xx}\} - [G] * d\{\epsilon_{xx}\}) dv \quad (2-2.11)$$

hence the equation (2-1.20) can be rewritten as

$$\begin{aligned} \delta J &= 0 \\ &= \int_{t_0}^{t_1} \left[\int_v \{\delta\sigma\}^T * d[\{\epsilon\} - [N']\{U\}] dv \right. \\ &+ \int_v d\rho \{\delta P\}^T * [\{P\} - [N_R]\{P_R\} - [N]\{\dot{U}\}] dv \\ &+ \int_{S_\sigma} \{d\delta g\}^T * (\{\bar{U}\} - [N]\{U\}) dS_\sigma \\ &+ \int_v d\{\delta U\}^T * [N]^T ([D]\{\sigma\} - \rho[N]\{\dot{P}\}) dv \\ &+ \int_{S_\sigma} d\{\delta U\}^T * [N]^T (\{\bar{g}\} - \{g\}) dS_\sigma \\ &+ d\{\delta r_o\}^T * \left(\int_{S_\sigma} \{\bar{g}\} dS_\sigma - \int_v \rho [N]\{\dot{P}\} dv \right) \\ &+ d\delta\bar{\theta}_j * [\int_{S_d} (\bar{r}x\bar{g}) dS + \int_v (\bar{r}x\rho\bar{P}) dv] \\ &+ \int_v d\{\delta\epsilon\}^T * (\{\sigma_{xx}\} - [G] * d\{\epsilon_{xx}\}) dv \left. \right] dt \quad (2-2.12) \end{aligned}$$

Focussing attention upon equation (2-2.7), this may be written as

$$\begin{aligned} & \int_V d\{\delta U\}^T [N]^T ([D]\{\sigma\} - \rho[N]\{\dot{P}\}) dv \\ &= \int_V d\{\delta U\}^T [N]^T ([D]\{\sigma_{xx}\} - \rho[N]\{\ddot{U}\} - \rho[N_R]\{\dot{P}_R\}) dv \end{aligned} \quad (2-2.13)$$

by utilising the equation (2-2.5). The first term of equation (2-2.13) may be subjected to integration-by-parts over x to yield

$$\begin{aligned} & \int_V d\{\delta U\}^T [N]^T (\partial/\partial x)\{\sigma_{xx}\} dv \\ &= \left[\int_A d\{\delta U\}^T [N]^T \{\sigma_{xx}\} dA \right]_x - \int_V d\{\delta U\}^T [N']\{\sigma_{xx}\} dv \end{aligned} \quad (2-2.14)$$

where $[N'] = (\partial/\partial x)[N]$

As stated in [62] consider an one dimensional finite element of length L , and cross sectional area A represented by a cartesian reference frame. If ox is the axial coordinate, then the unit vector on the end faces has the direction cosine $l = \pm 1$, $m = 0$, $n = 0$ and surface tractions are

$$\{g\} = \pm \{\sigma_{xx}\} \quad (2-2.15)$$

thus, equation (2-2.8) leads to

$$\begin{aligned} & \int_{S_\sigma} d\{\delta U\}^T [N]^T (\{\bar{g}\} - \{g\}) dS \\ &= \int_A d\{\delta U\}^T [U]^T (\{\bar{g}\} \pm \{\sigma_{xx}\}) dA \Big|_{x=0}^{x=L} \end{aligned} \quad (2-2.16)$$

The first term in the right hand side of equation (2-2.14) may be written as

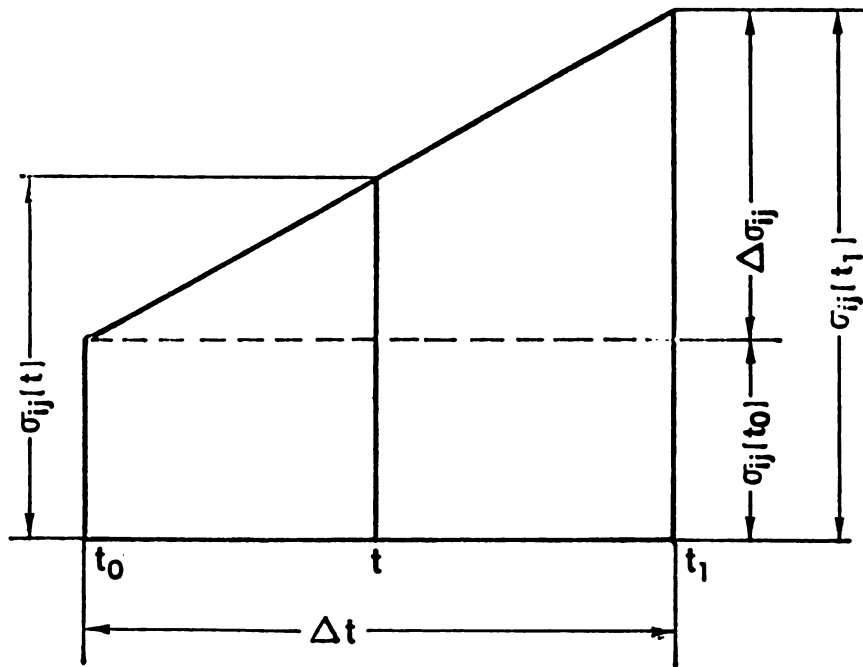


Figure 2-2.2 Finite difference representation

$$\int_A d\{\delta U\}^T \cdot [N]^T \{\sigma_{xx}\} dA \Big|_{x=L} - \int_A d\{\delta U\}^T \cdot [N]^T \{\sigma_{xx}\} dA \Big|_{x=0}$$

upon combining these terms with equation (2-2.16), terms cancel to give

$$\int_A d\{\delta U\}^T \cdot [N]^T \{\bar{g}\} dA \quad (2-2.17)$$

which is part of the equations of equilibrium.

The second term on the right-hand side of equation (2-2.14) may be written as

$$-\int_V d\{\delta U\}^T \cdot [N'] \{\sigma_{xx}\} dv$$

The the standard linear solid, presented in reference [63], will be employed to model the viscoelastic constitutive behavior, hence

$$\dot{\sigma}_{ij} + \beta \sigma_{ij} = 2\mu (\dot{\epsilon}_{ij} + \alpha \epsilon_{ij}) \quad (2-2.18)$$

Using Figure 5-2.2, which is a finite-difference representation of the materials' constitutive curve relating stress and strain, the left hand side of the equation (2-2.18) may be written as

$$\begin{aligned} \sigma_{ij} &= (1/2) [\sigma_{ij}(t_0) + \sigma_{ij}(t_1)] \\ &= \sigma_{ij}(t_0) + (\Delta \sigma_{ij} / 2) \end{aligned} \quad (2-2.19)$$

and, in addition,

$$\begin{aligned}\dot{\sigma}_{ij} &= (1/\Delta t)[\sigma_{ij}(t_1) - \sigma_{ij}(t_0)] \\ &= \Delta\sigma_{ij} / \Delta t\end{aligned}\quad (2-2.20)$$

Thus, the L.H.S. of the equation (2-2.18) becomes

$$\begin{aligned}\dot{\sigma}_{ij} + \beta\sigma_{ij} &= (\Delta\sigma_{ij}/\Delta t) + \beta\sigma_{ij}(t_0 + (\beta/2)\Delta t) \\ &= [(1/\Delta t) + (\beta/2)]\Delta\sigma_{ij} + \beta\sigma_{ij}(t_0)\end{aligned}\quad (2-2.21)$$

Similarly, applying the above procedure to the strain, the right hand side of equation (2-2.18) may be written as

$$2\mu\{[(1/\Delta t) + (\alpha/2)]\Delta\varepsilon_{ij} + \alpha\varepsilon_{ij}(t_0)\}$$

and hence equation (2-2.18) becomes

$$[(2/\Delta t) + \beta]\Delta\sigma_{ij} = 2\mu\{[(2/\Delta t) + \alpha]\Delta\varepsilon_{ij} + 2\alpha\varepsilon_{ij}(t_0)\} - 2\beta\sigma_{ij}(t_0)\quad (2-2.22)$$

Considering a one-dimensional model, equation (2-2.22) can be written as

$$\{\sigma_{xx}\} = B\{A\{\varepsilon_{xx} + 2\alpha\{\varepsilon_{xx}(t_0)\}\} - C\{\sigma_{xx}(t_0)\}\}\quad (2-2.23)$$

where

$$A=(2/\Delta t)+\alpha$$

$$B=2\mu/[(2/\Delta t)+\beta]$$

$$C=2\beta/[(2/\Delta t)+\beta]$$

where α , β , μ are constants.

$\varepsilon_{xx}(t_0)$ and $\sigma_{xx}(t_0)$ are the strain and stress at the previous time step of the numerical algorithm. Since

$$\{\varepsilon_{xx}\}=[N']\{U\} \quad (2-2.24)$$

the constitutive equation may be written as

$$\begin{aligned} & -\int_V d\{\delta U\}^T * [N']^T \left[AB[N']\{U\} + 2\alpha B\{\varepsilon_{xx}(t_0)\} - C\{\sigma_{xx}(t_0)\} \right] dv \\ & = -\int_V d\{\delta U\}^T * \left[AB[N']^T [N']\{U\} + 2\alpha B[N']^T \{\varepsilon_{xx}(t_0)\} - C[N']\{\sigma_{xx}(t_0)\} \right] dv \quad (2-2.25) \end{aligned}$$

by defining

$$[K] = \int_V AB[N']^T [N'] dv$$

$$[M] = \int_V [N]^T \rho [N] dv$$

$$[M_R] = \int_V [N]^T \rho [N_R] dv$$

and combining equation (2-2.25) with (2-2.17) and (2-2.13) the resulting

equations of motion are

$$d\{\delta U\}^T * \left[-[K]\{U\} - 2\alpha B[N']^T \{\varepsilon_{xx}(t_0)\} + C[N']^T \{\sigma_{xx}(t_0)\} - [M]\{\ddot{U}\} - [M_R]\{\dot{p}_R\} + \int_{S_\sigma} [N]^T \{\bar{g}\} dA \right] = 0$$

This may be written in a simpler form as

$$[K]\{U\} + [M]\{\dot{U}\} = \{f_{\text{visco}}\} - [M_R]\{\dot{P}_R\} + \int_{S_\sigma} [N']^T \{\bar{g}\} dA$$

where

$$\{f_{\text{visco}}\} = C[N']^T \{\sigma_{xx}(t_0)\} - 2\alpha B[N']^T \{\epsilon_{xx}(t_0)\}$$

Therefore, the final form of the variational equation of motion becomes

$$\delta J = 0$$

$$\begin{aligned} &= \int_{t_0}^{t_1} \left[\int_V d\{\delta\sigma_{xx}\}^T * \{ \{\epsilon_{xx}\} - [N']\{U\} \} dv \right. \\ &+ \int_V d\{\delta P\}^T * \rho \{ \{P\} - [N_R]\{P_R\} - [N]\{\dot{U}\} \} dv \\ &+ \int_{S_\sigma} d\{\delta g\}^T * (\{\bar{U}\} - [N]\{U\}) dS_\sigma \\ &+ d\{\delta U\}^T * [[K]\{U\} + [M]\{\dot{U}\} - \{f_{\text{visco}}\} + [M_R]\{\dot{P}_R\} - \int_{S_\sigma} [N]^T \{\bar{g}\} dS] dv \\ &+ d\{\delta r_0\}^T * (\int_{S_\sigma} \{\bar{g}\} dS_\sigma - \int_V \rho [N]\{\dot{P}\} dv) \end{aligned}$$

$$+d\delta\bar{\theta}_j * [\int_{S_d} (\bar{r}x\bar{g}) dS + \int_V (\bar{r}x\rho\bar{P}) dV]$$

$$+ \int_V d\{\delta e_{xx}\}^T * (\{\sigma_{xx}\} - [G] * d\{e_{xx}\}) dV] dt \quad (2-2.26)$$

Chapter 3

Mathematical Model of a Flexible Linkage

The objective of this chapter is to develop the finite element equations for a general planar elastic linkage which deforms principally in the axial and bending modes. In the course of this development, the nodal displacements, accelerations and shape functions expressions are derived. The stiffness matrix and mass matrix are also presented. The model for the viscoelastic material is in the last section. Some of the material presented in this chapter is based on reference [61].

3-1 Planar Beam Element

A general beam element is shown on the Fig. 3-1.1 in two reference frames. The global frame $O-X-Y$ and the local frame $o-x-y$. The x -axis of the local reference frame is parallel to the beam element axis. The dotted lines represent the rigid body position of the beam element and the solid lines show its elastically deformed configuration. The elastic deformation of the beam element could be described by six nodal displacements, here we denoted as $u_1, u_2, u_3, u_4, u_5, u_6$. These displacements are located at the deformed positions of the node A and node B. From the figure shown, the following relationships may be established in the global coordinates.

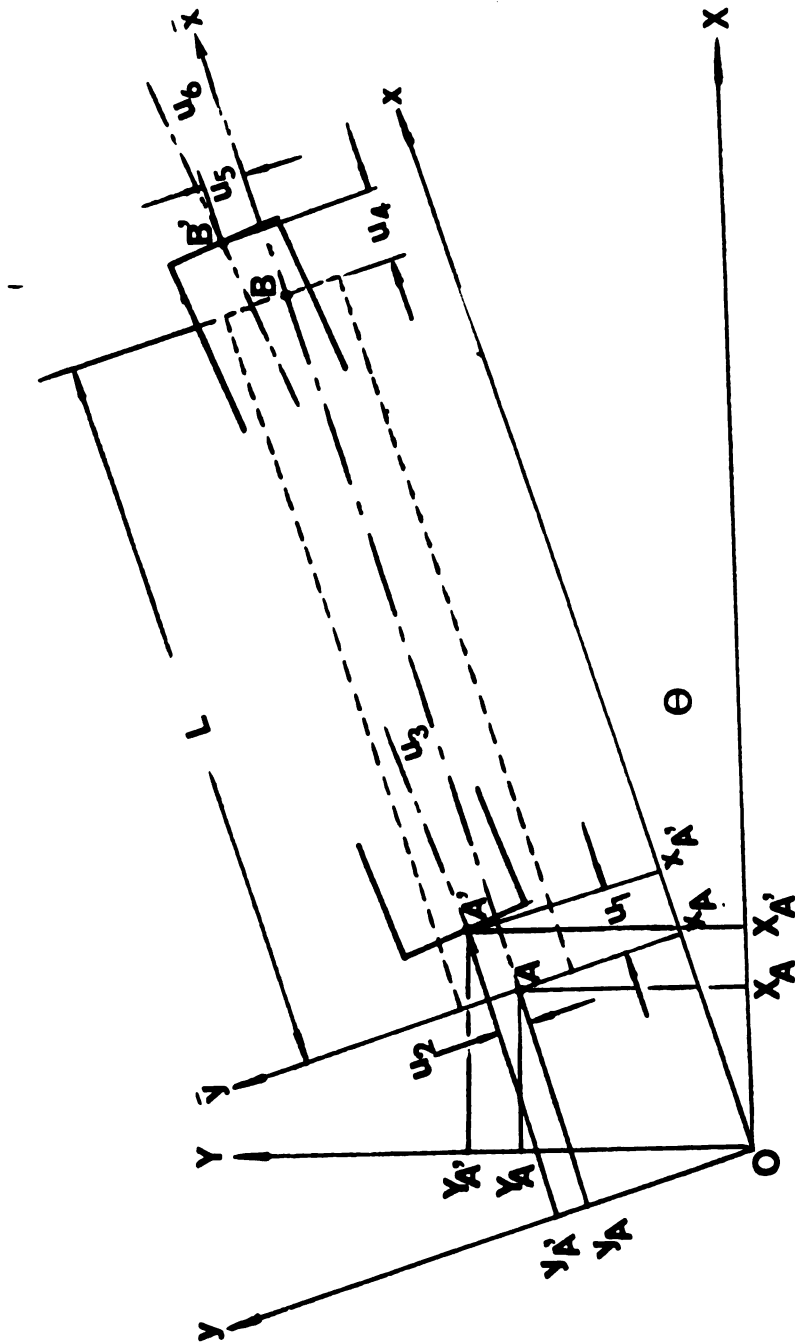


Figure 3-1.1 A General Beam Element

$$\begin{aligned}
X_{A'} &= X_A + u_1 \cos\theta - u_2 \sin\theta \\
Y_{A'} &= Y_A + u_1 \sin\theta + u_2 \cos\theta \\
\theta_{A'} &= \theta + u_3
\end{aligned}
\tag{3-1.1}$$

Differentiating equations above with respect to time, the velocity and the acceleration at node A can be expressed in the global coordinate as

$$\begin{aligned}
\dot{X}_{A'} &= \dot{X}_A + \dot{u}_1 \cos\theta - u_1 \dot{\theta} \sin\theta - \dot{u}_2 \sin\theta - u_2 \dot{\theta} \cos\theta \\
\dot{Y}_{A'} &= \dot{Y}_A + \dot{u}_1 \sin\theta + u_1 \dot{\theta} \cos\theta + \dot{u}_2 \cos\theta - u_2 \dot{\theta} \sin\theta \\
\dot{\theta}_{A'} &= \dot{\theta} + \dot{u}_3
\end{aligned}
\tag{3-1.2}$$

and

$$\begin{aligned}
\ddot{X}_{A'} &= \ddot{X}_A + \ddot{u}_1 \cos\theta - 2\dot{u}_1 \dot{\theta} \sin\theta - u_1 \dot{\theta}^2 \cos\theta - u_1 \ddot{\theta} \sin\theta - \ddot{u}_2 \sin\theta - 2\dot{u}_2 \dot{\theta} \cos\theta - u_2 \dot{\theta}^2 \sin\theta - u_2 \ddot{\theta} \cos\theta \\
\ddot{Y}_{A'} &= \ddot{Y}_A + \ddot{u}_1 \sin\theta + 2\dot{u}_1 \dot{\theta} \cos\theta - u_1 \dot{\theta}^2 \sin\theta + u_1 \ddot{\theta} \cos\theta + \ddot{u}_2 \cos\theta - 2\dot{u}_2 \dot{\theta} \sin\theta - u_2 \dot{\theta}^2 \cos\theta - u_2 \ddot{\theta} \sin\theta \\
\ddot{\theta}_{A'} &= \ddot{\theta} + \ddot{u}_3
\end{aligned}
\tag{3-1.3}$$

The absolute accelerations in equation (3-1.3) in global coordinates can be expressed in the local frame system with the following relations

$$\begin{aligned}
\bar{x}_A &= \bar{x}_A \cos\theta + \bar{y}_A \sin\theta \\
\bar{y}_A &= -\bar{x}_A \sin\theta + \bar{y}_A \cos\theta \\
\bar{\theta}_A &= \bar{\theta} + \bar{u}_3
\end{aligned} \tag{3-1.4}$$

combining equations (3-1.3) and (3-1.4), the resulting equations

$$\begin{aligned}
\bar{x}_A' &= \bar{x}_A + \bar{u}_1 - u_1 \dot{\theta}^2 - 2\dot{u}_2 \dot{\theta} - u_2 \ddot{\theta} \\
\bar{y}_A' &= \bar{y}_A + \bar{u}_2 - u_2 \dot{\theta}^2 - 2\dot{u}_1 \dot{\theta} + u_1 \ddot{\theta} \\
\bar{\theta}_A' &= \bar{\theta} + \bar{u}_3
\end{aligned} \tag{3-1.5}$$

Equation (3-1.5) is the absolute accelerations of node A of the beam element in the local frame.

Apply the same procedure to node B

$$\begin{aligned}
\bar{x}_B' &= \bar{x}_B + \bar{u}_4 - u_4 \dot{\theta}^2 - 2\dot{u}_5 \dot{\theta} - u_5 \ddot{\theta} \\
\bar{y}_B' &= \bar{y}_B + \bar{u}_5 - u_5 \dot{\theta}^2 - 2\dot{u}_4 \dot{\theta} + u_4 \ddot{\theta} \\
\bar{\theta}_B' &= \bar{\theta} + \bar{u}_6
\end{aligned} \tag{3-1.6}$$

Where \bar{x}_A , \bar{y}_A , $\dot{\theta}$, \bar{x}_B , \bar{y}_B , $\ddot{\theta}$ describe the rigid body motion of the beam element and are all kinematic quantities.

Defining

$$\{\ddot{u}_{ai}\} = \begin{pmatrix} \ddot{x}_{A'} \\ \ddot{y}_{A'} \\ \ddot{\theta}_{A'} \\ \ddot{x}_{B'} \\ \ddot{y}_{B'} \\ \ddot{\theta}_{B'} \end{pmatrix}, \text{ and } \{\ddot{u}_{ri}\} = \begin{pmatrix} \ddot{x}_A \\ \ddot{y}_A \\ \ddot{\theta} \\ \ddot{x}_B \\ \ddot{y}_B \\ \ddot{\theta} \end{pmatrix} \quad (3-1.7)$$

combining (3-1.5), (3-1.6), (3-1.7) in this section

$$\begin{pmatrix} \ddot{u}_{a1} \\ \ddot{u}_{a2} \\ \ddot{u}_{a3} \\ \ddot{u}_{a4} \\ \ddot{u}_{a5} \\ \ddot{u}_{a6} \end{pmatrix} = \begin{pmatrix} \ddot{u}_{r1} + \ddot{u}_1 - u_1 \dot{\theta}^2 & -2\dot{u}_2 \dot{\theta} & -u_2 \ddot{\theta} \\ \ddot{u}_{r2} + \ddot{u}_2 - u_2 \dot{\theta}^2 & +2\dot{u}_1 \dot{\theta} & +u_1 \ddot{\theta} \\ \ddot{u}_{r3} + \ddot{u}_3 & +0 & +0 \\ \ddot{u}_{r4} + \ddot{u}_4 - u_4 \dot{\theta}^2 & -2\dot{u}_5 \dot{\theta} & -u_5 \ddot{\theta} \\ \ddot{u}_{r5} + \ddot{u}_5 - u_5 \dot{\theta}^2 & -2\dot{u}_4 \dot{\theta} & +u_4 \ddot{\theta} \\ \ddot{u}_{r6} + \ddot{u}_6 & +0 & +0 \end{pmatrix} \quad (3-1.8)$$

this may be written as:

$$\{\ddot{u}_a\} = \{\ddot{u}_r\} + \{\ddot{u}\} + \{\ddot{u}_n\} + \{\ddot{u}_c\} + \{\ddot{u}_t\} \quad (3-1.9)$$

where

\ddot{u}_a : absolute acceleration

\ddot{u}_r : rigid body acceleration

\ddot{u} : elastic acceleration

\ddot{u}_n : normal acceleration

\ddot{u}_c : Coriolis acceleration

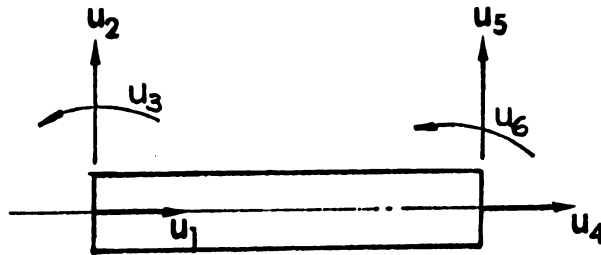
\ddot{u}_t : tangential acceleration

$\{\ddot{u}_n\}$, $\{\ddot{u}_c\}$, $\{\ddot{u}_t\}$ are the elastic and rigid body coupling terms. If the rigid body velocity and accelerations are small compared with those of the elastic nodal deflection, then in the equation (3-1.9) the product terms in vectors $\{\ddot{u}_c\}$, $\{\ddot{u}_c\}$, $\{\ddot{u}_t\}$ are also small compared to the corresponding terms in $\{\ddot{u}_r\} + \{\ddot{u}\}$. The analytical model presented here did not incorporate these coupling terms.

3-2 Shape Functions of Beam Element

The most widely used finite element approximation for representing the continuous function being studied, is the polynomial. Consider the beam element present in Figure 3-2.1, the shape functions for two kinds of deformations must be formulated. First, for the axial deformation, u_1 and u_2 , the choice of this shape function is a linear polynomial in x .

Figure 3-2.1 The Deformations of a Beam Element



$$u(x, t) = \phi_1(\bar{x})u_1(t) + \phi_4(\bar{x})u_4(t) \\ = a\bar{x} + b$$

(3-2.1)

where $\phi_1(\bar{x})$ and $\phi_4(\bar{x})$ are shape functions.

By virtue of fact that $u(x, t)$ must be such that

$$u(0, t) = u_1(t) = b$$

$$u(L, t) = u_4(t) = La + b$$

the functions $\phi_1(\bar{x})$ and $\phi_4(\bar{x})$ must satisfy boundary conditions

$$\phi_1(0) = 1 \quad , \quad \phi_1(L) = 0$$

$$\phi_4(0) = 0 \quad , \quad \phi_4(L) = 1$$

therefore

$$\phi_1 = (L - \bar{x})/L$$

$$\phi_4 = \bar{x}/L$$

Secondly, for the bending displacement field, the shape functions will

be described as a cubic polynomial in x . Hence

$$\begin{aligned} w(x, t) &= \phi_2(\bar{x})u_2(t) + \phi_3(\bar{x})u_3(t) + \phi_5(\bar{x})u_5(t) + \phi_6(\bar{x})u_6(t) \\ &= a_1 + a_2\bar{x} + a_3\bar{x}^2 + a_4\bar{x}^3 \end{aligned} \quad (3-2.2)$$

$$w(0, t) = u_2(t) = a_1$$

$$w(L, t) = u_3(t) = a_1 + a_2L + a_3L^2 + a_4L^3$$

$$w'(0, t) = u_5(t) = a_2$$

$$w'(L, t) = u_6(t) = a_2 + 2a_3L + 3a_4L^2$$

hence

$$\begin{aligned} a_3 &= (1/L^2)(-3\phi_1 - 2L\phi_2 + 3\phi_3 - L\phi_4) \\ a_4 &= (2/L^3)(\phi_1 + 2L\phi_2 - \phi_3 - (L/2)\phi_4) \end{aligned} \quad (3-2.3)$$

the shape functions are, therefore

$$\begin{aligned} \phi_2 &= 1 - (3\bar{x}^2/L^2) + (2\bar{x}^3/L^3) \\ \phi_3 &= (3\bar{x}^2/L^2) - (2\bar{x}^3/L^3) \\ \phi_5 &= \bar{x} - (2\bar{x}^2/L) + (\bar{x}^3/L^2) \\ \phi_6 &= -\bar{x}^2/L + (\bar{x}^3/L^2) \end{aligned} \quad (3-2.4)$$

The shape function of the beam element may; therefore, be written

as

$$\begin{aligned}
 \phi_1(\bar{x}) &= 1 - \bar{x}/L \\
 \phi_2(\bar{x}) &= 3((L-\bar{x})/L)^2 - 2((L-\bar{x})/L)^3 \\
 \phi_3(\bar{x}) &= \bar{x}((L-\bar{x})/L)^2 \\
 \phi_4(\bar{x}) &= \bar{x}/L \\
 \phi_5(\bar{x}) &= 3(\bar{x}/L)^2 - 2(\bar{x}/L)^3 \\
 \phi_6(\bar{x}) &= (L-\bar{x})(\bar{x}/L)^2
 \end{aligned} \tag{3-2.5}$$

The transverse displacement, $w(\bar{x}, t)$, may be written as:

$$w(\bar{x}, t) = \phi_2(\bar{x}) \cdot u_2(t) + \phi_3(\bar{x}) \cdot u_3(t) + \phi_5(\bar{x}) \cdot u_5(t) + \phi_6(\bar{x}) \cdot u_6(t) \tag{3-2.6}$$

and the axial displacement

$$u(\bar{x}, t) = \phi_1(\bar{x}) \cdot u_1(t) + \phi_4(\bar{x}) \cdot u_4(t) \tag{3-2.7}$$

3-3 Element Mass and Stiffness Matrices

Assume that the beam element has a uniform cross section, then the local mass and stiffness matrices are respectively $[\bar{m}]$ and $[\bar{k}]$, then

$$[\bar{m}] = \rho AL \begin{pmatrix} 1/3 & & & & & & \\ 0 & 13/35 & & & & & \\ 0 & 11L/210 & L^2/105 & & \text{Symmetric} & & \\ 1/6 & 0 & 0 & 1/3 & & & \\ 0 & 9/70 & 13L/420 & 0 & 13/35 & & \\ 0 & -13L/420 & -L^2/140 & 0 & -11L/210 & L^2/105 & \end{pmatrix} \quad (3-3.1)$$

$$[\bar{k}] = \begin{pmatrix} EA/L & & & & & & \\ 0 & 12EI/L^3 & & & \text{Symmetric} & & \\ 0 & 6EI/L^2 & 4EI/L & & & & \\ -EA/L & 0 & 0 & EA/L & & & \\ 0 & -12EI/L^3 & -6EI/L^2 & 0 & 12EI/L^3 & & \\ 0 & 6EI/L^2 & 2EI/L & 0 & -6EI/L^2 & 4EI/L & \end{pmatrix} \quad (3-3.2)$$

When deriving the stiffness properties of a beam finite element, using the small strain theory, it is assumed that the transverse displacements are independent of the axial displacements or forces. In reality, however, a compressive axial force would tend to increase any transverse displacement of the beam, thus effectively decreasing the

transverse stiffness of the beam. While a tensile axial force would have the opposite effect. This dependence of the stiffness matrix upon the axial loading is called geometric stiffening, and could become important in mechanism analysis where large axial forces are known to occur and also when the beam is very slender. One approximate method of including this effect is to calculate a geometric stiffness matrix $[k_G^0]$ based on large strain theory that would represent the coupling between the axial and transverse displacements. The geometric stiffness matrix for a beam element, which has been derived [46] and [64] is

$$[k_G^0] = (F/L) \begin{pmatrix} 0 & 0 & 0 & 0 & 0 & 0 \\ 0 & 6/5 & L/10 & 0 & -6/5 & L/10 \\ 0 & L/10 & 2L^2/15 & 0 & -L/10 & -L^2/30 \\ 0 & 0 & 0 & 0 & 0 & 0 \\ 0 & -6/5 & -L/10 & 0 & 6/5 & -L/10 \\ 0 & L/10 & -L^2/30 & 0 & -L/10 & 2L^2/15 \end{pmatrix} \quad (3-3.3)$$

where

F : the axial force in the element

This matrix $[k_G^0]$ represents the change in transverse stiffness due to an axial force in the element. To include this coupling effect in the equation of motion, the geometric stiffness matrix is simply added

to the element stiffness matrix $[\bar{k}]$.

3-4 Assembling the Mass and Stiffness Matrices of the Mechanis System

The finite element method generally requires the use of a global frame in order to assemble the element into a model for particular component. Therefore, a transfer matrix is necessary so as to transfer the stiffness matrix and mass matrix from the local frame to the global frame before the matrices of the system can be assembled to form a model for the complete mechanism system in which the links have differing orientations relative to the global frame.

Consider the beam element shown as Fig.3-4.1

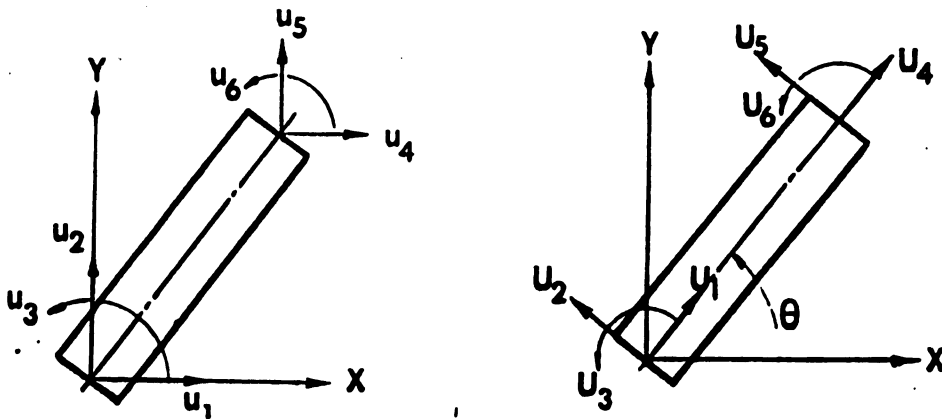


Figure 3-4.1 The Relation between Global and Local Coordinate

The relations between two different coordinate are:

$$\begin{aligned}
u_1 &= U_1 \cos\theta + U_2 \sin\theta \\
u_2 &= -U_1 \sin\theta + U_2 \cos\theta \\
u_3 &= U_3 \\
u_4 &= U_4 \cos\theta + U_5 \sin\theta \\
u_5 &= -U_4 \sin\theta + U_5 \cos\theta \\
u_6 &= U_6
\end{aligned}
\tag{3-4.1}$$

Thus, a transfer matrix may be written as:

$$[R] = \begin{pmatrix} \cos\theta & \sin\theta & 0 & 0 & 0 & 0 \\ -\sin\theta & \cos\theta & 0 & 0 & 0 & 0 \\ 0 & 0 & 1 & 0 & 0 & 0 \\ 0 & 0 & 0 & \cos\theta & \sin\theta & 0 \\ 0 & 0 & 0 & -\sin\theta & \cos\theta & 0 \\ 0 & 0 & 0 & 0 & 0 & 1 \end{pmatrix}
\tag{3-4.2}$$

and the global matrix $[m]$, is related to the local mass matrix $[\bar{m}]$

by the expression

$$[m] = [R]^T [\bar{m}] [R]
\tag{3-4.3}$$

similarly

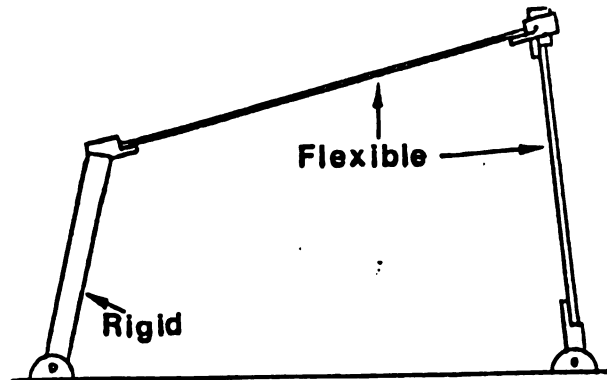
$$[k] = [R]^T [\bar{k}] [R]
\tag{3-4.4}$$

3-5 Linkage Model

For the finite element analysis, the linkage is regarded as an instantaneous structure at every position. Consequently, the stiffness and mass matrices are different at each mechanism position. Generalized coordinates representing deflections are assigned to every joint permitting the members to deflect in the horizontal or vertical directions. As illustrated above, the following steps should be satisfied in the computer program.

- 1) An idealization of linkage structure is needed. This will require selection of the type and the size of the finite element to generate the system mesh.
 - 2) The system-oriented element mass and stiffness matrices are generated for each element.
 - 3) These element mass and stiffness matrices are assembled systematically to develop the mass and stiffness matrices of the total linkage system.
 - 4) Determination of unknown model displacements of the problem involves solving a system of coupled ordinary differential equations.
- These equations are obtained by using the equilibrium condition at the nodes.

Figure 3-5.1 Four Bar Linkage Model with Flexible Coupler



The linkage model is shown in Figure 3-5.1, the crank element is considered to be rigid, while each flexible link, coupler and rocker, is divided into six elements. The element at both ends of the link, considered as joints made of aluminum, is treated differently because of the different material properties. In Figure 3-5.2, system-oriented generalized displacements are labeled to describe the structural deformation of the linkage as well as to maintain compatibility between the elements and nodes. For instance, at the joint between the coupler and the rocker, U_{14} and U_{15} represents the nodal translations and U_{36} and U_{16} describe the rotational deflection of the coupler and the rocker at that point. A rigid connection between two elements, will be simulated by only one rotational displacement.

3-6 Construction of system matrices

In Figure 3-6.1, appropriate displacements are labeled on each retaining compatibility at the nodes. The system mass and stiffness

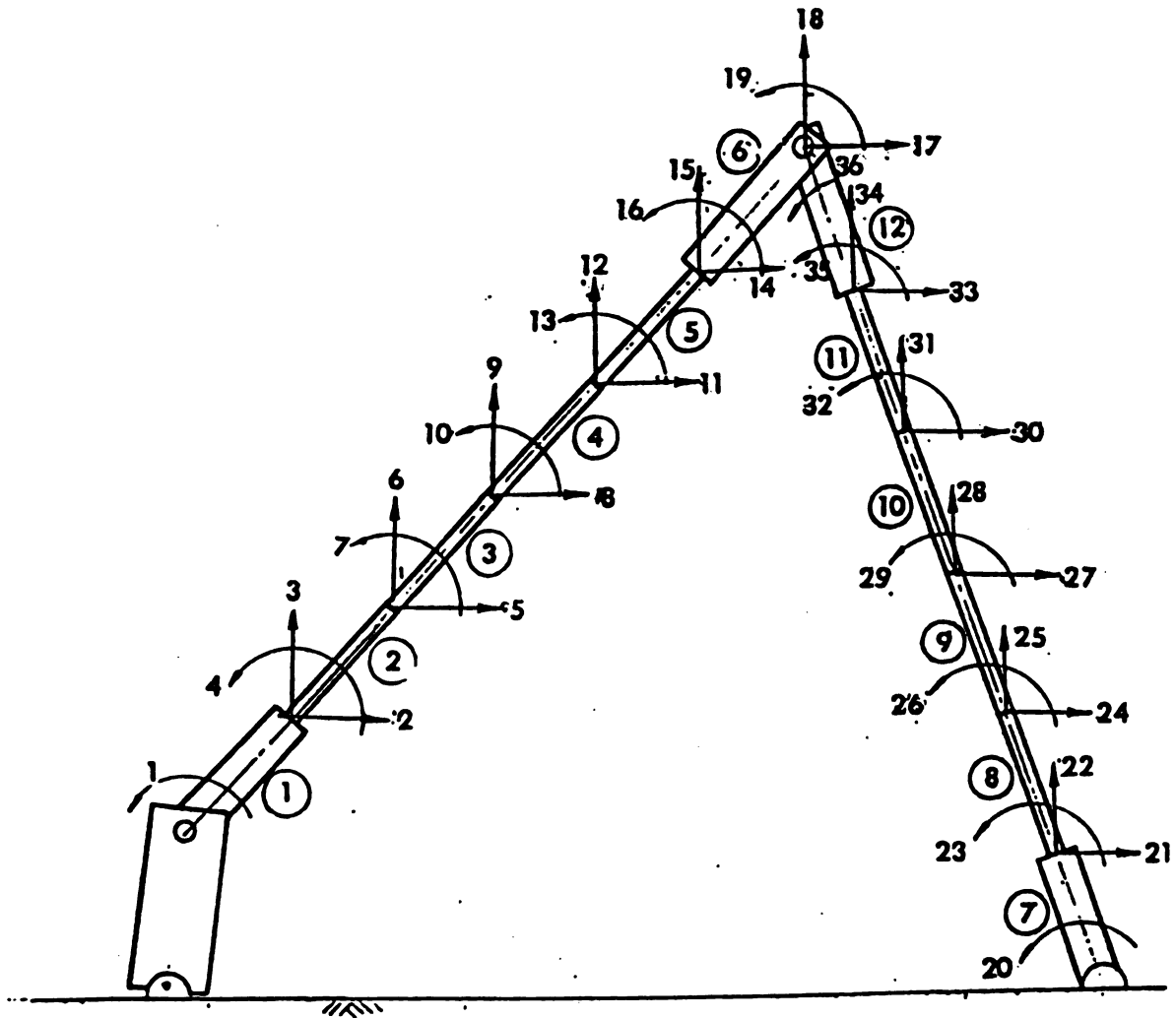


Figure 3-6.1 Finite Element Model for the Simulation

matrices of ith element are

$$\begin{aligned} [m_i] &= [R]_i^T [\bar{m}_i] [R]_i \\ [k_i] &= [R]_i^T [\bar{k}_i] [R]_i \end{aligned} \quad (3-6.1)$$

$i = 1, 2, 3, \dots, 12$

3-7. Modeling The Viscoelastic Constitutive Equations

The model representing a viscoelastic media is constructed to simulate the experimental behavior of viscoelastic material and involve differential equations relating strain, stress, and time. An important characteristic of these materials, especially when subjected to dynamic loading, is that they exhibited a time and rate dependence that is completely absent in the constitutive relations of elastic materials. Although these types of material have the capacity to respond instantaneously they also exhibit a delayed response. Thus the materials have the combined capacity of an elastic material to store energy and the capacity of a viscous material to dissipate energy. Materials with this type of behavior are termed viscoelastic materials and they have been the subject of several texts [48, 65-68], the topic for chapters in standard reference texts [69-71], and the objective of numerous papers [72-76]. For dynamic viscoelastic problems it is necessary to construct the entire solution without relying on the static elasticity results since after all, dynamic situations involve wave propagation phenomena, strain rate effects and attenuation characteristics. In this regard,

finite element solutions are proposed herein based on approximate forms for the constitutive equations because an exact solution requires the time history of the material to be known for all time, which is of course impractical.

The basic elements commonly used in the model representation are a spring and a dashpot. A spring, shown as Figure 3-7.1a, represents an elastic solid, and exhibits instantaneous elastic strain and elastic recovery as Figure 3-7.1b.

The equation relating stress and strain for a spring in time domain is

$$\sigma = E\varepsilon \quad \text{or} \quad \varepsilon = \sigma/E \quad (3-7.1)$$

A dashpot, as Figure 3-7.2a, represent a viscous element, and exhibits irreversible creep and permanent set as Figure 3-7.2b.

The differential equation relating stress and strain for a dashpot in time domain is

$$\sigma = \mu \dot{\varepsilon} \quad (3-7.2)$$

One of the combinations of the two basic elements is the Kelvin model, as Figure 3-7.3, which consists of a spring and dashpot in paral-



Figure 3-7.1a Spring.

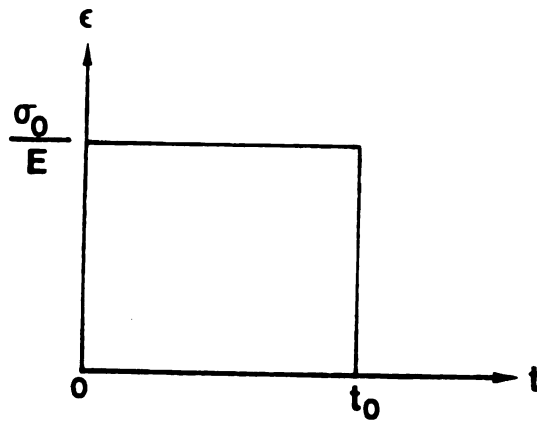


Figure 3-7.2b Strain-Time Relation of Dashpot.

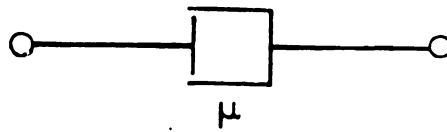


Figure 3-7.2a Dashpot.

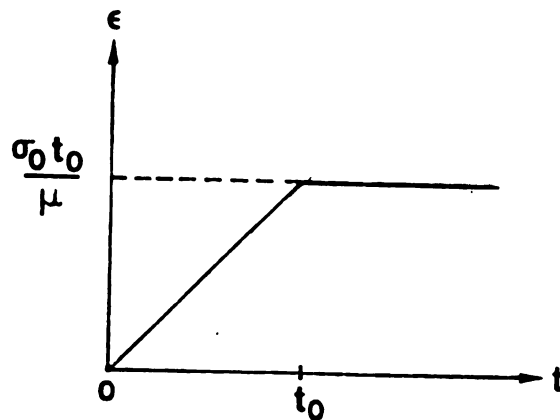


Figure 3-7.1b Strain-Time Relation of Spring.

1el. At all times the elongation ϵ of the two elements is the same, and the total force σ will split into σ_1 (for the spring) and σ_2 (for the dashpot) in whichever way to make ϵ the same. When applied to this model

$$\begin{aligned}\sigma_1 &= E_1 \epsilon \\ \sigma_2 &= \mu \dot{\epsilon}\end{aligned}\tag{3-7.3}$$

and from these two relations

$$\begin{aligned}\sigma &= \sigma_1 + \sigma_2 \\ &= E_1 \epsilon + \mu \dot{\epsilon}\end{aligned}\tag{3-7.3}$$

Various combinations of the basic elements are also possible. The standard linear model, as Figure 3-7.4, representing a first order linear differential equation of stress and strain. This is a three parameter model which consists of a spring in series with a Kelvin unit. The differential equation relating stress and strain for this model are

$$(\mu_1/E_1) \dot{\sigma} + [1 + (E_1/E_2)] \sigma = \mu_1 \dot{\epsilon} + E_1 \epsilon\tag{3-7.4}$$

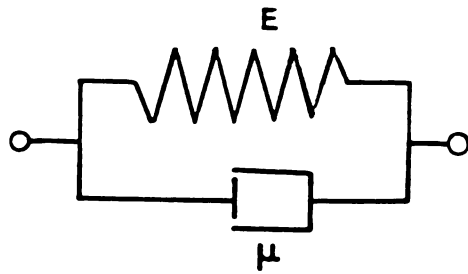


Figure 3-7.3 Kelvin Model.

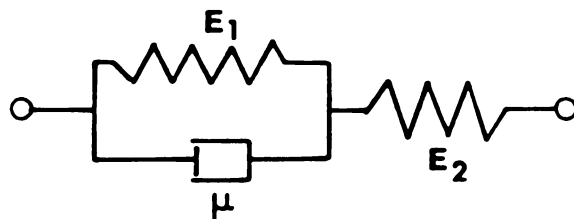


Figure 3-7.4 Standard Linear Solid Model

Chapter 4

Experimental Investigation

4-1. Material Characterization Studies

The experimental results concerning the material properties were developed by Mr.C.K.Sung and Mr.J.Cuccio under the instructions of Dr. B.S.Thompson in August 1983 in Michigan State University [78].

The main cause of link deformations in a flexible mechanism is either the bending, or the flexural, mode and the associated deflection field is governed by the flexural rigidity, which is the product of the Young's modulus (E) of the material and the second moment of the cross-section area of the link (I).

The materials chosen for the experimental work were a low carbon steel and a graphite-epoxy laminate with a symmetrical ply layup of ± 45 degrees relative to the longitudinal axis of the link.

The modulus of elasticity of the steel link specimens were obtained from supplier's data sheets, and the specimens were not subjected to mechanical testing. However, the composite materials have a greater variability of mechanical properties, hence the characteristics of the laminates need to be examined and quantified carefully. In order to

determine whether it is elastic, viscoelastic, or plastic.

The purpose for the testing was to investigate the mechanical properties of the ± 45 degrees graphite-epoxy laminates. At first, the specimens were subjected to dynamic testing, which required the specimen to gain a prescribed maximum load 0.258 MPa over a range of time intervals. Thus Figure 4-1 presents the results of the tests performed on the ± 45 degrees laminate and the maximum stress level was reached in 0.5, 1, 10, 100 and 1000 seconds during the four tests.

The results presented in Figure 4-1 suggest that the behavior of the material is certainly dependent on the rate of application of the loading. Thus, the ± 45 degrees laminate is a viscoelastic material, and the response curve implies that the constitutive relationship of strain and stress is nonlinear.

In order to verify the deductions made from these test data, another test was undertaken to study the creep response of the materials. The results are presented in the Figure 4-2. The creep data in Figure 4-2 verifies that the ± 45 degrees composite is truly a viscoelastic material.

The following method was adopted in order to incorporate the data from the material characterization studies into the mathematical model. The objective was to determine the relaxation function relating stress and time. Firstly, the maximum strain was measured on the response

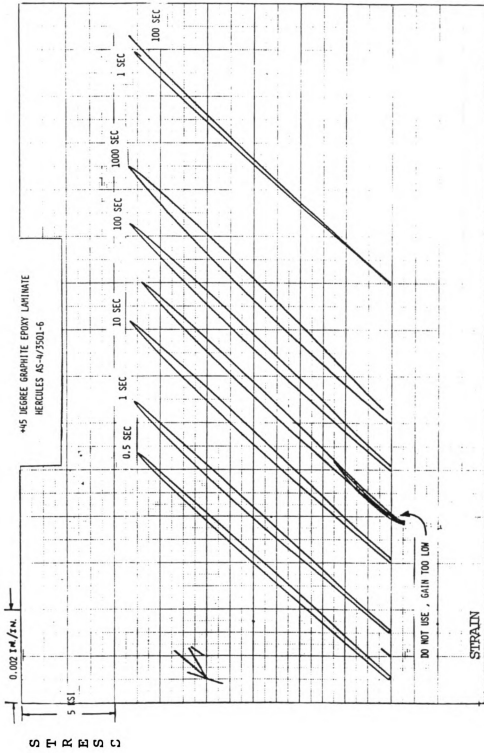


Figure 4-1 Result for Material Testing

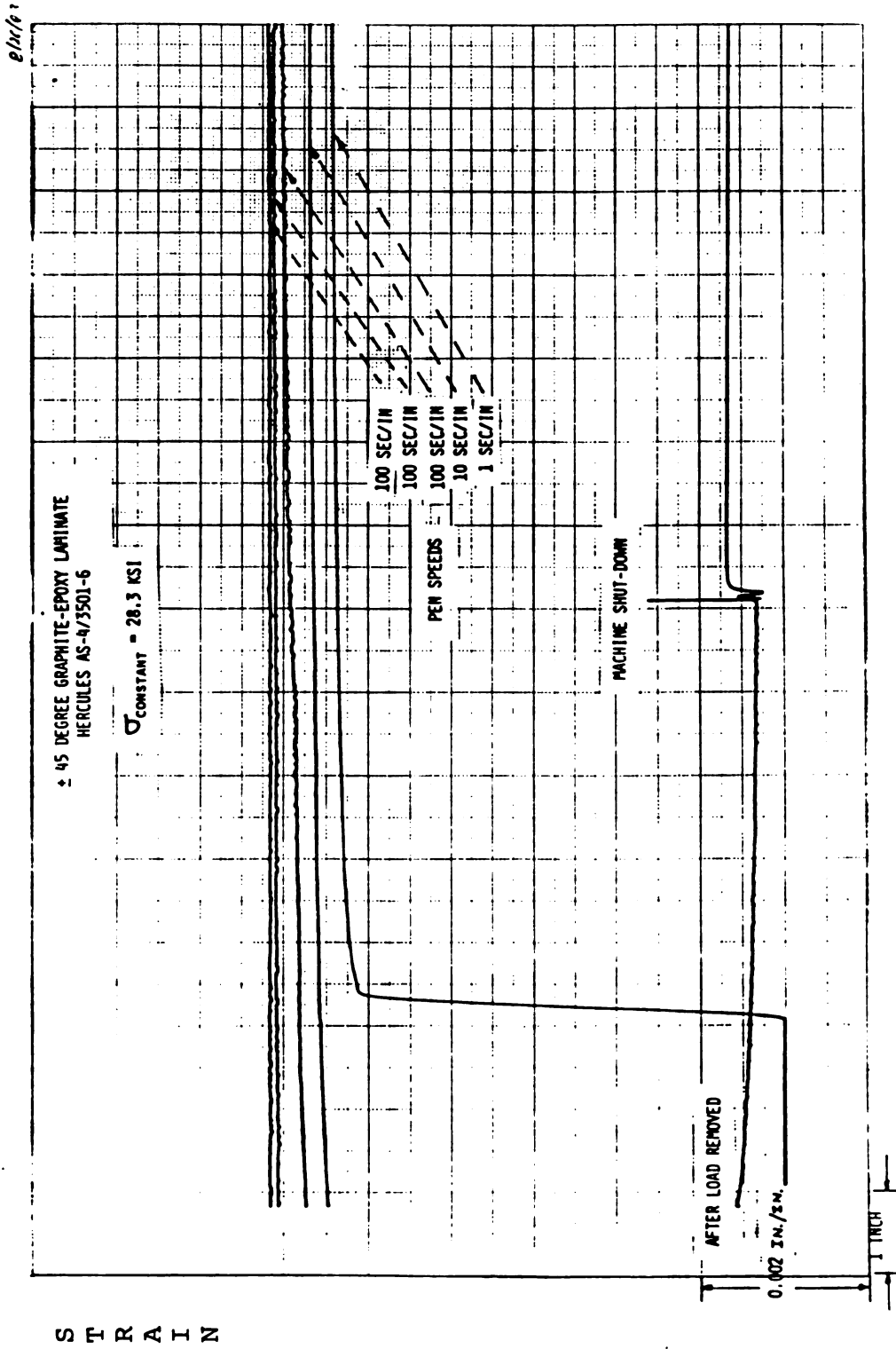


Figure 4-2 Result for Creep Testing

curve extreme left. This corresponded to a stress of 0.258 MPa. at 0.5 second after the load was initially applied.

Then using this magnitude of strain, a horizontal line was measured from the point of load initiation on each of the response curve in Figure 4-1 and a vertical perpendicular line constructed until it intersected each response curve on the increasing load (upper) portion of the curve. This permitted the stress to be obtained and assuming that the rate of application of load was constant (it was programmed to be constant on the MTS testing machine) this operation permitted a stress-time graph to be plotted. This is presented in Figure 4-3. Then using a PRIME 750 curve fitting software "CURVFIT" by changing the values of the parameters A, B in the equation

$$Y(t) = (A-B)e^{-at} + B \quad (4-1)$$

and the data presented in Figure 4-4, which is a curve of the standard linear solid model, the curve presented in Figure 4-5 was generated. By plotting the constants E_1 , E_2 , μ_1 of the relaxation modulus, [79], can be obtained from the following procedures

$$\begin{aligned} G(t) &= E_1 e^{-t/\mu_1} + (E_1/E_2)(1 - e^{-t/\mu_1}) \\ &= [E_1 - (E_1/E_2)]e^{-at} + (E_1/E_2) \end{aligned} \quad (4-2)$$

so

$$E_1 = A$$

$$E_2 = A/B$$

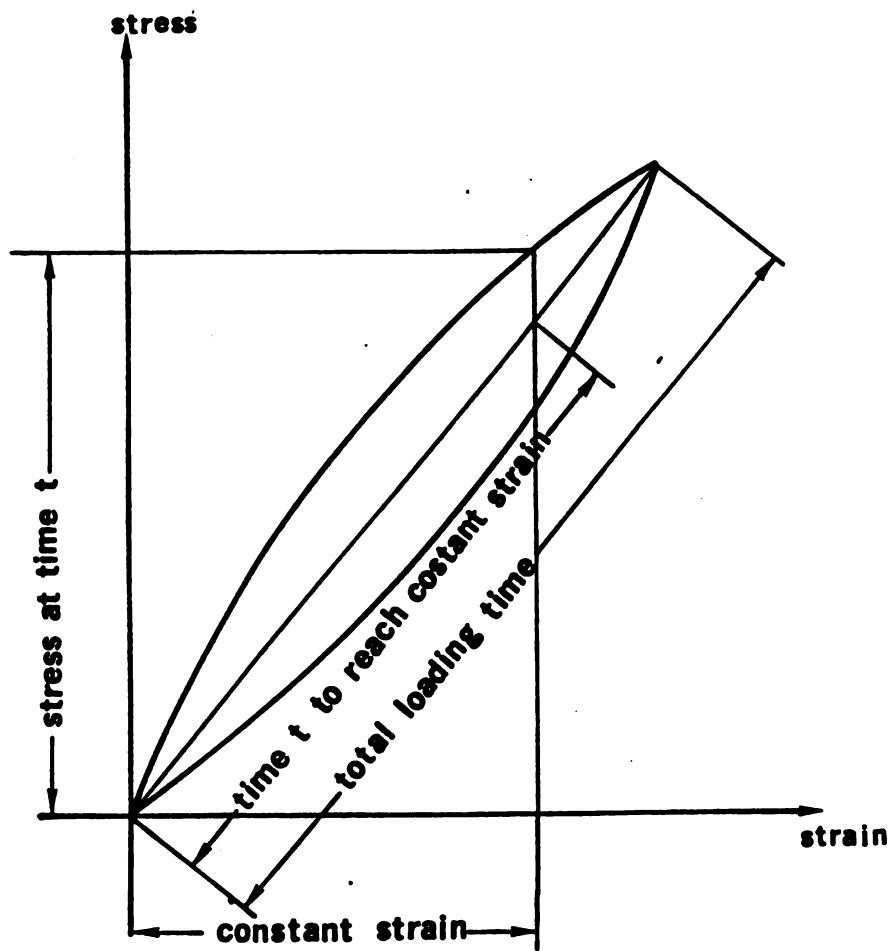


Figure 4-3 Method to Obtain the Relaxation Function

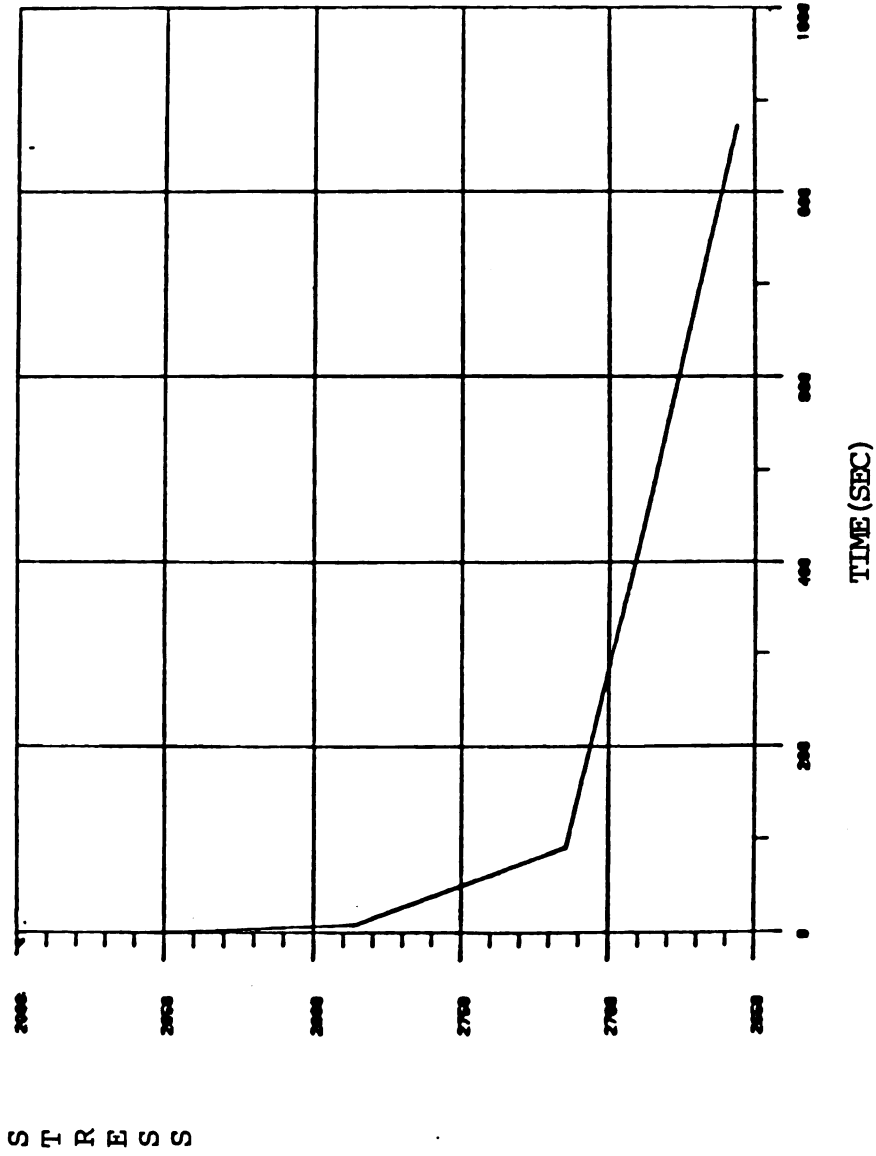


Figure 4-4 Relaxation Function Obtained from Material Testing

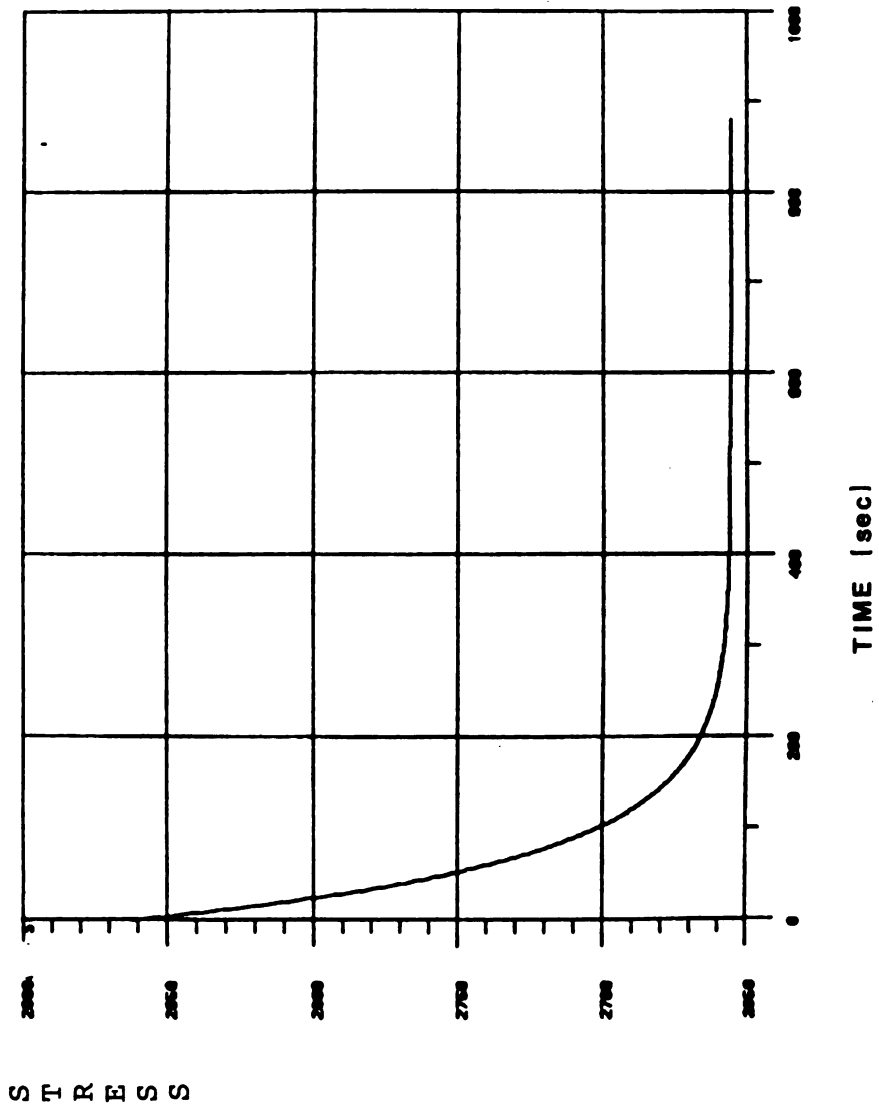


Figure 4-5 Relaxation Function Obtained from Curve Fitting

$$\mu_1 = 1/a$$

After the dynamic and creep testing of the laminate is completed, the response data provides the foundations of several investigations. The ± 45 degrees laminate has a complex response because the stress-strain relation is not linear, and the gradient depends on the strain rate. Obviously, a wide range of different Young's modulus could be determined from the experimental data depended on the assumptions that considered to be necessary. Because a link of any mechanism experiences rapidly fluctuating stress levels, the response curve on the extreme left of Figure 4-1 was selected to provide the basis for the Young's modulus because this records the highest strain rate of any specimen.

The approach was to draw a tangent to the response curve out the lower end of the upper portion of the curve in the region recording, the initial response immediately following load application. The effective Young's modulus for this viscoelastic material was calculated to be 3.143×10^6 lbf/in² while a mean value of 2.834×10^6 lbf/in² was calculated for the line joining the points defining the maximum and minimum stress levels.

The final objective of the material characterization studies was to determine the material damping of the material. Each link specimen was clamped at one end to develop a cantilever configuration prior to

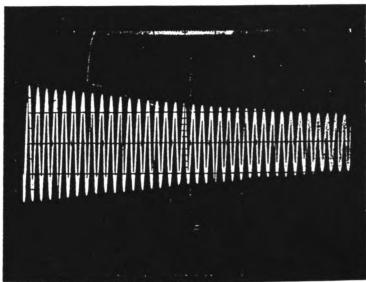


Figure 4-6 Natural Frequency of the Steel Link

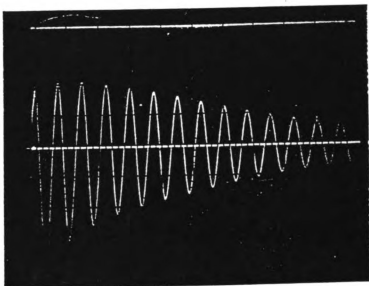


Figure 4-7 Natural Frequency of the Composite Link

deflecting and releasing the other end and recording the transient vibration. Besides obtaining the natural frequency of the link from the trace on the oscilloscope screen, simple logarithmic decrement calculations were undertaken to calculate the damping ratio (ξ). The results are presented in Figure 4-5 for steel and Figure 4-6 for composite laminate. Thus it is evident that of the laminate has a much higher damping ratio than the steel, and this property can be utilised in mechanism design to eliminate undesirable vibrations.

4-2 Experimental Apparatus

Specimens were prepared to form matched pairs in the two link materials. At the end of each link, two clearance holes were drilled. These accommodated socket screws which clamped each specimen to the bearing housing and permitted the experimental four bar linkage to be constructed. The flexible links were fixed to the aluminum bearing housing by two socket screw at either ends with a flat plate. The small plate which was shown in Figure 4-7 ensured a smooth load transfer between the principle components of each link.

The experimental four bar linkage presented in Fig.4-7 was located on a large cast iron table which was bolted to the ground and wall of the laboratory. It had a rigid crank with a link length of 63.5 mm (2.5 inches), while the lengths of the two flexible links, the coupler and rocker, were changeable.

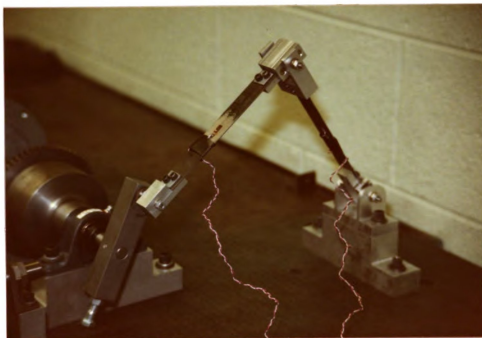


Figure 4-8 Joint connecting the flexible coupler and rocker

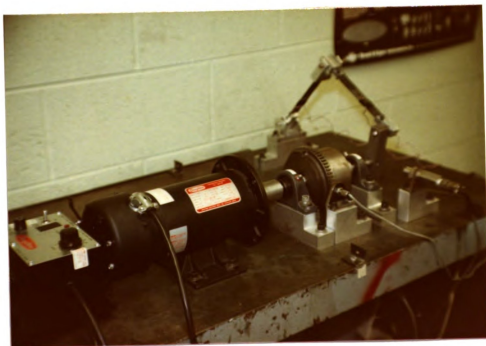


Figure 4-9 Experimental Four Bar Mechanism

The coupler and rocker links were supported on matched pairs of ball bearing (FAG R3 DB R12) of 0.25 inches in bore. Every bearing was preloaded using a Dresser torque limiting screw driver with ± 1 in-lbf preloading. This procedure is to ensure that bearing clearance is eliminated. The impact loading associated with bearing clearances would cause the links to have large deflections. Nevertheless, where the bearings were assembled with large axial preloading, the deflections of the linkages will be decayed. Owing to these affects, the torque limit device must be employed to accurately preload the joints.

A 0.75 hp variable speed D-C motor (Dayton 2Z846) powered the crank through a 0.625 inch diameter shaft supported by a cast iron pillow box bearings. A 4 inch diameter fly wheel was keyed to the shaft thereby providing a large inertia to ensure a constant crank frequency, when operating in unison with the motor's speed controller.

4-3 Instrumentation

The instrumentation flow chart in the experimental work is shown in the Figure 4-9. The rated speed of the electric motor was measured to three decimal places by a HP 5314A universal counter which was actived by a digital-magnetic pickup, model 58423, by Electro corporation. These devices allowed the operator to adjust the speed controller of the motor in order to achieve the desired speed.

The experimental results present the variation of link deflections

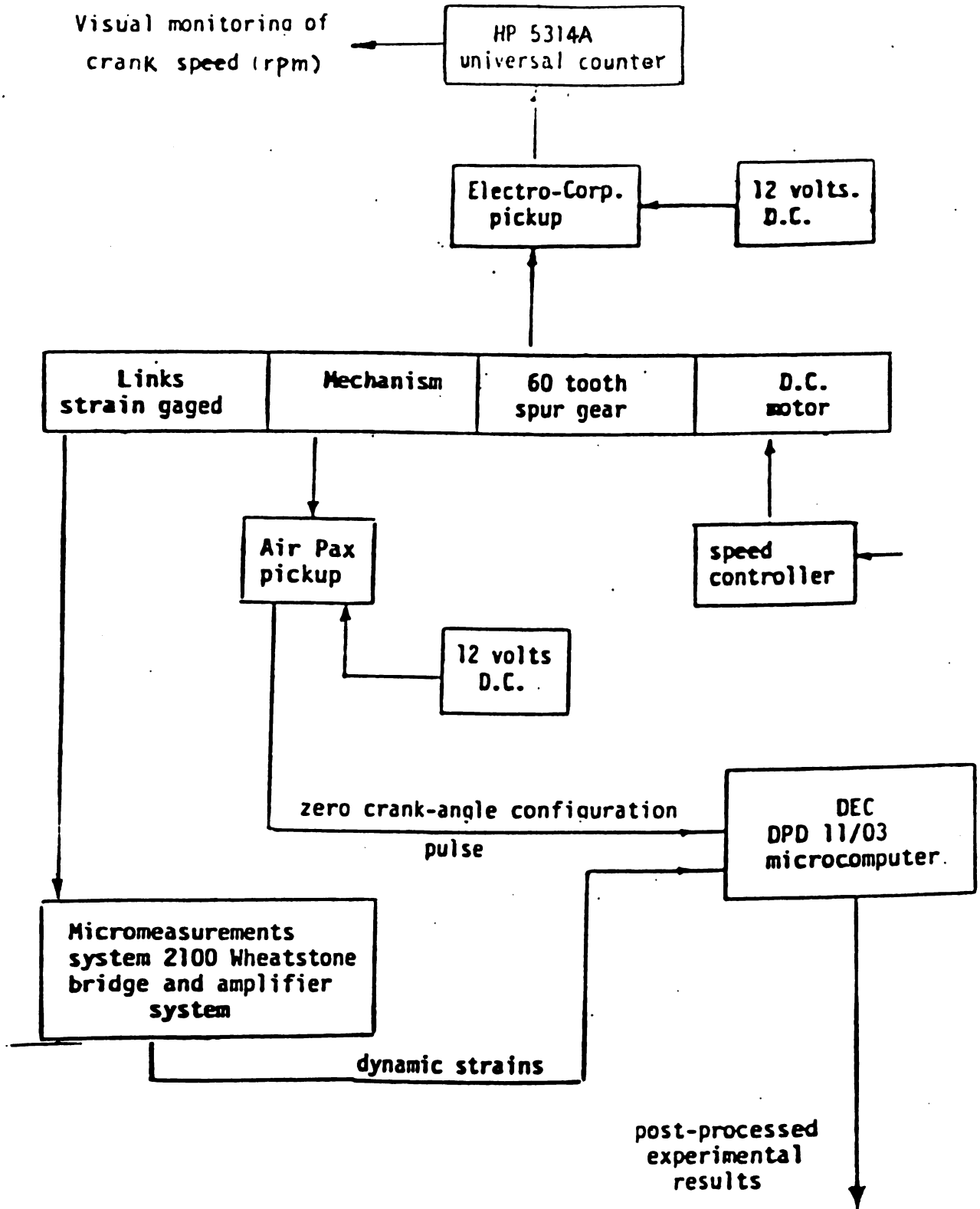


Figure 4-10 Experimental Apparatus Flow Chart.

with crank angle. Strain gages were bonded to the midspans of the coupler and rocker links of the four bar mechanism and shielded cables were used to reduce the effect of electromagnetic fields which can introduce spurious noise into the signals. In fact, noise from electromagnetic fields and other sources, which was superimposed upon the strain gage signals, was considered to be a major signal conditioning problem in this experimental work. A low pass filter was built to eliminate the high frequency noise from the signal and the filter had a variable cut-off frequency.

In order to relate the strain gage signal to the configuration of the experimental mechanism, another transducer arrangement was established. A zero velocity digital pick up, Airpax 14-0001, was located so as to sense the bolt head at the end of the crank when the four-bar-linkage was in the position of zero-degree crank angle.

This mechanism configuration signal and the output from the gages were either fed to the oscilloscope with a C-5C camera attachment for photographically recording the response, or to a digital data acquisition system (a DEC PDP-11/03 microcomputer with 5 Mb hard disk).

The BNC cables from the experimental apparatus were connected to a input-output module. This device had 16 analog-digital channels, 4 digital-analog channels and two schmidt triggers. Using the code developed for digital data acquisition, the flexural response signal was recorded from the zero crank angle position through 360 degrees by fir-

ing on of the schmidt triggers.

Chapter 5

Experimental and Computational Results

The analytical and experimental results are obtained by using the finite element method and the equations were solved by the Newmark method [77]. The $[K_G^e]$ matrix described in the chapter 3 was included in the mechanism model developed for the elastic material. Each flexible link was divided into six elements, and the element at both ends of the link considered as bearing housing made of aluminum that need to input the different material properties and dimensions into the simulations. These analytical results are then compared with experimentally obtained strain data in order to verify the correlation between the analytical and experimental results.

The main assumptions made formulating the computer model for the simulations are

- 1) All bearings were considered frictionless and without clearance.
- 2) Out-of-plane motions were disregarded.
- 3) Only small elastic deformations from the rigid body equilibrium position were assumed.
- 4) Gravitational acceleration was considered to be smaller than the elastodynamic accelerations.

- 5) The crank speed was assumed constant.
- 6) The natural frequency and damping ratios were calculated from experimental work.

In Figure 5-1, it shows the dynamic response of the coupler taken by C-5C camera from T-912 oscilloscope. The material used was a low carbon steel. Figure 5-2 presents a comparison of the dynamic responses of the analytical and experimental investigations. It shows good correlation between the two. The dimensions of the link and other necessary data were listed below.

Link lengths:

Ground 16 inches

Crank 2.25 inches

Coupler 12 inches

Rocker 12 inches

RPM of the mechanism:

342 RPM

Cross sectional area of the flexible links:

Width 0.75 inch (in the plane perpendicular to the mechanism)

Depth 0.055 inch (in the plane of mechanism)

Young's Modulus 30×10^6 psi

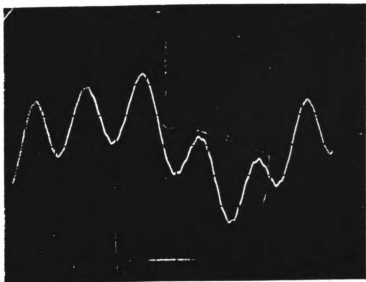


Figure 5-1 Steel Coupler Response Operated at 342 RPM
(Oscilloscope Photograph)

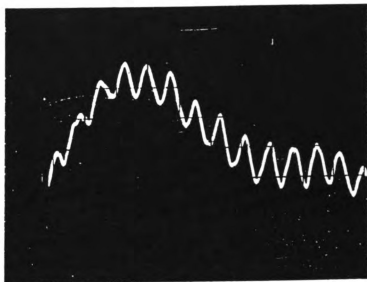


Figure 5-3 45 Composite Coupler Response operated at 280 RPM
(Oscilloscope Photograph)

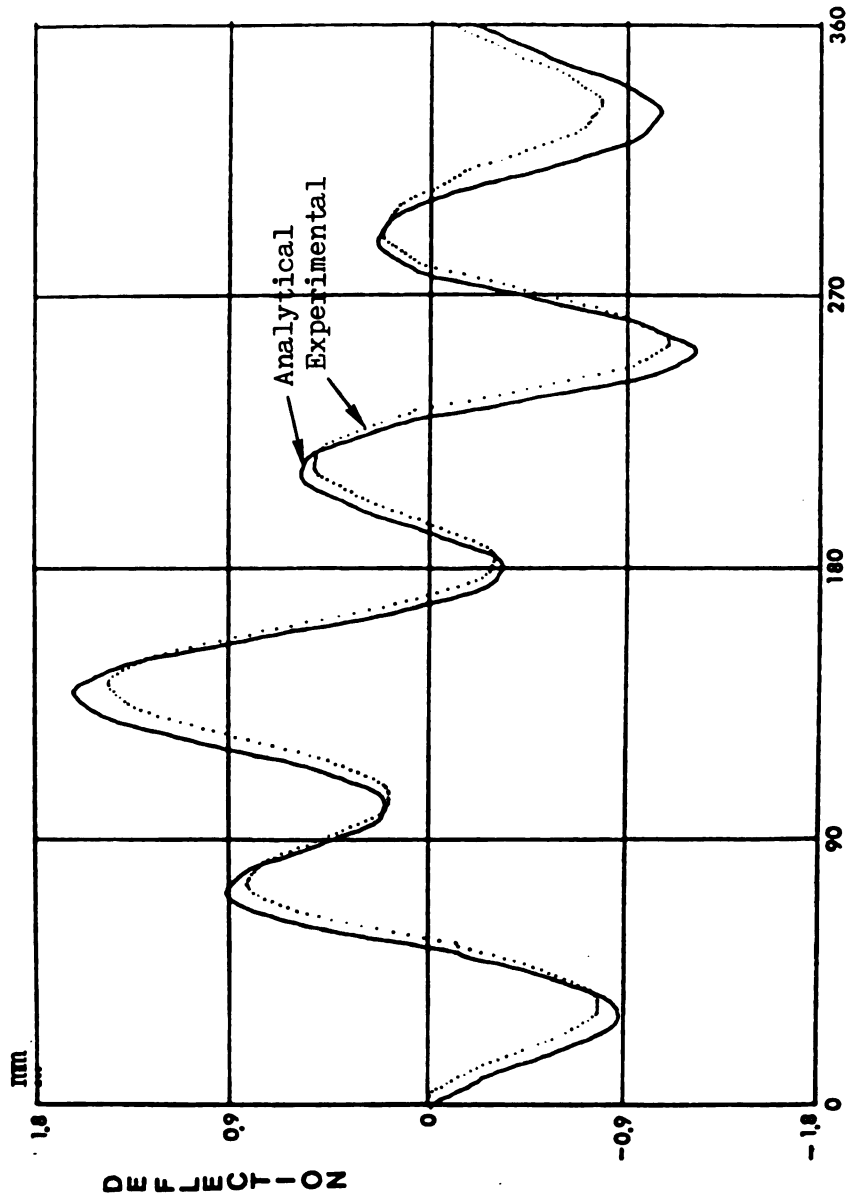


Figure 5-2 Steel Coupler Response at 342 RPM

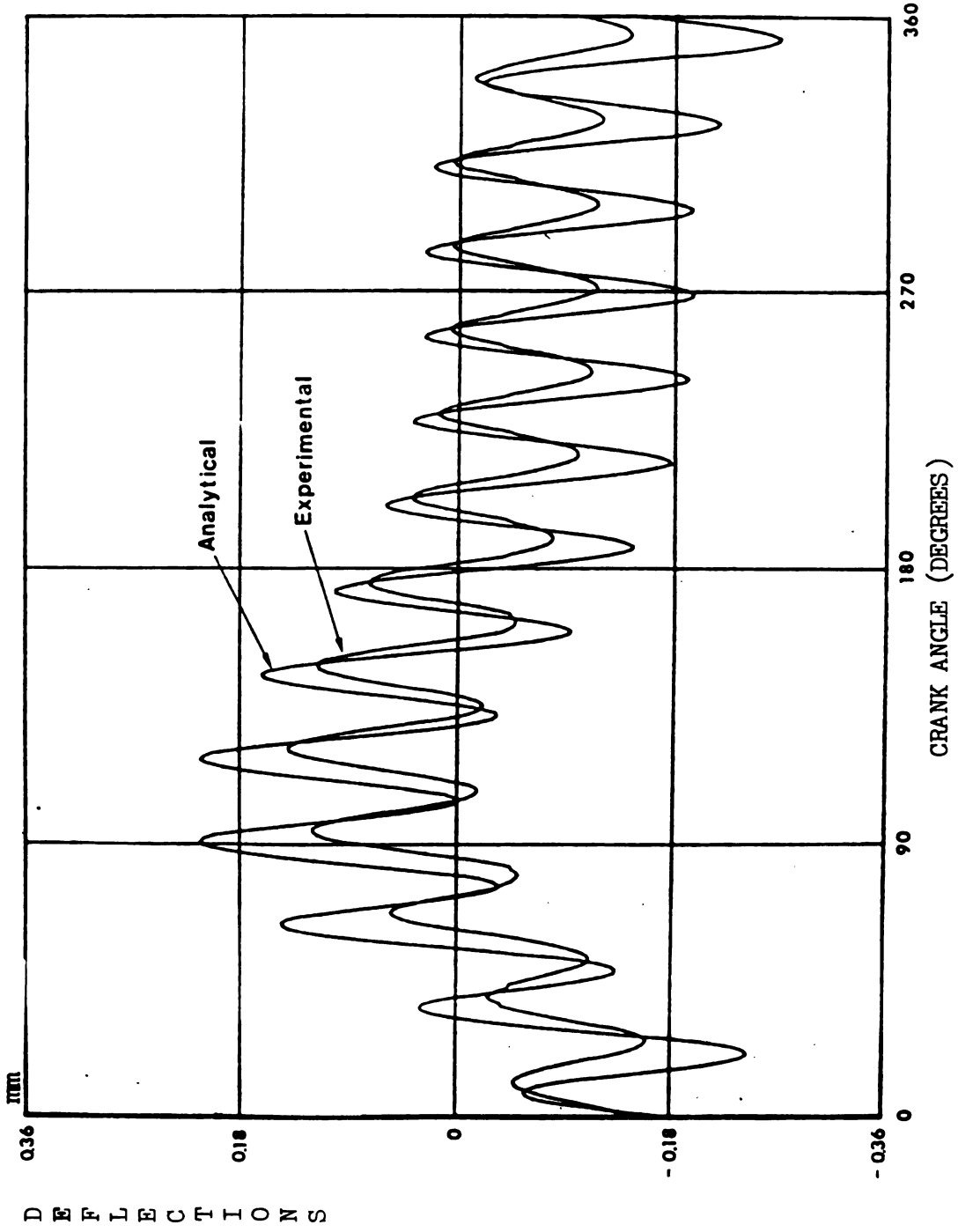


Figure 5-4 45 Degree Composite Coupler Response at 280 RPM

Figure 5-3 is the photograph of the dynamic response for the composite laminate coupler and Figure 4-4 is the comparison of the simulation result and experimental data. The relevant dimensions for the composite mechanism are:

Link lengths:

Ground 12 inches

Rocker 2.25 inches

Coupler 9 inches

Rocker 9 inches

RPM of the Mechanism:

280 RPM

Cross sectional area of the flexible links

Width 0.092 inch (in the plane perpendicular to the mechanism)

Depth 0.045 inch (in the plane of the mechanism)

Young's Modulus 1.38×10^6 psi

Figure 5-5, 5-7 and 5-9 are the responses of the coupler obtained at 205 RPM, 255 RPM and 297 RPM respectively. Figure 5-6, 5-8 and 5-10 are the rocker responses obtained from 205 RPM, 255 RPM and 297 RPM.

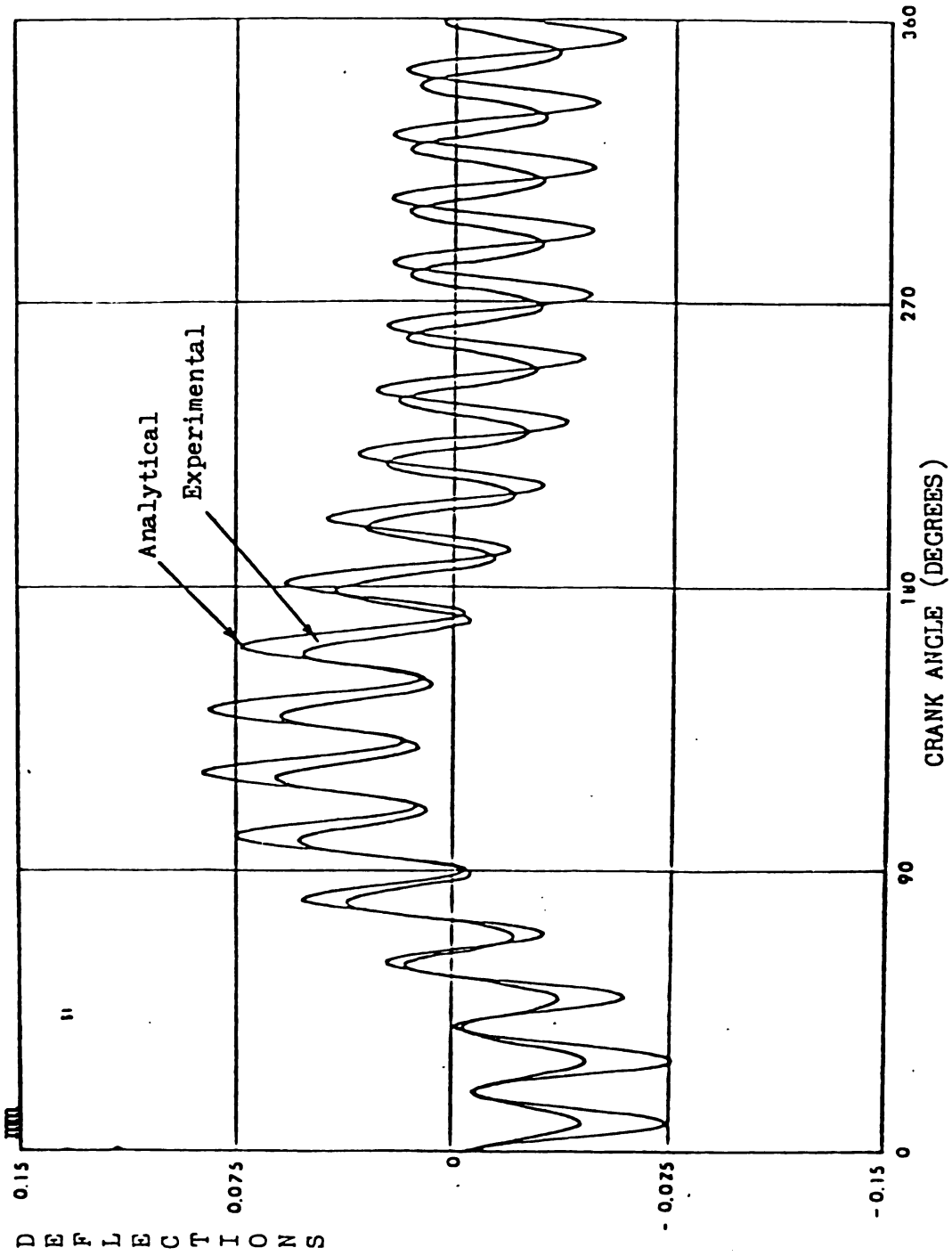


Figure 5-5 45 Composite Coupler Response at 205 RPM

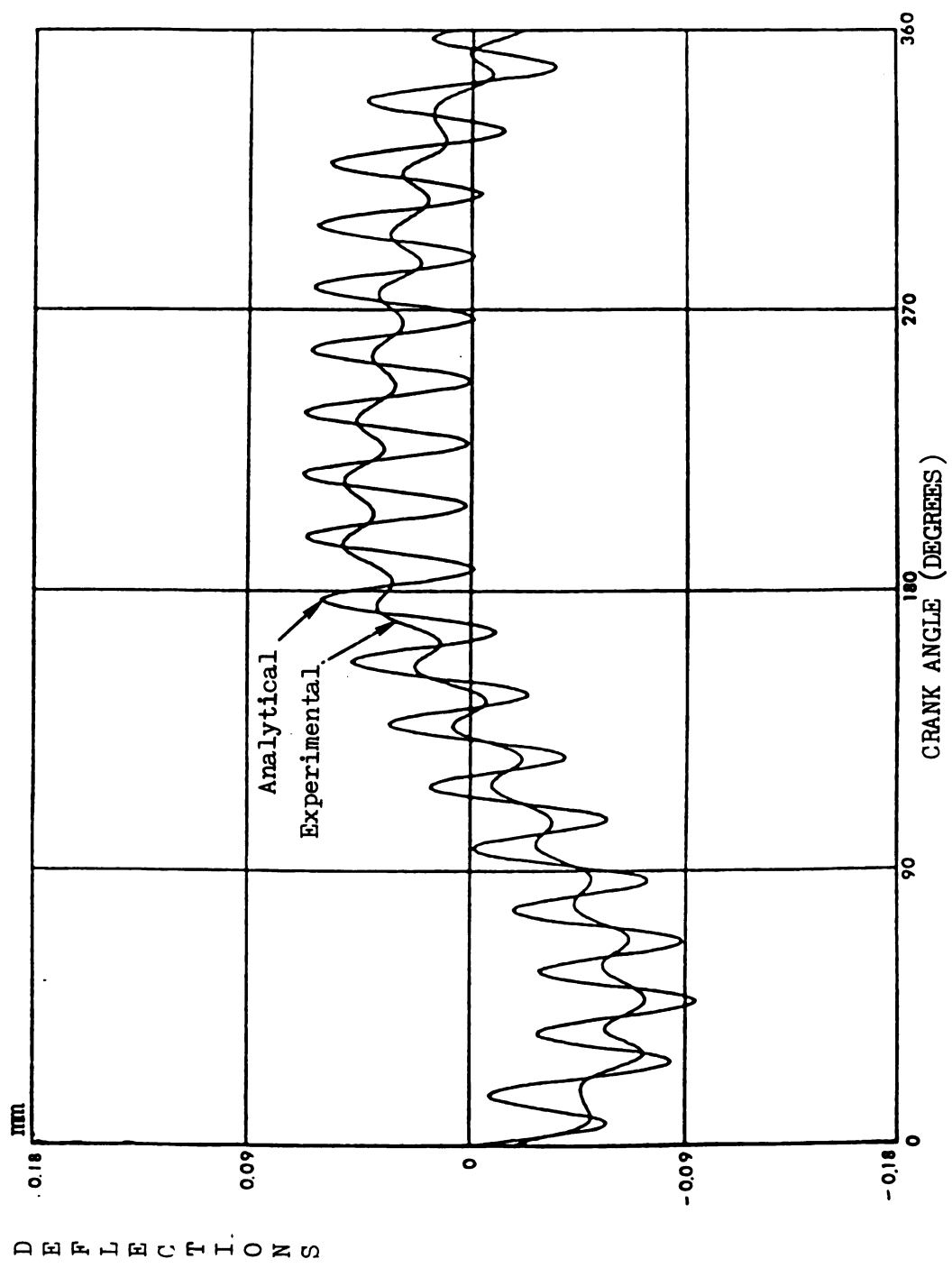


Figure 5-6 45 Degree Composite Rocker Response at 205 RPM

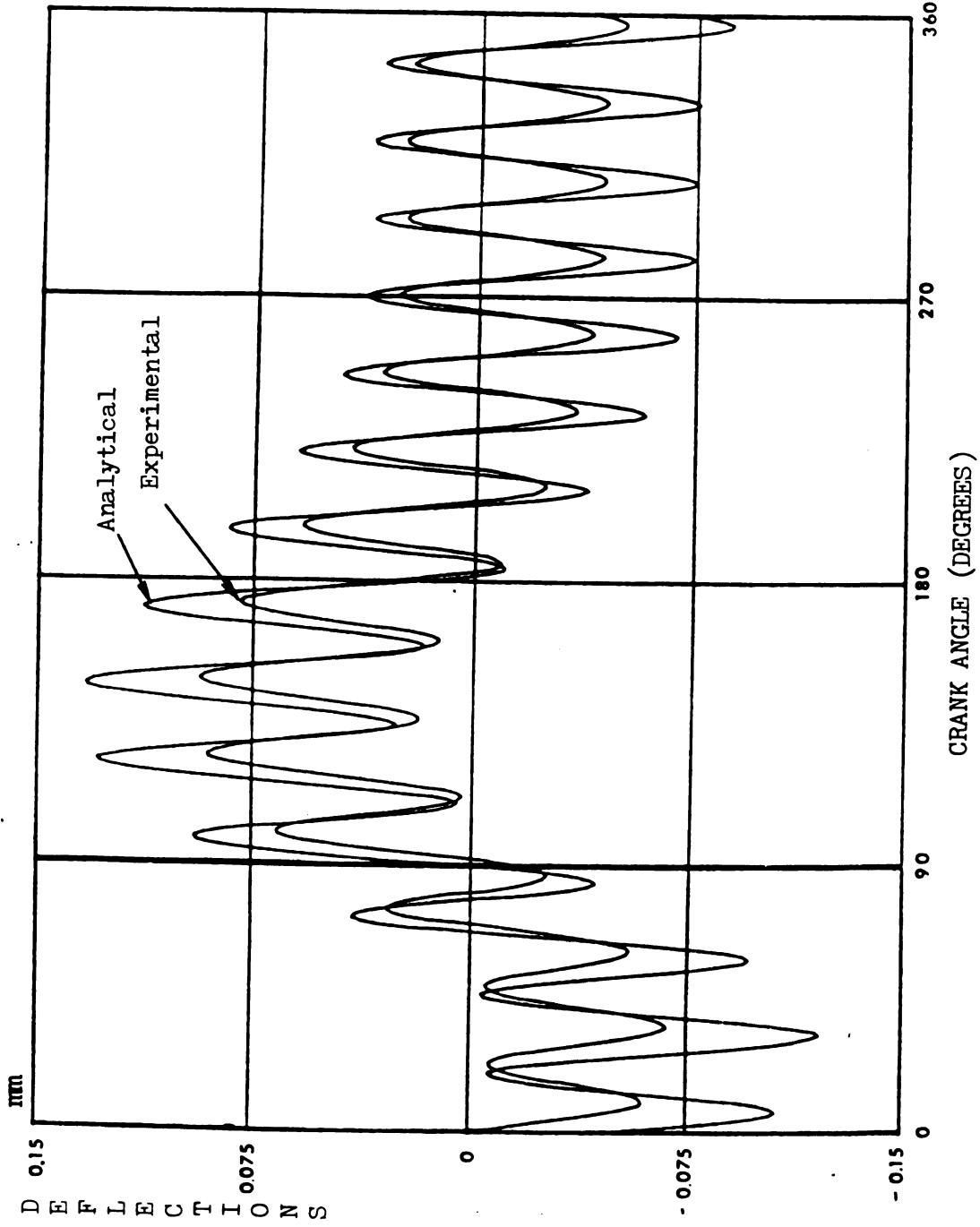


Figure 5-7 45 Degree Composite Coupler Response at 255 RPM

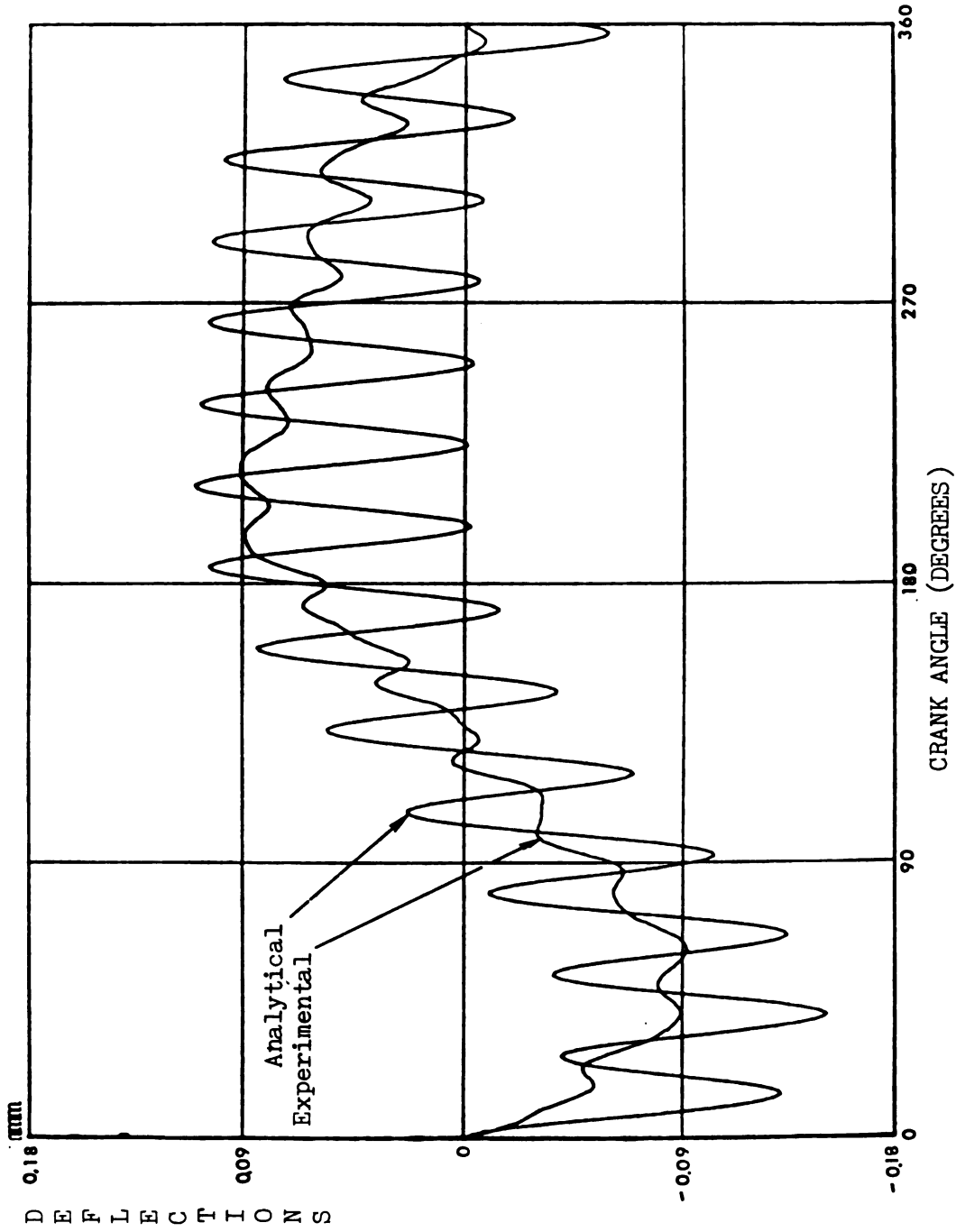


Figure 5-8 45 Degree Composite Rocker Response at 255 RPM

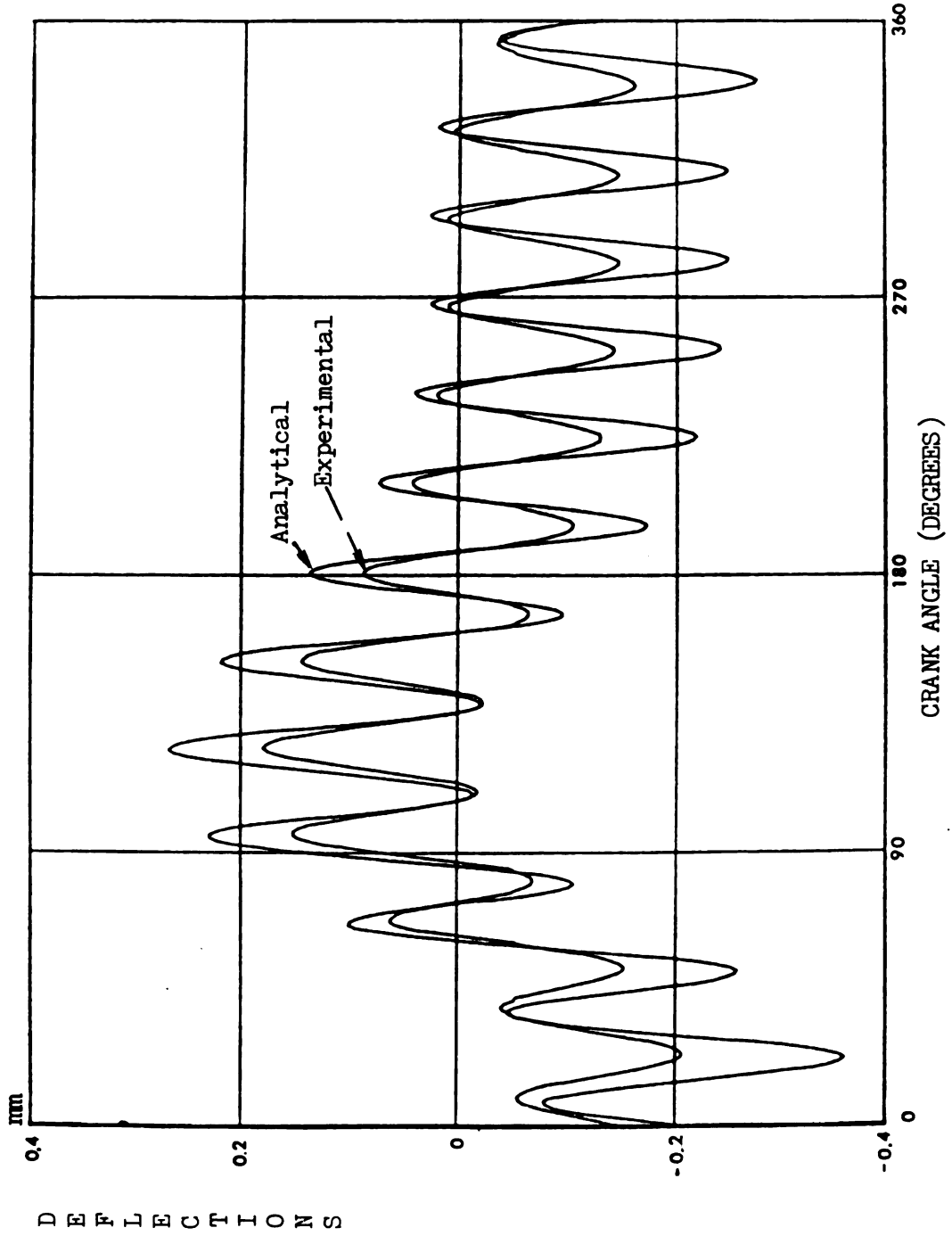


Figure 5-9 . 45 Degree Composite Coupler Response at 297 RPM

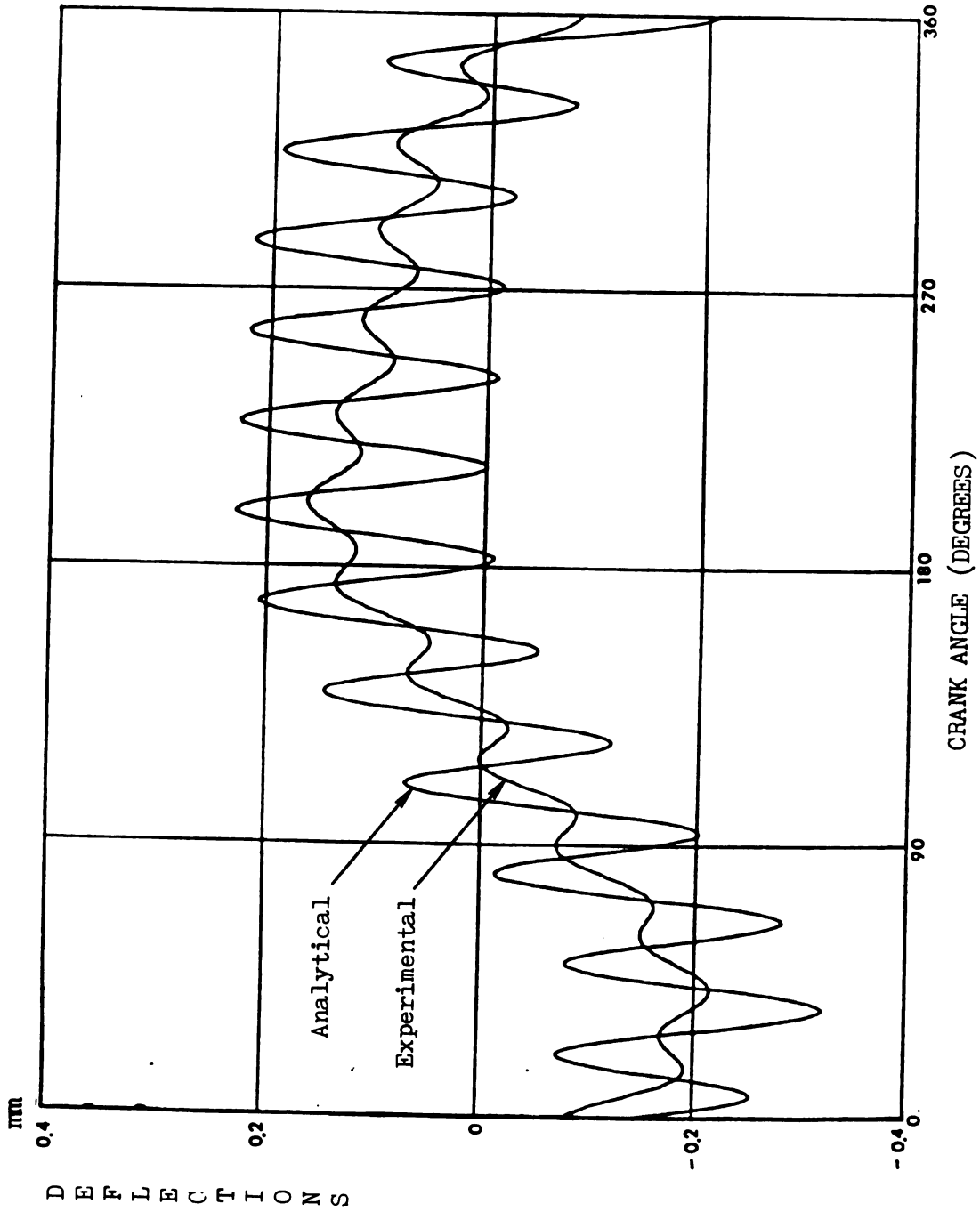


Figure 5-10 45 Degree Composite Rocker Response at 297 RPM

†

Chapter 6

Discussion of Results

Figure 5-2 shows that the correlation between the analytical results and the experimental response are extremely good, thus proving that the variational theorem has been successfully applied and the correct model has been used to formulate the elastic linkages. However, the results for the composite material presented in the previous chapter do not have such a good correlation between the analytical and the experimental responses. The difference in amplitude between the two results at 280 RPM for the coupler is about 0.09 mm, which is an extremely small deflection, as shown in Figure 5-4. All the rocker responses have larger differences between two curves if compared with the coupler. Plausible explanations for the difference in the two classes of waveform will now be discussed.

Firstly, the alignment of the experimental mechanism introduces an error. Since several specimens with different lengths were employed, upon completing each set of tests it was necessary reconstruct the mechanism ; therefore, it was necessary to change the position of the rocker ground joint. Whenever this joint was moved back or forth, the alignment had to be carefully reconfigured. Furthermore, the clearance holes on the specimens for the socket screws will affect the alignment. The alignment can only be improved by considerable care prior to under-

taking the experimental work.

Secondly, the value of the second moment of area of model for the joints in the mathematical representation are only approximate values. The cross section area of the real joints are rather complex, while the cross-section area being used in the simulation are the values of rectangular cross sections. Also, the lengths of the joints used in the simulation are the lengths from the centerline of the bearing to the other end of the joint, these lengths are a little bit shorter than the true lengths of the joints. However, the model of the joint did include the total mass of the joints.

Thirdly, the dynamic responses of the experimental work were often disturbed by unknown sources of electromagnetic noise and the results are not always repeatable. Thus, it was necessary to take several data sets for the same RPM and select the best curve after first eliminating the noise disturbance using the Fast Fourier Transform program FILTER developed in the laboratory. This was developed using FORTRAN and MACRO. Further discussion concerning the stability of the response in the experimental work has been discussed in [51] but is outside the scope of this thesis.

Forthly, the sampling rate of the digital data acquisition may not be high enough to adequately represent the signals being monitored. In the present program, the PDP-11 can pick up one datum in 0.000363467 second; therefore, the curve obtained from PDP-11 were often more than

one revolution. If the experimental result is to be superimposed on the analytical result, judgements, based on the oscilloscope photograph were necessary in order to decide the starting point as well as the ending point of the revolution. Misjudgement of this activity may be resulted in a phase shift.

The technique of calibration is considered to be the most critical reason which resulted in the difference between two response curves. This is because that the results of the calibration govern the magnitude of the experimental results. To do the calibration, a load was applied at the midpoint of the specimen which was configured as a simply supported beam, then recorded the deflection read from the dial gage. At the same time, the response was recorded from the oscilloscope so as to measure the voltage (strain) developed by the gage. The problem here is that the dial gage, must be observed by the operator in addition to recording the oscilloscope deflection and also apply the load on the link. Thus there are too many operations to be performed simultaneously. Two experimentalists, operating in unison improved the accuracy of this procedure, but a more accurate instrument for calibration is considered to be necessary, such as a calibration fixture.

Chapter 7

Conclusions

A variational theorem has been developed and has been shown to provide a variable formulation for the finite element analysis of an experimental linkage fabricated with a viscoelastic material using a three parameter solid model representing the material constitutive equations. Although differences between the experimental and analytical results exist, these are rather small if attention is focused on the quasi-static response. The limitations in predicating the dynamic response are probably due to the first order model of viscoelastic material. As discussed previously, advanced approaches exist and these should probably be adopted a future work. The simulations do, however, provide a conservative prediction for the dynamic response hence this model could be used with confidence in an industrial computer aided design environment for the design of high speed mechanism systems and robotic manipulators.

References

1. Smith, M.R. and Maunder, L., "Inertia Force in a Four Bar Linkage," *Journal of Mechanical Engineering Science*, 1967, Vol. 9, No. 3, pp.218-225.
2. Elliott, J.L. and Tesar, D., "The Theory of Torque Shaking Force, and Shaking Moment Balancing of Four Link Mechanism," *ASME Journal of Engineering for Industry*, 1977, Vol. 99B, pp. 715-721.
3. Orlandea, N., Chace, M.a. and Calahan, D.A., "A Sparsity-Oriented Approach to the Dynamic Analysis and Design of Mechanical Systems-Part 1 and 2," *ASME Journal of Engineering for Industry*, Vol. 99, No. 3, 1977 , pp. 773-779.
4. Chace, M.A. and Smith, D.A., "DAMN, A Digital Computer Program for the Dynamic analysis of Generalized Mechanical System," *SAE Paper 710244*, SAE Annual Meeting, Detroit, Jan. 1971.
5. Sheth, D.N. and Vicker, J.J., "IMP(Intergrated Mechanism Program) A Computer-Aided Design Analysis System for Mechanism and Linkages," *ASME Journal of Engineering for Industry*, Vol.94, 1972, pp. 454-464.

6. Thompson, B.S. and Barr, A.D.S., "A Variational Principle for the Motion of Components of Elastic Mechanisms." 1975, Proceeding of the Fourth World Congress on the Theory of Machines and Mechanism, Newcastle Upon Tyne, U.K., Paper No. 43.

7. Viscomi, B.V. and Ayre, R.S., "Nonlinear Dynamic Response of Elastic Slider-Crank Mechanism," ASME Journal of Engineering for Industry, 1971, Vol. 93B, pp. 251-262.

8. Neubauer, A.H., Cohen, R. and Hall, A.S., "An Analytical Study of the Dynamics of an Elastic Linkage," ASME Journal of Engineering for Industry, 1966, Vol. 88B, pp.311-317.

9. Jasinski, P.W., Lee, H.C. and Sandor, G.N., "Vibrations of Elastic Connecting Rod of a High-Speed Slider-Crank Mechanism," ASME Journal of Engineering for Industry, 1971, Vol.94, pp. 636-644.

10. Sadler, J.P., "On the Analytical Lumped Mass Model of an Elastic Four-Bar Linkage Mechanism," ASME Journal of Engineering for Industry, 1975, Vol. 97B, pp. 561-565.

11. Sadler, J.P. and Sandor, G.N., "A Lumped Parameter Approach to the Vibration and Stress Analysis of Elastic Linkages," ASME Journal of Engineering for Industry, 1973, Vol. 95B, pp. 549-557.

12. Sadler, J.P. and Sandor, G.N., "Nonlinear Vibration Analysis

of Elastic Four-Bar Linkages," ASME Journal of Engineering for Industry, 1974, Vol. 96B, pp. 411-419.

13. Kalaycioglu, S. and Bagci, C., "Determination of the Critical Operating Speeds of Planar Mechanisms by the Finite Element Method Using Planar Actual Line Elements and Lumped Mass Systems," ASME Journal of Mechanical Design, Vol. 101, No. 2, 1979, pp. 210-223.

14. Bagci, C. and Kalaycioglu, S., "Elastodynamics of Planar Mechanisms Using Planar Actual Finite Line Elements, Lumped Mass Systems, Matrix-Exponential Method, and the Method of Critical-Geometry-Kineto- Elasto-Statics," ASME Journal of Mechanical Design, Vol. 101, No.3, 1979, pp. 417-427.

15. Thompson, B.S. and Barr, A.D.S., " Variational Principle for the Elastodynamic Motion of Planar Linkages," ASME Journal of Engineering for Industry, Vol. 98B 1976, pp. 1306-1312.

16. Jandrasits, W.G. and Lowen, G.G., "The Elasto-Dynamic Behavior of a Counter-weighted Rocker Link with an Overhanging Endmass in a Four-bar Linkage. Part I- Theory. Part II - Application and Experiment," ASME Journal of Mechanical Design. Vol. 101, No. 1, 1979, pp. 77-98.

17. Imam, I., Sandor, G.N. and Kramer, S.N., "Deflection and Stress analysis in High Speed Planar Mechanisms with Elastic Links,"

ASME Journal of Engineering for Industry, 1973, Vol. 95B, pp. 541-548.

18. Erdman, A.G., Sandor, G.N. and Oakberg, R.G., "A General Method for Kineto-Elastodynamic Analysis of Mechanisms," ASME Journal of Engineering for Industry, 1972, Vol. 94B, pp. 1193-1205.

19. Midha, A., Erdman, A.G. and Frohrib, D.A., "An Approximate Method for the Dynamic Analysis of Elastic Linkages," ASME Journal of Engineering for Industry, 1977, Vol. 99B, pp. 449-455.

20. Midha, A., Erdman, A.G. and Frohrib, D.A., "A Closed-Form Numerical Algorithm, for the Periodic Response of High-Speed Elastic Linkages," ASME Journal of Mechanical Design, 1979, Vol. 101, No.1, pp. 154-162.

21. Midha, A., Erdman, A.G. and Frohrib, D.A., "A Computationally Efficient Numerical Algorithm for the Transient Response of High Speed Elastic Linkages," ASME Journal of Mechanical Design, 1979, Vol. 101, No. 1, pp. 138-148.

22. Winfrey, R.C., "Elastic Link Mechanisms Dynamics," ASME Journal of Engineering for Industry, 1968, Vol. 91B, pp. 268-272.

23. Bahgat, B.M. and Willmert, K.D., "Finite Element Vibrational Analysis of Planar Mechanisms," Mechanism and Machine Theory, 1976, Vol. 11, pp. 47-71.

24. Thompson, B.S., "A Variational Formulation for the Finite Element Analysis of High-Speed Machinery," ASME Paper No. 80-WA/DSC-38.

25. Allen, R.R., "Dynamics of Mechanisms and Machine Systems in Accelerating Reference Frames," ASME Journal of Dynamic Systems, Measurement, and Control, Vol. 103, 1981, pp. 395-403.

26. Allen, R.R. and Dubowsky, S., "Mechanisms as Components of Dynamic Systems: A Bond Graph Approach," ASME Journal of Engineering for Industry, Vol. 99, No. 1, 1977, pp. 104-111.

27. Karnopp, D. and Margolis, D., "Analysis and Simulation of Planar Mechanism Systems Using Bond Graphs," ASME Journal of Mechanical Design, Vol. 101, No. 2, 1979, pp. 187-191.

28. Tadjbakhsh, I.G., "Stability of Motion of Elastic Planar Linkages with Application to Slider Crank Mechanism," ASME Journal of Mechanical Design, 1981.

29. Sanders, J.R. and Tesar, D., "The Analytical and Experimental Evaluation of Vibratory Oscillations in Relativistically Proportional Mechanisms," ASME Journal of Mechanical Design, vol. 100, No. 3, 1978, pp. 762-768.

30. Yang, A.T., Pennock, G.R. and Hsia, L.M., "Stress Fluctuation in High-Speed Mechanisms," ASME Journal of Mechanical Design, Vol. 103,

No.4, 1981, pp. 736-742.

31. Lowen, G.G. and Jandrasits, W.G., "Survey of Investigation into the Dynamic Behavior of Mechanisms Containing Links with Distributed Mass and Elasticity," *Mechanism and Machine Theory*, Vol. 7, 1972, pp.3-17.

32. Erdman, A.G. and Sandor, G.N., "Kineto-Elasto-Dynamics - A Review of the State-of-Art and Trends," *Mechanism and Machine Theory*, Vol. 7, 1972, pp. 19-33.

33. Imam, I. and Sandor, G.N., "A General Method for Kinetoelastodynamic Design of High-Speed Mechanisms," *Mechanism and Machine Theory*, Vol. 8, No. 4, 1973, pp. 497-516.

34. Imam, I. and Sandor, G.N., "High Speed Mechanism Design - A General Analytical Approach," *Journal of Engineering for Industry*, Trans. ASME, Vol. 97, 1975, pp. 609-628.

35. Khan, M.R., Thornton, W.A. and Willmert, K.D., "Optimality Criterion techniques Applied to Mechanism Design," *Journal of Mechanical Design*, Trans. ASME, Vol. 100, 1978, pp. 319-327.

36. Thornton, W.A., Willmert, K.D. and Khan, M.R., "Mechanism Optimization via Optimality Criterion Techniques," *Journal of Mechanical Design*, Trans. ASME. Vol. 1979, pp. 392-397.

37. Cleghorn, W.L., Fenton, R.G. and Tabarrok, B., "Optimum Design of High Speed Flexible Mechanisms," Mechanism and Machine Theory, Vol. 16, No. 4, 1981, pp. 399-406.

38. Jones, R.M., Mechanics of Composite Materials, McGraw-Hill book Company, 1975.

39. Tsai, S.W., Halpin, J.C. and Pagano, N.J. (eds.), Composite Materials Workshop, Technomac Publishing Company, Sanford, CA, 1968.

40. Christensen, R.M., Mechanics of Composite Materials, Wiley, NY, 1979

41. Sendeckyj, G.P. (Ed.), Mechanics of Composite Materials, Composite Materials Series, Vol. 2, by Broutman, L.J. and Krock, R.M., (Eds.) Academic, 1974.

42. Dietz, A.G.H. (Ed.), Composite Engineering Laminates, Wiley, NY, 1969.

43. Berg, C.A., McGarry, F.J. and Elliott, S.Y. (Coords.), Composite Materials: Testing and Design, Third Conference, March 1973, Williamsburg, VA, American Society for Testing and Materials, STP546.

44. Herrman, G. (Ed.), Dynamics of Structured Solids, ASME Applied Mechanics Division Publication, 1972.

45. Lee, E.H. (Ed.), Dynamics of Composite Materials, ASME Applied Mechanics Division Publication, 1972.

46. Thompson, B.S. and Sung, C.K., "A Variational Formulation for the Nonlinear Finite Element Analysis of Flexible Linkages, Part 1: Theoretical Development," ASME Journal of Mechanisms, Transmissions and Automation in Design, submitted January 1984.

47. Sung, C.K., Xing, T.M., Wang, C.H., Thompson, B.S. and Crowley, P., "A Higher Order Variational Formulation for the Finite Element Analysis of Flexible Linkages, Part II: Application and Experiment," ASME Journal of Mechanisms, Transmissions and Automation in Design, submitted January 1984.

48. Christensen, R.M., Theory of Viscoelasticity: An Introduction, Academic Press, NY, 1971.

49. Gurtin, M.E. and Sternberg, E., "On the Linear Theory of Viscoelasticity," Archives for Rational Mechanics and Analysis, Vol. 11, 1962, pp. 261-356.

50. Leitman, M.J., "Variational Principles in the Linear Dynamic Theory of Viscoelasticity," Quarterly of Applied Mathematics, Vol. 24, 1966, pp. 37-46.

51. Schapery, R.A., "On the Time Dependence of Viscoelastic Varia-

tional Solutions," Quarterly of Applied Mathematics, Vol. 22, 1964, pp. 207-215.

52. Gurtin, M.E., "Variational Principles in the Linear Theory of Viscoelasticity," Archives for Rational Mechanics and Analysis, Vol. 13, 1963, pp. 179-191.

53. Leitman, M.J. and Fisher, G.M.C., "The Linear Theory of Viscoelasticity," in Handvuch der Physik (S. Flugge, Ed.), Vol. 6a/3, Springer Verlag, Berlin, 1973, pp. 1-123.

54. Kline, K.A., "Variational Principles in the Linear Theory of Viscoelastic Media with Microstructure," Quarterly of Applied Mathematics, Vol. 28, NO. 1, 1970, pp. 69-80.

55. Onat, E.T., "On a Variational Principle in Linear Viscoelasticity," Journal of Mdcanique, Vol. I, No. 2, June 1962, pp. 135-140.

56. Christensen, R.M., "Variational and Minimum Theorems for the Linear Theory of Viscoelasticity," Zeitschnift fur Angewandt Mathematik und Physik, Vol. 19, 1968, pp. 233-241.

57. Thompson, B.S. and Sung, C.K., "A Variational Theorem for the Viscoelastodynamic Analysis of High-Speed Machinery Fabricated from Composite Materials," ASME Paper No. 83-DET-6.

58. Zienkiewicz, O.C. and Watson, M., "Some Creep Effects in Stress Analysis with Particular Reference to Concrete Pressure Vessels." Nuclear Engineering and Design, North-Holland Publishing Co., 1966, pp 406-442.

59. Adey, R.A. and Brebbia, C.A., "Efficient Method for Solution of Viscoelastic Problems," Journal of The Engineering Mechanics Division, 1973.

60. Zienkiewicz, O.C., Watson, M. and Kino, I.P., "A Numerical Method of Viscoelastic Stress Analysis," International Journal of Mechanical Science, Vol. 10, 1968, pp 807-827.

61. Midha, A., Erdman, A.G. and Frohrib, D.A., "Finite Element Approach to Mechanical Modeling of High-Speed Elastic Linkages," mechanical and Machine Theory, Vol. 13, 1978, pp 603-618.

62. Gandhi, M.V. and Thompson, B.S., "The Finite Element Analysis of Flexible Components of Mechanical Systems Using a Mixed Variational Principle," ASME Paper No. 80-DET-64.

63. Aoki, S., Fishimoto, K, Izumihara, Y. and Sakata, M., "Dynamic analysis of cracked linear viscoelastic solid by finite element method using singular element," International Journal of Fracture, Vol.16, No.2 April, 1980.

64. Przemieniecki, J.S., Theory of Matrix Structural Analysis, McGraw-Hill, 1971.

65. Flugge, W., Viscoelasticity, Blaisdell Publishing Company, Waltham, MA, 1976.

66. Gross, B., Mathematical Structure of the Theories of Viscoelasticity, Hermann, Paris, 1953.

67. Bland, D.R., The Theory of Linear Viscoelasticity, Pergamon Press, Oxford, 1960.

68. Lockett, F.J., Nonlinear Viscoelastic Solids, Academic Press, London, 1972.

69. Truesdell, C. and Noll, W., in Handbuch der Physik (S. Flugge, Ed.), Vol. 3, NO. 3, Springer Verlag, Berlin, 1965.

70. Malvern, L.E., Introduction to the Mechanics of a Continuous Medium, Prentice-Hall, Englewood Cliffs, 1969.

72. Hashin, Z., "Viscoelastic Fiber Reinforced Materials," AIAA Journal, Vol. 4, No. 8, 1966, pp. 1411-1417. < 5063 92 AS

73. Grot, R.A. and Achenbach, J.D., "Linear Anisothermal Theory for a Viscoelastic Laminated Composite," Acta Mechanica, Vol. 9, 1970,

Appendix

-

```

C*****
C
C      V      V  III  SSSSSSS  CCCCCC  0000000  *
C      V      V  I    S          C      C  0      0  *
C      V      V  I    SSSSSSS  C          0      0  *
C      V V      I      S  C          C  0      0  *
C      V      III  SSSSSSS  CCCCCC  0000000  *
C

```

```

C*****

```

```

C
C      THIS PROGRAM IS DESIGNED TO SEEK THE
C      RESPONSE OF THE FOUR BAR MECHANISM CONSTRUCTED
C      BY VISCOELASTIC COMPOSITE MATERIAL
C

```

```

C      The mechanism have two flexible parts, coupler
C      and rocker. Each flexible link consist of
C      6 elements, the two element at both ends are
C      the joint elements that have different material
C      properties and dimensions as the flexible link.
C      The flexible part equally divided into four
C      element. We are seeking the step-by step
C      solution by using the Newmark intergration
C      method.

```

```

C      (Ref: Bathe,K.J.and Wilson, E.L.," The Numerical*
C      Method in Finite Element Analysis"
C

```

```

C*****

```

```

C
C
C      REAL GG1,GG2,NTA
C      REAL EL1,EL2,G11(36,36)
C      REAL KLI(6,6),Q(36,1),MK(36,36),XG(40,40),KLJ(6,6)
C      REAL G1(36,36),MLI(6,6),KX(40,40),MLJ(6,6)
C      REAL YY(36,1),CC(36,36),OUT(36),WK(37,37),WORK(6,6)
C      REAL RA(36,1),MASS ,P(36,1)
C      REAL U(36),U1(36),U2(36),RCAP(36,36)
C      REAL Y(36,1),B(36,1),F(12)
C      REAL UL(36),QCAP(36),BB(36,1),MR(36,36)
C      REAL AC(40),KI(6,6),KJ(6,6),KN(36,36)
C      REAL KL1(6,6),KL2(6,6),KL3(6,6),KL4(6,6)
C      REAL ML1(6,6),ML2(6,6),ML4(6,6),ML3(6,6)
C      REAL R4(6,6),RT4(6,6),R3(6,6),RT3(6,6)
C      REAL RI,RI1,RI2,RI3,RI4,XLEN1,XLEN2,XLEN3,XLEN4
C      REAL MASS1,MASS2,MASS3,MASS4
C      REAL XKL I(6,6),XKLJ(6,6),XKL1(6,6)
C      REAL XKL2(6,6),XKL3(6,6),XKL4(6,6)
C      REAL XML I(6,6),XMLJ(6,6),XML1(6,6)
C      REAL XML2(6,6),XML3(6,6),XML4(6,6)
C      REAL BB1(1,6),BB2(1,6),BBT1(6,1),BBT2(6,1)

```

```

C
C=====
C

```

```

C      THE DIMENSIONS FOR FINDING THE STRAIN AND STRESS

```



```

C
REAL ALPHA, BETA, DELT, MU, ETA
REAL EBS2(1,1), EBS3(1,1), EBS4(1,1), EBS5(1,1)
REAL EBS8(1,1), EBS9(1,1), EBS10(1,1), EBS11(1,1)
REAL TAW2(1,1), TAW3(1,1), TAW4(1,1), TAW5(1,1)
REAL TAW8(1,1), TAW9(1,1), TAW10(1,1), TAW11(1,1)
C
C THESE ARE THE STRAIN ATRESS AS THE INITIAL FOR NEXT STEP
C
REAL EBSB2(1,1), EBSB3(1,1), EBSB4(1,1), EBSB5(1,1)
REAL EBSB8(1,1), EBSB9(1,1), EBSB10(1,1), EBSB11(1,1)
REAL TAWB2(1,1), TAWB3(1,1), TAWB4(1,1), TAWB5(1,1)
REAL TAWB8(1,1), TAWB9(1,1), TAWB10(1,1), TAWB11(1,1)
C
C=====
C
REAL U2L(6,1), U3L(6,1), U4L(6,1), U5L(6,1)
REAL U8L(6,1), U9L(6,1), U10L(6,1), U11L(6,1)
REAL X2(6,1), X3(6,1), X4(6,1), X5(6,1)
REAL X8(6,1), X9(6,1), X10(6,1), X11(6,1)
REAL XT2(6,1), XT3(6,1), XT4(6,1), XT5(6,1)
REAL XT8(6,1), XT9(6,1), XT10(6,1), XT11(6,1)
REAL G5(36,1)
C
REAL Y2(6,1), Y3(6,1), Y4(6,1), Y5(6,1)
REAL Y8(6,1), Y9(6,1), Y10(6,1), Y11(6,1)
REAL YT2(6,1), YT3(6,1), YT4(6,1), YT5(6,1)
REAL YT8(6,1), YT9(6,1), YT10(6,1), YT11(6,1)
REAL Q2(36,1)
C
REAL ZT2(6,1), ZT3(6,1), ZT4(6,1), ZT5(6,1)
REAL ZT8(6,1), ZT9(6,1), ZT10(6,1), ZT11(6,1)
C=====
OPEN(7, FILE='COM1')
C
C KL LOCAL STIFFNESS MATRIX
C XG GLOBAL STIFFNESS MATRIXAND MASS MATRIX
C WITHOUT B. C.
C G1 GLOBAL STIFFNESS MATRIX INCORPORATING B.C.'S
C ML (1 TO 4) LOCAL MASS MATRIX
C MK GLOBAL MASS MATRIX INCORPORATING B.C.'S
C EL1 ELEMENT LENGTH FOR THE COUPLER
C EL2 ELEMENT LENGTH FOR THE ROCKER
C XLEN (1 TO 4) LENGTHES FOR THE JOINTS
C E YOUNG'S MODULUS OF THE FLEXIBLE PART
C ES YOUNG'S MODULUS OF THE JOINTS
C RHO MASS DENSITY
C U DEFLECTION
C U1 VELOCITY
C U2 ACCELERATION
C=====
C
C IN NEWMARK METHOD.

```

```

C
C      Q      LOAD VECTOR
C      RA     ACC. VALUES FROM FLEX PROGRAM
C      QCAP   THE EFFECTIVE LOAD VECTOR BEFORE USING THE
C             SUBROUTINE 'LEQT1F' AFTERWARDS IT IS THE DYNAMIC
C             DEFLECTIONS DUE TO THE MODE OF OPERATION OF
C             THIS IMSL PACKAGE.
C      G5     ONE OF THE VISCO TERM (CONSIST OF THE STRESS TERM)
C      Q2     ONE OF THE VISCO TERM (CONSIST OF THE STRAIN TERM)
C      UL     THE DYNAMIC DEFLECTIONS IN THE LOCAL FRAME
C      P      THE ACCELERATION VALUES FROM FLEX AFTER THEY
C             ARE CHANGED FROM RA.
C
C=====
C      INPUT THE CONSTANTS IN THE CONSTITUTIVE EQUATION
C=====
      PRINT *, 'THE VALUE OF G1,G2,NTA'
      READ(1,*)GG1,GG2,NTA
      ALPHA=GG2/NTA
      BETA=(GG1+GG2)/NTA
      MU=GG1/2.
      PRINT *, 'ENTER RPM OF THE MECHANISM'
      READ(1,*)RPM
C=====
C      THE LENGTHS OF LINKS
C=====
      L1=12.
      L2=2.5
      L3=9.0
      L4=9.0
C=====
C      THE LENGTH OF EACH JOINT ELEMENT
C=====
      XLEN1=1.5
      XLEN2=1.5
      XLEN3=1.75
      XLEN4=1.5
C=====
C      THE LENGTHS OF THE ELEMENT OF THE FLEXIBLE LINK
C=====
      EL1=(L3-XLEN1-XLEN2)/4.
      EL2=(L4-XLEN3-XLEN4)/4.
C=====
C      MATERIAL PROPERTIES FOR JOINTS ELE.
C=====
      RHO=0.1
      ES=10.3E+6
C=====
C      THE NECESSARY DATA FOR JOINT 1 ( ELE 1 )
C=====
      WID1=0.75
      DEP1=0.75
      A1=WID1*DEP1

```

```

      MASS1=(RHO/384.)*A1
      RI1=(1.0/12.0)*(WID1*DEP1**3)
C=====
C      THE NECESSARY DATA FOR JOINT 2 ( ELE 6)
C=====
      WID2=1.25
      DEP2=0.75
      A2=WID2*DEP2
      MASS2=(RHO/384.)*A2
      RI2=(1.0/12.0)*(WID2*DEP2**3)
C=====
C      THE NECESSARY DATA FOR JOINT 3 ( ELE 12)
C=====
      WID3=1.75
      DEP3=0.27
      A3=WID3*DEP3
      MASS3=(RHO/384.)*A3
      RI3=(1.0/12.0)*(WID3*DEP3**3)
C=====
C      THE NECESSARY DATA FOR JOINT 4 ( ELE 7)
C=====
      WID4=1.25
      DEP4=0.75
      A4=WID4*DEP4
      MASS4=(RHO/384.)*A4
      RI4=(1.0/12.0)*(WID4*DEP4**3)
C=====
C      MATERIAL PROPERTIES OF COMPOSITE(45 DEG)
C=====
      E=1.328E+06
      DEP=0.135
      RHO1=0.06
      WID=1.36
      A=WID*DEP
      MASS=(RHO1/384.)*A
      RI=(1.0/12.0)*(WID*DEP**3)
C=====
C      INITIALIZE THE CRANK ANGLE
C=====
      TH2=0.0
C=====
C      INITIALIZE STRAIN AND STRESS FOR THE FIRST STEP
C=====
      EBS2(1,1)=0.
      EBS3(1,1)=0.
      EBS4(1,1)=0.
      EBS5(1,1)=0.
      EBS8(1,1)=0.
      EBS9(1,1)=0.
      EBS10(1,1)=0.
      EBS11(1,1)=0.
C
      TAW2(1,1)=0.

```

```

TAW3(1,1)=0.
TAW4(1,1)=0.
TAW5(1,1)=0.
TAW8(1,1)=0.
TAW9(1,1)=0.
TAW10(1,1)=0.
TAW11(1,1)=0.
C=====
C      INITIALIZE THE DEFLECTION OF EACH ELEMENT
C      IN LOCAL FRAME THE BETWEEN U_L STANDS
C      FOR THE ELEMENT N
C=====
      U2L(6,1)=0.
      U3L(6,1)=0.
      U4L(6,1)=0.
      U5L(6,1)=0.
      U8L(6,1)=0.
      U9L(6,1)=0.
      U10L(6,1)=0.
      U11L(6,1)=0.
C=====
C      DEFINE TIME STEP AND RPM OF CRANK LINK
C=====
      TH21=RPM*2.0*3.1415927/60.0
      TSTEP=1.0
      STEP=1.0/TSTEP
C=====
C      TO EVALUATE THE CONSTANTS FOR THE NEWARK METHOD
C=====
      PAR=0.5
      AA=0.25
      T=1./(RPM/60.0*360.0*STEP)
      SSO=(1./(AA*T**2))
      SS1=PAR/(AA*T)
      SS2=1./(AA*T)
      SS3=(1./(2.*AA))-1.
      SS4=PAR/AA-1.
      SS5=(T/2.)*(PAR/AA-2.)
      SS6=T*(1.-PAR)
      SS7=PAR*T
C=====
C      TO INITIALIZE U,U1,U2 AND UL AND Q
C=====
      DO 877 I=1,36
      U(I)=0.
      U1(I)=0.
      U2(I)=0.
      UL(I)=0.
      Q(I,1)=0.
877  CONTINUE
      DO 889 I=1,36
      DO 889 J=1,36
889  KN(I,J)=0.

```

```

C=====
C      BUILD UP THE MATRIX WITH SECOND DERIVATIVE
C      OF SHAPE FUNC.
C=====
      CALL SSP(EL1, BBT1, BB1)
      CALL SSP(EL2, BBT2, BB2)
C=====
C      DEFINE LOCAL STIFFNESS _MASS MATRICES
C=====
      CALL LOL(E, A, EL1, RI, MASS, KLI, MLI)
      CALL LOL(E, A, EL2, RI, MASS, KLJ, MLJ)
      CALL LOL(ES, A1, XLEN1, RI1, MASS1, KL1, ML1)
      CALL LOL(ES, A2, XLEN2, RI2, MASS2, KL2, ML2)
      CALL LOL(ES, A3, XLEN3, RI3, MASS3, KL3, ML3)
      CALL LOL(ES, A4, XLEN4, RI4, MASS4, KL4, ML4)
C
C*****
C
C      THIS IS THE START OF THE MAIN LOOP
C
C*****
      DO 765 K=1,360
C=====
C      FIND THE ACCELERATION OF THE LINK
C=====
      CALL KIN(RA, TH2, TH3, TH4, TH21, STEP, XLEN1,
      *        XLEN2, AC, XLEN3, XLEN4, L1, L2, L3, L4)
C=====
C      THE RIGHT HAND SIDE OF THE EQ. OF MOTION
C      IS -MK*P(I), SO THE FOLLOWING STEP IS NECESSARY
C=====
      DO 990 I=1,36
      990 P(I,1)=-RA(I,1)
C
      TT3=TH3
      TT4=TH4
      S3=SIN(TT3)
      C3=COS(TT3)
      S4=SIN(TT4)
      C4=COS(TT4)
C=====
C      BUILD UP TRANSFER MATRICES
C=====
      CALL RMTR(R3, RT3, TT3)
      CALL RMTR(R4, RT4, TT4)
C=====
C      TRANSFER [K] MATRICES TO GLOBAL FRAME
C=====
      CALL MMLT(WORK, KLI, R3, 6, 6, 6)
      CALL MMLT(XKLI, RT3, WORK, 6, 6, 6)
C
      CALL MMLT(WORK, KL1, R3, 6, 6, 6)
      CALL MMLT(XKL1, RT3, WORK, 6, 6, 6)

```

```

C
  CALL MMLT(WORK, KL2, R3, 6, 6, 6)
  CALL MMLT(XKL2, RT3, WORK, 6, 6, 6)
C
  CALL MMLT(WORK, KLJ, R4, 6, 6, 6)
  CALL MMLT(XKLJ, RT4, WORK, 6, 6, 6)
C
C
  CALL MMLT(WORK, KL3, R4, 6, 6, 6)
  CALL MMLT(XKL3, RT4, WORK, 6, 6, 6)
C
  CALL MMLT(WORK, KL4, R4, 6, 6, 6)
  CALL MMLT(XKL4, RT4, WORK, 6, 6, 6)
C=====
C      CONSTRUCT THE GLOBAL STIFFNESS MATRIX
C=====
      CALL GLOLIN(XKLI, XKLJ, XKL1, XKL2, XKL3, XKL4, XG, G1)
C=====
C      TRANSFER [M] MATRICES TO GLOBAL FRAM
C=====
      CALL MMLT(WORK, MLI, R3, 6, 6, 6)
      CALL MMLT(XMLI, RT3, WORK, 6, 6, 6)
C
      CALL MMLT(WORK, ML1, R3, 6, 6, 6)
      CALL MMLT(XML1, RT3, WORK, 6, 6, 6)
C
      CALL MMLT(WORK, ML2, R3, 6, 6, 6)
      CALL MMLT(XML2, RT3, WORK, 6, 6, 6)
C
      CALL MMLT(WORK, MLJ, R4, 6, 6, 6)
      CALL MMLT(XMLJ, RT4, WORK, 6, 6, 6)
C
C
      CALL MMLT(WORK, ML3, R4, 6, 6, 6)
      CALL MMLT(XML3, RT4, WORK, 6, 6, 6)
C
      CALL MMLT(WORK, ML4, R4, 6, 6, 6)
      CALL MMLT(XML4, RT4, WORK, 6, 6, 6)
C=====
C      CONSTRUCT THE GLOBAL MASS MATRIX
C=====
      CALL GLOLIN(XMLI, XMLJ, XML1, XML2, XML3, XML4, XG, MK)
C
      IF(K.EQ.1)GOTO 10007
C
C=====
C      CHANGE THE NOTATION OF THE DEFLECTION FORM
C      SYSTEM TO ELEMENTS
C=====
      DO 201 I=1,6
      J=I+1
201  U2L(I,1)=UL(J)
      DO 2011 I=1,6

```

```

      J=I+4
2011  U3L(I,1)=UL(J)
      DO 2012 I=1,6
      J=I+7
2012  U4L(I,1)=UL(J)
      DO 2013 I=1,6
      J=I+10
2013  U5L(I,1)=UL(J)
      DO 2014 I=1,6
      J=I+20
2014  U8L(I,1)=UL(J)
      DO 2015 I=1,6
      J=I+23
2015  U9L(I,1)=UL(J)
      DO 2016 I=1,6
      J=I+26
2016  U10L(I,1)=UL(J)
      DO 2017 I=1,6
      J=I+29
2017  U11L(I,1)=UL(J)
C=====
C      CALCULATE THE STRAIN OF EACH FLEXIBLE ELE.
C=====
C      THIS IS FOR THE ELEMENTS ON THE COUPLER
C
      CALL MMLT(EBS2, BB1, U2L, 1, 6, 1)
      CALL MMLT(EBS3, BB1, U3L, 1, 6, 1)
      CALL MMLT(EBS4, BB1, U4L, 1, 6, 1)
      CALL MMLT(EBS5, BB1, U5L, 1, 6, 1)
C=====
C      THIS IS FOR THE ELEMENT ON THE ROCKER
C
      CALL MMLT(EBS8, BB2, U8L, 1, 6, 1)
      CALL MMLT(EBS9, BB2, U9L, 1, 6, 1)
      CALL MMLT(EBS10, BB2, U10L, 1, 6, 1)
      CALL MMLT(EBS11, BB2, U11L, 1, 6, 1)
C
C=====
C      CALCULATE STRESS OF EACH FLEXIBLE ELEMENT
C
      CALL STRESS(TAW2, TAWB2, EBSB2, EBS2, ALPHA, BETA, MU)
      CALL STRESS(TAW3, TAWB3, EBSB3, EBS3, ALPHA, BETA, MU)
      CALL STRESS(TAW4, TAWB4, EBSB4, EBS4, ALPHA, BETA, MU)
      CALL STRESS(TAW5, TAWB5, EBSB5, EBS5, ALPHA, BETA, MU)
      CALL STRESS(TAW8, TAWB8, EBSB8, EBS8, ALPHA, BETA, MU)
      CALL STRESS(TAW9, TAWB9, EBSB9, EBS9, ALPHA, BETA, MU)
      CALL STRESS(TAW10, TAWB10, EBSB10, EBS10, ALPHA, BETA, MU)
      CALL STRESS(TAW11, TAWB11, EBSB11, EBS11, ALPHA, BETA, MU)
C=====
C      CALCULATE THE LOAD VECTOR Q=(M)*(P)
C=====
10007      CALL MMLT(Q, MK, P, 36, 36, 1)
C=====

```

DELT=60./RPM/360.
ETA=2*DELT/(2+BETA*DELT)

C=====

C CALCULATE (B)*TAW*A *ETA

C=====

DO 202 I=1,6

X2(I,1)=BBT1(I,1)*TAW2(1,1)*A*ETA

X3(I,1)=BBT1(I,1)*TAW3(1,1)*A*ETA

X4(I,1)=BBT1(I,1)*TAW4(1,1)*A*ETA

X5(I,1)=BBT1(I,1)*TAW5(1,1)*A*ETA

X8(I,1)=BBT2(I,1)*TAW8(1,1)*A*ETA

X9(I,1)=BBT2(I,1)*TAW9(1,1)*A*ETA

X10(I,1)=BBT2(I,1)*TAW10(1,1)*A*ETA

X11(I,1)=BBT2(I,1)*TAW11(1,1)*A*ETA

202 CONTINUE

C=====

C TRANSFER X2....X5, X8....X11 TO GLOBAL FRAME

C=====

CALL MMLT(XT2,RT3,X2,6,6,1)

CALL MMLT(XT3,RT3,X3,6,6,1)

CALL MMLT(XT4,RT3,X4,6,6,1)

CALL MMLT(XT5,RT3,X5,6,6,1)

CALL MMLT(XT8,RT4,X8,6,6,1)

CALL MMLT(XT9,RT4,X9,6,6,1)

CALL MMLT(XT10,RT4,X10,6,6,1)

CALL MMLT(XT11,RT4,X11,6,6,1)

C

C=====

C CALCULATE ONE OF THE VISCO TERM

C=====

CALL GLOS(XT2,XT3,XT4,XT5,XT8,XT9,XT10,XT11,G5)

C=====

C CALCULATE (K)*(U2L.....U11L)

C=====

CALL MMLT(Y2,KLI,U2L,6,6,1)

CALL MMLT(Y3,KLI,U3L,6,6,1)

CALL MMLT(Y4,KLI,U4L,6,6,1)

CALL MMLT(Y5,KLI,U5L,6,6,1)

CALL MMLT(Y8,KLJ,U8L,6,6,1)

CALL MMLT(Y9,KLJ,U9L,6,6,1)

CALL MMLT(Y10,KLJ,U10L,6,6,1)

CALL MMLT(Y11,KLJ,U11L,6,6,1)

C=====

C TRANSFER TO THE GLOBAL FRAME

C=====

CALL MMLT(YT2,RT3,Y2,6,6,1)

CALL MMLT(YT3,RT3,Y3,6,6,1)

CALL MMLT(YT4,RT3,Y4,6,6,1)

CALL MMLT(YT5,RT3,Y5,6,6,1)

CALL MMLT(YT8,RT4,Y8,6,6,1)

CALL MMLT(YT9,RT4,Y9,6,6,1)

CALL MMLT(YT10,RT4,Y10,6,6,1)

CALL MMLT(YT11,RT4,Y11,6,6,1)


```

C=====
C      TIME ALPHA AND ETA
C=====
      DO 203 I=1,6
      ZT2(I,1)=YT2(I,1)*ALPHA*ETA/E
      ZT3(I,1)=YT3(I,1)*ALPHA*ETA/E
      ZT4(I,1)=YT4(I,1)*ALPHA*ETA/E
      ZT5(I,1)=YT5(I,1)*ALPHA*ETA/E
      ZT8(I,1)=YT8(I,1)*ALPHA*ETA/E
      ZT9(I,1)=YT9(I,1)*ALPHA*ETA/E
      ZT10(I,1)=YT10(I,1)*ALPHA*ETA/E
      ZT11(I,1)=YT11(I,1)*ALPHA*ETA/E
203  CONTINUE
C=====
C      ASSEMBLY ONE TERM OF THE VISCO PROPERTIES
C=====
      CALL GLO5(ZT2,ZT3,ZT4,ZT5,ZT8,ZT9,ZT10,ZT11,Q2)
C=====
C      TO CREATE THE TERMS INSIDE THE SECOND BRACKET
C      ON LINE B1 P323 BW
C=====
      DO 890 I=1,36
      890 Y(I,1)=SS0*U(I) +SS2*U1(I) +SS3*U2(I)
C=====
C      TO CREATE THE SECOND TERM ON LINE B1
C      M*(A0*UT+A2*U1T+A3*U2T)
C=====
      CALL MMLT(B,MK,Y,36,36,1)
C=====
C      TO CREATE LINE B1 P232 BW
C      QCAP ETC THE EFFECTIVE LOAD
C=====
      DO 894 I=1,36
894  QCAP(I)=Q(I,1)+B(I,1)+G5(I,1)-Q2(I,1)
C=====
C      TO CREATE THE EFFECTIVE STIFFNESS MATRIX
C      LINE A4 P232 BW
C=====
      DO 888 I=1,36
      DO 888 J=1,36
888  RCAP(I,J)=G11(I,J)+SS0*MK(I,J)+SS1*CC(I,J)
C=====
C      TO SOLVE THE LINEAR EQUATIONS BY GAUSS ELIMINATION.
C=====
      CALL LINEQ(OUT,QCAP,RCAP,WK,36,37,IERR)
C=====
C      TO CREATE LINES B3 AND LINES B4 P232 BW
C=====
      DO 896 I=1,36
      UD=U(I)
      UV=U1(I)
      UA=U2(I)
      U(I)=OUT(I)

```

```

      U2(I)=SS0*(U(I)-UD)-SS2*UV-SS3*UA
      U1(I)=UV+SS6*UA+SS7*U2(I)
896  CONTINUE
C=====
C    TREAT STRAIN AND STRESS AS THE INITIAL OF NEXT STEP
C=====
      ESB2(1,1)=EBS2(1,1)
      TAWB2(1,1)=TAW2(1,1)
      ESB3(1,1)=EBS3(1,1)
      TAWB3(1,1)=TAW3(1,1)
      ESB4(1,1)=EBS4(1,1)
      TAWB4(1,1)=TAW4(1,1)
      ESB5(1,1)=EBS5(1,1)
      TAWB5(1,1)=TAW5(1,1)
      ESB8(1,1)=EBS8(1,1)
      TAWB8(1,1)=TAW8(1,1)
      ESB9(1,1)=EBS9(1,1)
      TAWB9(1,1)=TAW9(1,1)
      ESB10(1,1)=EBS10(1,1)
      TAWB10(1,1)=TAW10(1,1)
      ESB11(1,1)=EBS11(1,1)
      TAWB11(1,1)=TAW11(1,1)
C=====
C    TO DEFINE THE DYNAMIC DEFLECTIONS IN THE
C    LOCAL FRAMES
C=====
      DO 100 I=2,17,3
        J=I+1
100    UL(I)=OUT(I)*C3+OUT(J)*S3
C
      DO 200 I=3,18,3
        J=I-1
200    UL(I)=-OUT(J)*S3+OUT(I)*C3
C
      DO 300 I=21,33,3
        J=I+1
300    UL(I)=OUT(I)*C4+OUT(J)*S4
C
      DO 400 I=22,34,3
        J=I-1
400    UL(I)=-OUT(J)*S4+OUT(I)*C4
C
      DO 500 I=1,19,3
500    UL(I)=OUT(I)
      DO 600 I=20,35,3
600    UL(I)=OUT(I)
      UL(36)=OUT(17)*C4+OUT(18)*S4
C
      RK11=(K-1)/1.0
C=====
C    THIS IS FOR THE PLOTTING , IT
C    GIVES THE CRANK ANGLE.
C    UL(9)  DEFORMATION AT MIDPOINT OF COUPLER

```

```
C          UL(28) DEFORMATION AT MIDPOINT OF ROCKER
C=====
      WRITE(1,153)RK11,UL(9),UL(28)
765  CONTINUE
153  FORMAT(F14.8,1X,F14.10)
      CLOSE(7,STATUS='KEEP')
      STOP
      END
.jμ.fμ.s 2
```

```

C*****
C
C      EEEEEEE L          A      SSSSSSS TTTTTTT 000000      *
C      E       L          A  A  S          T      0    0      *
C      EEEEEEE L          A  A  SSSSSSS T          0    0      *
C      E       L          AAAAAA          S      T      0    0      *
C      EEEEEEE LLLLLLL A  A  SSSSSSS T          000000      *
C
C*****
C
C      This program is designed to seek the dynamic response      *
c      of the elastic four bar mechanism, the material            *
c      properties and the link length are changable.              *
C
C*****
      REAL EL1,EL2
      REAL KLI(6,6),Q(36,1),MK(36,36),KLJ(6,6)
      REAL G1(36,36),MLI(6,6),MLJ(6,6)
      REAL YY(36,1),CC(36,36),OUT(36),WK(37,37),WORK(6,6)
      REAL RA(36,1),MASS ,P(36,1)
      REAL U(36),U1(36),U2(36),RCAP(36,36)
      REAL Y(36,1),B(36,1),F(12)
      REAL UL(36),QCAP(36),BB(36,1),MR(36,36)
      REAL KN(36,36),KG1(6,6),KG2(6,6),KG3(6,6),KG4(6,6),KI(6,6),KJ(6,6)
      REAL KG5(6,6),KG6(6,6),KG7(6,6),KG8(6,6),KG9(6,6),AC(40)
      REAL KG10(6,6),KG11(6,6),KG12(6,6)
      REAL KGI(6,6),KGJ(6,6),KGM(6,6),K GK(6,6)
      REAL KS(36,36),KL1(6,6),KL2(6,6),KL3(6,6),KL4(6,6)
      REAL AST(2),ML1(6,6),ML2(6,6),ML4(6,6),ML3(6,6),R3(6,6),RT3(6,6)
      REAL R4(6,6),RT4(6,6)
      REAL RI,RI1,RI2,RI3,RI4,XLEN1,XLEN2,XLEN3,XLEN4
      REAL MASS1,MASS2,MASS3,MASS4
      REAL XKLI(6,6),XKLJ(6,6),XKL1(6,6),XKL2(6,6),XKL3(6,6),XKL4(6,6)
      REAL XMLI(6,6),XMLJ(6,6),XML1(6,6),XML2(6,6),XML3(6,6),XML4(6,6)
      REAL KM1(6,6),KM2(6,6),KM3(6,6),KM4(6,6),KM5(6,6),KM6(6,6)
      REAL KM7(6,6),KM8(6,6),KM9(6,6),KM10(6,6),KM11(6,6),KM12(6,6)
C*****
C      KL          LOCAL STIFFNESS MATRIX
C      XG          GLOBAL STIFFNESS MATRIXAND MASS MATRIX WITHOUT B. C.
C      G1          GLOBAL STIFFNESS MATRIX INCORPORATING B.C.'S
C      ML          (1 TO 4) LOCAL MASS MATRIX
C      MK          GLOBAL MASS MATRIX INCORPORATING B.C.'S
C      EL          ELEMENTLENGTH FOR THE LINKAGE (COUPLER AND ROCKER)
C      XLEN        (1 TO 4) LENGTH FOR THE JOINT
C      E           YOUNGS MODULUS FOR THE LINK DESIRED
C      EJ          YOUNGS MODULUS FOR THE JOINTS
C      RHO         MASS DENSITY
C      U           DEFLECTION
C      U1          VELOCITY
C      U2          ACCELERATION
C*****
C      IN NEWMARK METHOD.
C*****

```

```

C      Q      LOAD VECTOR
C      RA      ACC. VALUES FROM FLEX PROGRAM
C      QCAP     IS THE EFFECTIVE LOAD VECTOR BEFORE USING THE
C              SUBROUTINE 'LEQTI1F' AFTERWARDS IT IS THE DYNAMIC
C              DEFLECTIONS DUE TO THE MODE OF OPERATION OF
C              THIS IMSL PACKAGE.
C      UL      ARE THE DYNAMIC DEFLECTIONS IN THE LOCAL FRAME
C      P      IS THE ACCELERATION VALUES FROM FLEX AFTER THEY
C              ARE CHANGED FROM RA.
C-----
C      INPUT THE LINK LENGTH DESIRED
C-----
      PRINT *, 'WHAT KIND OF LINK LENGTH DO YOU WANT'
      PRINT *, 'ENTER 1 FOR LONG LINKS'
      PRINT *, 'ENTER 2 FOR SHORT LINKS'
      READ(1,*)XLL
      IF(XLL.EQ.1)THEN
        GOTO 1
      ELSE IF(XLL.EQ.2) THEN
        GO TO 2
      ELSE
        GOTO 3
      ENDIF
C-----
C      THE LENGTHES OF THE LONG LINKS
1      L1=16.12
      L2=2.25
      L3=12.0
      L4=12.
C-----
C      THE LENGTHES OF THE SHORT LINKS
2      L1=12.
      L2=2.25
      L3=9.
      L4=9.
3      CONTINUE
C-----
C      DECIDE WHAT KIND OF MATERIAL YOU WANT
C-----
      PRINT *, 'WHAT KIND OF MATERIAL YOU WANT!'
      PRINT *, ' 1,  STEEL'
      PRINT *, ' 2,  ALUMINUM'
      PRINT *, ' 3,  UNICOMPOSTE'
      READ (1,*)XMAT
      IF(XMAT.EQ.1)THEN
        GO TO 11
      ELSEIF(XMAT.EQ.2)THEN
        GO TO 12
      ELSE IF(XMAT.EQ.3)THEN
        GO TO 13
      ELSE
        GO TO 14
      END IF

```

C=====

C DEFINE THE MATERIAL PROPERTIES

C=====

C MATERIAL PROPERTIES FOR ALUMINUM

12 E=10.3E+06
 WID=0.58
 DEP=0.0795
 A=WID*DEP
 RHO=0.100
 DR=0.0048
 XF=60.
 BELTA=2.0*DR*XF
 OPEN(7,FILE='A')
 GO TO 14

C=====

C MATERIAL PROPERTIES FOR STEEL

11 E=30.0E+06
 WID=0.75
 DEP=0.062
 RHO=0.3
 A=WID*DEP
 DR=0.01
 XF=31.1
 BELTA=2.0*DR*XF
 OPEN(7,FILE='ST')
 GO TO 14

C=====

C MATERIAL PROPERTIES FOR UNIDIRECTIONAL COMPOSITE

13 E=20.5E+6
 RHO=0.06
 WID=0.75
 DEP=0.08
 A=WID*DEP
 DR=0.00984
 XF=100.0
 BELTA=2.0*DR*0.01/XF
 OPEN(7,FILE='UNIC')
 GO TO 14

14 CONTINUE

C=====

C THE LENGTH OF EACH JOINT ELEMENT

EJ=10.3E+6
 RHOJ=0.1
 XLEN1=1.5
 XLEN2=1.5
 XLEN3=1.75
 XLEN4=1.5

C=====

C THE LENGTH OF THE FLEXIBLE ELEMENT

EL1=(L3-XLEN1-XLEN2)/4.
 EL2=(L4-XLEN3-XLEN4)/4.

C=====

C THE DIMENSIONS FOR JOINT 1 (ELE 1)

```

WID1=0.75
DEP1=0.75
A1=WID1*DEP1
MASS1=(RHOJ/384.)*A1
RI1=(1.0/12.0)*(WID1*DEP1**3)
C=====
C   THE DIMENSIONS FOR JOINT 2 ( ELE 6 )
WID2=1.25
DEP2=0.75
A2=WID2*DEP2
MASS2=(RHOJ/384.)*A2
RI2=(1.0/12.0)*(WID2*DEP2**3)
C=====
C   THE DIMENSIONS FOR JOINT 3 ( ELE 12 )
WID3=1.75
DEP3=0.27
A3=WID3*DEP3
MASS3=(RHOJ/384.)*A3
RI3=(1.0/12.0)*(WID3*DEP3**3)
C=====
C   THE DIMENSIONS FOR JOINT 4 ( ELE 7 )
WID4=1.25
DEP4=0.75
A4=WID4*DEP4
MASS4=(RHOJ/384.)*A4
RI4=(1.0/12.0)*(WID4*DEP4**3)
C=====
MASS=(RHO/384.) *A
RI=(1.0/12.0)*(WID*DEP**3)
C=====
C   INITIALIZE THE CRANK ANGLE
TH2=0.0
C=====
C   DEFINE TIME STEP AND RPM OF CRANK LINK
RPM=340.0
TH21=RPM*2.0*3.1415927/60.0
STEP=1.0
TSTEP=1.0/STEP
C=====
C   TO EVALUATE THE CONSTANTS FOR THE NEWARK METHOD
PAR=0.5
AA=0.25
T=1./(RPM/60.0*360.0*STEP)
SS0=(1./(AA*T**2))
SS1=PAR/(AA*T)
SS2=1./(AA*T)
SS3=(1./(2.*AA))-1.
SS4=PAR/AA-1.
SS5=(T/2.)*(PAR/AA-2.)
SS6=T*(1.-PAR)
SS7=PAR*T
C=====
C   TO INITIALIZE U,U1,U2 AND UL AND Q

```

```

DO 887 I=1,36
  U(I) =0.0
  U1(I)=0.0
  U2(I)=0.0
  UL(I)=0.0
  Q(I,1)=0.0
887  CONTINUE
      DO 889 I=1,36
      DO 889 J=1,36
889  KN(I,J)=0.
C=====
C   DEFINE LOCAL STIFFNESS _MASS MATRICES
      CALL LOL(E,A,EL1,RI,MASS,KLI,MLI)
      CALL LOL(E,A,EL2,RI,MASS,KLJ,MLJ)
      CALL LOL(EJ,A1,XLEN1,RI1,MASS1,KL1,ML1)
      CALL LOL(EJ,A2,XLEN2,RI2,MASS2,KL2,ML2)
      CALL LOL(EJ,A3,XLEN3,RI3,MASS3,KL3,ML3)
      CALL LOL(EJ,A4,XLEN4,RI4,MASS4,KL4,ML4)
C*****
C   THIS IS THE START OF THE MAIN LOOP          *
C*****
C   CALCULATE THE ACCELERATION OF THE LINKS
      DO 765 K=1,360
      CALL KIN1(RA,TH2,TH3,TH4,TH21,STEP,XLEN1,XLEN2
      *          ,AC,XLEN3,XLEN4,L1,L2,L3,L4)
C=====
      DO 990 I=1,36
      990 P(I,1)=-RA(I,1)
C   THIS IS NECESSARY BECAUSE THE R.H.S. OF
C   THE EQ. OF MOTION IS -MK*P(I)
C=====
      TT3=TH3
      TT4=TH4
      S3=SIN(TT3)
      C3=COS(TT3)
      S4=SIN(TT4)
      C4=COS(TT4)
C=====
C   BUILD UP TRANSFER MATRICES
      CALL RMTR(R3,RT3,TT3)
      CALL RMTR(R4,RT4,TT4)
C=====
C   TRANSFER [K] MATRICES TO GLOBAL FRAME
      CALL MMLT(WORK,KLI,R3,6,6,6)
      CALL MMLT(XKLI,RT3,WORK,6,6,6)
      CALL MMLT(WORK,KL1,R3,6,6,6)
      CALL MMLT(XKL1,RT3,WORK,6,6,6)
      CALL MMLT(WORK,KL2,R3,6,6,6)
      CALL MMLT(XKL2,RT3,WORK,6,6,6)
      CALL MMLT(WORK,KLJ,R4,6,6,6)
      CALL MMLT(XKLJ,RT4,WORK,6,6,6)
      CALL MMLT(WORK,KL3,R4,6,6,6)
      CALL MMLT(XKL3,RT4,WORK,6,6,6)

```



```

CALL MMLT(WORK, KL4, R4, 6, 6, 6)
CALL MMLT(XKL4, RT4, WORK, 6, 6, 6)
CALL GLOLIN(XKLI, XKLJ, XKL1, XKL2, XKL3, XKL4, XG, G1)

```

```

C=====

```

```

C   TRANSFER [M] MATRICES TO GLOBAL FRAM
CALL MMLT(WORK, MLI, R3, 6, 6, 6)
CALL MMLT(XMLI, RT3, WORK, 6, 6, 6)
CALL MMLT(WORK, ML1, R3, 6, 6, 6)
CALL MMLT(XML1, RT3, WORK, 6, 6, 6)
CALL MMLT(WORK, ML2, R3, 6, 6, 6)
CALL MMLT(XML2, RT3, WORK, 6, 6, 6)
CALL MMLT(WORK, MLJ, R4, 6, 6, 6)
CALL MMLT(XMLJ, RT4, WORK, 6, 6, 6)
CALL MMLT(WORK, ML3, R4, 6, 6, 6)
CALL MMLT(XML3, RT4, WORK, 6, 6, 6)
CALL MMLT(WORK, ML4, R4, 6, 6, 6)
CALL MMLT(XML4, RT4, WORK, 6, 6, 6)
CALL GLOLIN(XMLI, XMLJ, XML1, XML2, XML3, XML4, XG, MK)

```

```

C=====

```

```

IF(K.EQ.1) GOTO 10007

```

```

C=====

```

```

C   DEFINE LOCAL NONLINER MATRICES FOR EACH KIND OF ELE
CALL LONON(E, A, UR, EL1, UL, KI)
CALL LONON(E, A, UR, EL2, UL, KJ)
CALL LONON(EJ, A1, UR, XLEN1, UL, KGI)
CALL LONON(EJ, A2, UR, XLEN2, UL, KGJ)
CALL LONON(EJ, A3, UR, XLEN3, UL, KGK)
CALL LONON(EJ, A4, UR, XLEN4, UL, KGM)

```

```

C=====

```

```

C   CALCULATE KG FOR EVERY ELEMENT
CON1=E*A/EL1
F(1)=EJ*A1/XLEN1*UL(2)
DO 101 I=2,5
DO 101 J=2,11,3
KK=J+3
F(I)=CON1*(UL(KK)-UL(J))
101  CONTINUE
F(6)=EJ*A2/XLEN2*(UL(17)-UL(14))
F(7)=EJ*A4/XLEN4*UL(21)
CON2=E*A/EL2
DO 102 I=8,11
DO 102 J=24,33,3
M=J-3
F(I)=CON2*(UL(J)-UL(M))
102  CONTINUE
F(12)=EJ*A3/XLEN3*(UL(36)-UL(33))
DO 832 I=1,6
DO 832 J=1,6
KG1(I, J)=F(1)/XLEN1*KGI(I, J)
KG2(I, J)=F(2)/EL1*KI(I, J)
KG3(I, J)=F(3)/EL1*KI(I, J)
KG4(I, J)=F(4)/EL1*KI(I, J)
KG5(I, J)=F(5)/EL1*KI(I, J)

```

```

KG6(I,J)=F(6)/XLEN2*KGJ(I,J)
KG7(I,J)=F(7)/XLEN4*KGM(I,J)
KG8(I,J)=F(8)/EL2*KJ(I,J)
KG9(I,J)=F(9)/EL2*KJ(I,J)
KG10(I,J)=F(10)/EL2*KJ(I,J)
KG11(I,J)=F(11)/EL2*KJ(I,J)
KG12(I,J)=F(12)/XLEN3*KGK(I,J)

```

```
832  CONTINUE
```

```
C
```

```
C=====
```

```
C
```

```
C
```

```
TRANSFER KG TO THE GLOBAL FRAME
```

```
C
```

```
CALL MMLT(WORK,KG1,R3,6,6,6)
CALL MMLT(KM1,RT3,WORK,6,6,6)
```

```
C
```

```
CALL MMLT(WORK,KG2,R3,6,6,6)
CALL MMLT(KM2,RT3,WORK,6,6,6)
```

```
C
```

```
CALL MMLT(WORK,KG3,R3,6,6,6)
CALL MMLT(KM3,RT3,WORK,6,6,6)
```

```
C
```

```
CALL MMLT(WORK,KG4,R3,6,6,6)
CALL MMLT(KM4,RT3,WORK,6,6,6)
```

```
C
```

```
CALL MMLT(WORK,KG5,R3,6,6,6)
CALL MMLT(KM5,RT3,WORK,6,6,6)
```

```
C
```

```
CALL MMLT(WORK,KG6,R3,6,6,6)
CALL MMLT(KM6,RT3,WORK,6,6,6)
```

```
C
```

```
CALL MMLT(WORK,KG7,R4,6,6,6)
CALL MMLT(KM7,RT4,WORK,6,6,6)
```

```
C
```

```
CALL MMLT(WORK,KG8,R4,6,6,6)
CALL MMLT(KM8,RT4,WORK,6,6,6)
```

```
C
```

```
CALL MMLT(WORK,KG9,R4,6,6,6)
CALL MMLT(KM9,RT4,WORK,6,6,6)
```

```
C
```

```
CALL MMLT(WORK,KG10,R4,6,6,6)
CALL MMLT(KM10,RT4,WORK,6,6,6)
```

```
C
```

```
CALL MMLT(WORK,KG11,R4,6,6,6)
CALL MMLT(KM11,RT4,WORK,6,6,6)
```

```
C
```

```
CALL MMLT(WORK,KG12,R4,6,6,6)
CALL MMLT(KM12,RT4,WORK,6,6,6)
```

```
C
```

```
C=====
```

```
C
```

```
C
```

```
CONSTRUCT THE GLOBAL [KG]MATRIX
```

```
C
```

```

      CALL GLONON(KN, KM1, KM2, KM3, KM4, KM5, KM6, KM7, KM8,
*           KM9, KM10, KM11, KM12, KX)
C
C=====
C
C      TO CREATE THE LOAD VECTOR "Q".
C
10007      CALL MMLT(Q, MK, P, 36, 36, 1)
C
C=====
C
C      TO CREATE THE TERMS INSIDE THE SECOND BRACKET
C      ON LINE B1 P323 BW
C
      DO 890 I=1,36
890 Y(I,1)=SS0*U(I) +SS2*U1(I) +SS3*U2(I)
C
C=====
C
C      TO CREATE THE SECOND TERM ON LINE B1
C      M*(A0*UT+A2*U1T+A3*U2T)
C
      CALL MMLT(B, MK, Y, 36, 36, 1)
C
C=====
C
C      TO CREATE THE TERMS INSIDE THE THIRD BRACKET ON LINE
C
      DO 8900 I=1,36
8900 YY(I,1)=SS1*U(I)+SS4*U1(I)+SS5*U2(I)
C
      DO 8901 I=1,36
      DO 8901 J=1,36
8901 CC(I,J)=BELTA*MK(I,J)
      CALL MMLT(BB, CC, YY, 36, 36, 1)
C
C=====
C
C      TO CREATE LINE B1 P232 BW
C      QCAP ETC THE EFFECTIVE LOAD
C
      DO 894 I=1,36
894 QCAP(I)=Q(I,1)+B(I,1)+BB(I,1)
C
C=====
C
C      TO CREATE THE EFFECTIVE STIFFNESS MATRIX
C      LINE A4 P232 BW
C
      DO 888 I=1,36
      DO 888 J=1,36
888 RCAP(I,J)=G1(I,J)+SS0*MK(I,J)+KN(I,J)+SS1*CC(I,J)
C

```

```

C=====
C
C      TO SOLVE THE LINEAR EQUATIONS BY GAUSS ELIMINATION.
C
C      CALL LINEQ(OUT, QCAP, RCAP, WK, 36, 38, IERR)
C
C=====
C
C      TO CREATE LINES B3 AND LINES B4 P232 BW
C
C      DO 896 I=1,36
C      UD=U(I)
C      UV=U1(I)
C      UA=U2(I)
C      U(I)=OUT(I)
C      U2(I)=SS0*(U(I)-UD)-SS2*UV-SS3*UA
C      U1(I)=UV+SS6*UA+SS7*U2(I)
896    CONTINUE
C
C=====
C
C      TO DEFINE THE DYNAMIC DEFLECTIONS IN THE LOCAL FRAMES
C
C      DO 100 I=2,17,3
C      J=I+1
100    UL(I)=OUT(I)*C3+OUT(J)*S3
C
C      DO 200 I=3,18,3
C      J=I-1
200    UL(I)=-OUT(J)*S3+OUT(I)*C3
C
C      DO 300 I=21,33,3
C      J=I+1
300    UL(I)=OUT(I)*C4+OUT(J)*S4
C
C      DO 400 I=22,34,3
C      J=I-1
400    UL(I)=-OUT(J)*S4+OUT(I)*C4
C
C      UL(36)=OUT(17)*C4+OUT(18)*S4
C
C      RK11=(K-1)/1.0
C
C=====
C      THIS IS FOR THE PLOTTING , IT
C      GIVES THE CRANK ANGLE.
C      UL(9) IS THE DEFLECTION IN THE MIDPOINT OF COUPLER
C      UL(28) IS THE DEFLECTION IN THE MIDPOINT OF ROCKER
C=====
C      WRITE(7,153)RK11,UL(9),UL(28)
C=====
765    CONTINUE
153    FORMAT(F14.8,1X,F14.10)

```

```
CLOSE(7, STATUS='KEEP')  
STOP  
END
```

```

C*****
C
C      L          00000          L          *
C      L          0  0          L          *
C      L          0  0          L          *
C      L          0  0          L          *
C      LLLLLLL  00000          LLLLLLL  *
C
C
C      THIS SUBROUTINE IS USED TO GET LINEAR *
C      LOCAL STIFFNESS AND MASS MATRICES *
C
C*****
      SUBROUTINE LOL(E,A,EL,RI,MASS,KL,ML)
      REAL MASS,KL(6,6),ML(6,6),EL,E,RI
C=====
C      INITIALIZE THE ENTRY OF STIFFNESS MATRIX
C=====
      DO 1 I=1,6
      DO 1 J=1,6
1      KL(I,J)=0.0
C=====
C      TO DEFINE THE LOCAL STIFFNESS MATRIX
C=====
      KL(1,1)=E*A/EL
      KL(2,2)=12.*E*RI/EL**3.
      KL(3,3)=4.*E*RI/EL
      KL(4,4)=KL(1,1)
      KL(5,5)=KL(2,2)
      KL(6,6)=KL(3,3)
      KL(1,4)=-KL(1,1)
      KL(2,3)=6.*E*RI/EL**2
      KL(2,5)=-KL(2,2)
      KL(2,6)=KL(2,3)
      KL(3,5)=-KL(2,3)
      KL(3,6)=2.*E*RI/EL
      KL(5,6)=-KL(2,3)
C
      DO 2 I=2,6
      I1=I-1
      DO 2 J=1,I1,1
2      KL(I,J)=KL(J,I)
C
C=====
C      INITIALIZE THE ENTRY OF MASS MATRIX
C=====
      DO 100 I=1,6
      DO 100 J=1,6
100     ML(I,J)=0.0
C=====
C      TO CREATE THE LOCAL MASS MATRIX.
C=====
      ML(1,1)=140.

```

```
ML(2,2)=156.  
ML(3,3)=4.*EL**2  
ML(4,4)=ML(1,1)  
ML(5,5)=ML(2,2)  
ML(6,6)=ML(3,3)  
ML(1,4)=70.  
ML(2,3)=22.*EL  
ML(2,5)=54.  
ML(2,6)=-13.*EL  
ML(3,5)=-ML(2,6)  
ML(3,6)=-3.*EL**2  
ML(5,6)=-ML(2,3)  
C  
DO 103 I=2,6  
  I1=I-1  
DO 103 J=1, I1  
103 ML(I,J)=ML(J,I)  
C  
DO 104 I=1,6  
DO 104 J=1,6  
104 ML(I,J)=ML(I,J)*(MASS*EL)/420.  
RETURN  
END
```

```

C*****
C
c      GGGGG L      00000 L      III N N      *
C      G      L      0 0 L      I  NN N      *
C      G GG L      0 0 L      I  N NN      *
C      G  G L      0 0 L      I  N NN      *
C      GGGGG LLLLL 00000 LLLLL III N N      *
C
C      THIS SUBROUTINE IS DESIGNED TO CONSTRUCTED
C      THE GLOBAL STIFFNESS AND MASS MATRICES
C
C*****
C
      SUBROUTINE GLOLIN(X,XJ,X1,X2,X3,X4,XG,XM)
      REAL X(6,6),X1(6,6),X2(6,6),X3(6,6),X4(6,6),XJ(6,6)
      REAL XG(40,40),XM(36,36)

C
C=====
C      INITIALIZE EVERY ENTRY OF THE MATRIX
C=====
      DO 111 I=1,40
      DO 111 J=1,40
111  XG(I,J)=0.0
C=====
C      CONSTRUCTED THE 40 BY 40 MATRIX WITHOUT B. C.
C=====
      DO 10 I=1,3
      DO 10 J=1,6
10  XG(I,J)=X1(I,J)
C
      DO 20 I=4,6
      DO 20 J=4,6
      K=I-3
      M=J-3
20  XG(I,J)=X1(I,J)+X(K,M)
C
      DO 30 I=4,6
      DO 30 J=7,9
      K=I-3
      M=J-3
30  XG(I,J)=X(K,M)
C
      XG(7,7)=X(4,4)+X(1,1)
      XG(7,8)=X(4,5)+X(1,2)
      XG(7,9)=X(4,6)+X(1,3)
C
      XG(8,7)=X(5,4)+X(2,1)
      XG(8,8)=X(5,5)+X(2,2)
      XG(8,9)=X(5,6)+X(2,3)
C
      XG(9,7)=X(6,4)+X(3,1)
      XG(9,8)=X(6,5)+X(3,2)
      XG(9,9)=X(6,6)+X(3,3)

```



```

C
DO 40 I=7,9
DO 40 J=10,12
K=I-6
M=J-6
40 XG(I,J)=X(K,M)
C
DO 60 I=10,12
DO 60 J=10,12
K=I-3
M=J-3
60 XG(I,J)=XG(K,M)
C
DO 70 I=10,12
DO 70 J=13,15
K=I-9
M=J-9
70 XG(I,J)=X(K,M)
C
DO 80 I=13,15
DO 80 J=13,15
K=I-3
M=J-3
80 XG(I,J)=XG(K,M)
C
DO 90 I=13,15
DO 90 J=16,18
K=I-12
M=J-12
90 XG(I,J)=X(K,M)
C
XG(16,16)=X(4,4)+X2(1,1)
XG(16,17)=X(4,5)+X2(1,2)
XG(16,18)=X(4,6)+X2(1,3)
C
XG(17,16)=X(5,4)+X2(2,1)
XG(17,17)=X(5,5)+X2(2,2)
XG(17,18)=X(5,6)+X2(2,3)
C
XG(18,16)=X(6,4)+X2(3,1)
XG(18,17)=X(6,5)+X2(3,2)
XG(18,18)=X(6,6)+X2(3,3)
C
DO 100 I=16,18
DO 100 J=19,21
K=I-15
M=J-15
100 XG(I,J)=X2(K,M)
C
XG(19,19)=X2(4,4)+X3(4,4)
XG(19,20)=X2(4,5)+X3(4,5)
XG(19,21)=X2(4,6)
C

```

```

XG(20,19)=X2(5,4)+X3(5,4)
XG(20,20)=X2(5,5)+X3(5,5)
XG(20,21)=X2(5,6)
C
XG(21,19)=X2(6,4)
XG(21,20)=X2(6,5)
XG(21,21)=X2(6,6)
C
XG(19,37)=X3(4,1)
XG(19,38)=X3(4,2)
XG(19,39)=X3(4,3)
XG(19,40)=X3(4,6)
C
XG(20,37)=X3(5,1)
XG(20,38)=X3(5,2)
XG(20,39)=X3(5,3)
XG(20,40)=X3(5,6)
C
DO 110 I=22,24
DO 110 J=22,24
K=I-21
M=J-21
110 XG(I,J)=X4(K,M)
C
DO 1101 I=22,24
DO 1101 J=25,27
K=I-21
M=J-21
1101 XG(I,J)=X4(K,M)
C
XG(25,25)=X4(4,4)+XJ(1,1)
XG(25,26)=X4(4,5)+XJ(1,2)
XG(25,27)=X4(4,6)+XJ(1,3)
C
XG(26,25)=X4(5,4)+XJ(2,1)
XG(26,26)=X4(5,5)+XJ(2,2)
XG(26,27)=X4(5,6)+XJ(2,3)
C
XG(27,25)=X4(6,4)+XJ(3,1)
XG(27,26)=X4(6,5)+XJ(3,2)
XG(27,27)=X4(6,6)+XJ(3,3)
C
DO 120 I=25,27
DO 120 J=28,30
K=I-24
M=J-24
120 XG(I,J)=XJ(K,M)
C
XG(28,28)=XJ(1,1)+XJ(4,4)
XG(28,29)=XJ(1,2)+XJ(4,5)
XG(28,30)=XJ(1,3)+XJ(4,6)
C
XG(29,28)=XJ(2,1)+XJ(5,4)

```

```

XG(29,29)=XJ(2,2)+XJ(5,5)
XG(29,30)=XJ(2,3)+XJ(5,6)
C
XG(30,28)=XJ(3,1)+XJ(6,4)
XG(30,29)=XJ(3,2)+XJ(6,5)
XG(30,30)=XJ(3,3)+XJ(6,6)
C
DO 130 I=28,30
DO 130 J=31,33
K=I-27
M=J-27
130 XG(I,J)=XJ(K,M)
C
DO 140 I=31,33
DO 140 J= 31,33
K=I-3
M=J-3
140 XG(I,J)=XG(K,M)
C
DO 150 I=31,33
DO 150 J=34,36
K=I-30
M=J-30
150 XG(I,J)=XJ(K,M)
C
DO 160 I=34,36
DO 160 J=34,36
K=I-3
M=J-3
160 XG(I,J)=XG(K,M)
C
DO 170 I=34,36
DO 170 J=37,39
K=I-33
M=J-33
170 XG(I,J)=XJ(K,M)
C
XG(37,37)=XJ(4,4)+X3(1,1)
XG(37,38)=XJ(4,5)+X3(1,2)
XG(37,39)=XJ(4,6)+X3(1,3)
XG(37,40)=X3(1,6)
C
XG(38,37)=XJ(5,4)+X3(2,1)
XG(38,38)=XJ(5,5)+X3(2,2)
XG(38,39)=XJ(5,6)+X3(2,3)
XG(38,40)=X3(2,6)
C
XG(39,37)=XJ(6,4)+X3(3,1)
XG(39,38)=XJ(6,5)+X3(3,2)
XG(39,39)=XJ(6,6)+X3(3,3)
XG(39,40)=X3(3,6)
C
XG(40,40)=X3(6,6)

```

```
C
      DO 180 I=1,40
      DO 180 J=1,40
180   XG(J,I)=XG(I,J)
C=====
C      PUT B.C. IN THE MATRIX REDUCED TO 36 BY 36 MATRIX
C=====
      DO 181 I=1,36
      DO 181 J=1,36
181   XM(I,J)=0.
C
      DO 190 I=1,19
      DO 190 J=1,19
      K=I+2
      M=J+2
190   XM(I,J)=XG(K,M)
C
      DO 200 I=20,36
      DO 200 J=20,36
      K=I+4
      M=J+4
200   XM(I,J)=XG(K,M)
C
      RETURN
      END
```

```

C*****
C
c      L      000000  NN  N  000000  NN  N      *
C      L      0   0   NN  N  0   0   NN  N      *
C      L      0   0   N  NN  0   0   N  NN      *
C      L      0   0   N  NN  0   0   N  NN      *
C      LLLLLL 000000  N   N  000000  N   N      *
C
C      THIS SUBROUTINE IS TO GENERATE NONLINEAR
C      LOCAL STIFFNESS MATRIX
C
C*****
C
C      KG(1-12)----NONLINEAR LOCAL STIFFNESS MATRIX
C
C      SUBROUTINE LONON(E, A, UR, EL, UL, KG)
C      REAL UR(6),KG(6,6),E
C=====
C      INITIALIZE EVERY ENTRY OF THE MATRIX
C=====
      DO 830 I=1,6
      DO 830 J=1,6
830    KG(I,J)=0.0
C
      KG(2,2)=6.0/5.0
      KG(3,3)=2.0*EL**2/15.0
      KG(5,5)=KG(2,2)
      KG(6,6)=KG(3,3)
      KG(2,3)=EL/10.0
      KG(2,5)=-KG(2,2)
      KG(2,6)=KG(2,3)
      KG(3,2)=KG(2,3)
      KG(3,5)=-KG(2,3)
      KG(3,6)=-EL**2/30.0
      KG(5,2)=-KG(2,2)
      KG(5,3)=-KG(2,3)
      KG(5,6)=-KG(2,3)
      KG(6,2)=KG(2,3)
      KG(6,3)=KG(3,6)
      KG(6,5)=-KG(2,3)
C
      RETURN
      END

```

```

C*****
C
C      GGGGGG   L       000000   NN   N   000000   NN   N
C      G       L       0   0   N N N   0   0   N N N
C      G GGG   L       0   0   N N N   0   0   N N N
C      G   G   L       0   0   N   NN   0   0   N   NN
C      GGGGGG   LLLLLL  000000   N     N   000000   N     N
C
C      BUILD UP GLOBAL MATRICES (NONLINEAR PART OF THE PROGRAM)
C
C      KM---GLOBAL MATRICES FOR EVERY ELEMENT
C
C      KX---GLOBAL MATRICES FOR THE MECHANISM WITHOOUT B.C.
C
C      KN---GLOBAL MATRICES FOR THE MECHANISM WITH B. C.
C*****
C
C      SUBROUTINE GLONON(KN,KM1,KM2,KM3,KM4,KM5,KM6,
*      KM7,KM8,KM9,KM10,KM11,KM12,KX)
C      REAL KN(36,36),KX(40,40)
C      REAL KM1(6,6),KM2(6,6),KM3(6,6),KM4(6,6),KM5(6,6),KM6(6,6)
C      REAL KM7(6,6),KM8(6,6),KM9(6,6),KM10(6,6),KM11(6,6),KM12(6,6)
C
C      DO 111 I=1,40
C      DO 111 J=1,40
111  KX(I,J)=0.
C
C      DO 10 I=1,3
C      DO 10 J=1,6
10   KX(I,J)=KM1(I,J)
C
C      DO 20 I=4,6
C      DO 20 J=4,6
C      K=I-3
C      M=J-3
20   KX(I,J)=KM1(I,J)+KM2(K,M)
C
C      DO 30 I=4,6
C      DO 30 J=7,9
C      K=I-3
C      M=J-3
30   KX(I,J)=KM2(K,M)
C
C      DO 201 I=7,9
C      DO 201 J=7,9
C      K=I-3
C      M=J-3
C      KK=I-6
C      MM=J-6
201  KX(I,J)=KM2(K,M)+KM3(KK,MM)
C
C

```

```

DO 40 I=7,9
DO 40 J=10,12
K=I-6
M=J-6
40  KX(I,J)=KM3(K,M)
C

DO 60 I=10,12
DO 60 J=10,12
K=I-6
M=J-6
KK=I-9
MM=J-9
60  KX(I,J)=KM3(K,M)+KM4(KK,MM)
C
C

DO 70 I=10,12
DO 70 J=13,15
K=I-9
M=J-9
70  KX(I,J)=KM4(K,M)
C

DO 80 I=13,15
DO 80 J=13,15
K=I-9
M=J-9
KK=I-12
MM=J-12
80  KX(I,J)=KM4(K,M)+KM5(KK,MM)
C

DO 90 I=13,15
DO 90 J=16,18
K=I-12
M=J-12
90  KX(I,J)=KM5(K,M)
C

DO 901 I=16,18
DO 901 J=16,18
K=I-12
M=J-12
KK=I-15
MM=J-15
901 KX(I,J)=KM5(K,M)+KM6(KK,MM)
C

DO 100 I=16,18
DO 100 J=19,21
K=I-15
M=J-15
100 KX(I,J)=KM6(K,M)
C

KX(19,19)=KM6(4,4)+KM12(4,4)
KX(19,20)=KM6(4,5)+KM12(4,5)
KX(19,21)=KM6(4,6)
C

```

```

KX(20,19)=KM6(5,4)+KM12(5,4)
KX(20,20)=KM6(5,5)+KM12(5,5)
KX(20,21)=KM6(5,6)
C
KX(21,19)=KM6(6,4)
KX(21,20)=KM6(6,5)
KX(21,21)=KM6(6,6)
C
KX(19,37)=KM12(4,1)
KX(19,38)=KM12(4,2)
KX(19,39)=KM12(4,3)
KX(19,40)=KM12(4,6)
C
KX(20,37)=KM12(5,1)
KX(20,38)=KM12(5,2)
KX(20,39)=KM12(5,3)
KX(20,40)=KM12(5,6)
C
DO 110 I=22,24
DO 110 J=22,27
K=I-21
M=J-21
110 KX(I,J)=KM7(K,M)
C
DO 1101 I=25,27
DO 1101 J=25,27
K=I-21
M=J-21
KK=I-24
MM=J-24
1101 KX(I,J)=KM7(K,M)+KM8(KK,MM)
C
DO 120 I=25,27
DO 120 J=28,30
K=I-24
M=J-24
120 KX(I,J)=KM8(K,M)
C
DO 1201 I=28,30
DO 1201 J=28,30
K=I-24
M=J-24
KK=I-27
MM=J-27
1201 KX(I,J)=KM8(K,M)+KM9(KK,MM)
C
DO 130 I=28,30
DO 130 J=31,33
K=I-27
M=J-27
130 KX(I,J)=KM9(K,M)
C
DO 140 I=31,33

```



```

DO 140 J=31,33
K=I-27
M=J-27
KK=I-30
MM=J-30
140 KX(I,J)=KM9(K,M)+KM10(KK,MM)
C
DO 150 I=31,33
DO 150 J=34,36
K=I-30
M=J-30
150 KX(I,J)=KM10(K,M)
C
DO 160 I=34,36
DO 160 J=34,36
K=I-30
M=J-30
KK=I-33
MM=J-33
160 KX(I,J)=KM10(K,M)+KM11(KK,MM)
C
DO 170 I=34,36
DO 170 J=37,39
K=I-33
M=J-33
170 KX(I,J)=KM11(K,M)
C
KX(37,37)=KM11(4,4)+KM12(1,1)
KX(37,38)=KM11(4,5)+KM12(1,2)
KX(37,39)=KM11(4,6)+KM12(1,3)
KX(37,40)=KM12(1,6)
C
KX(38,37)=KM11(5,4)+KM12(2,1)
KX(38,38)=KM11(5,5)+KM12(2,2)
KX(38,39)=KM11(5,6)+KM12(2,3)
KX(38,40)=KM12(2,6)
C
KX(39,37)=KM11(6,4)+KM12(3,1)
KX(39,38)=KM11(6,5)+KM12(3,2)
KX(39,39)=KM11(6,6)+KM12(3,3)
KX(39,40)=KM12(3,6)
C
KX(40,40)=KM12(6,6)
C
DO 180 I=1,40
DO 180 J=1,40
180 KX(J,I)=KX(I,J)
C
DO 191 I=1,36
DO 191 J=1,36
191 KN(I,J)=0.
C
C*****

```

```
C
C   PUT BOUNDARY CONDITIONS IN
C
C*****
C
      DO 56 I=1,36
      DO 56 J=1,36
      IIM=I+2
      JIM=J+2
      IF(I.GE.20)IIM=I+4
      IF (J.GE.20)JIM=J+4
      KN(I,J)=KX(IIM, JIM)
56  CONTINUE
C
      RETURN
      END
```

```

C*****
C
C      K  K          III      N   N
C      K  K          I       NN  N
C      K  KK         I       N  N  N
C      KK  K         I       N   N  N
C      K   K         III      N   NN
C
C      THIS SUBROUTINE IS DESIGNED TO CALCULATE
C      THE ACCLERATION AND ANGULAR DISPLACEMENT
C
C      PROGRAM IS BASED ON THE PAPER BY SMITH AND MAUNDER(1967)
C*****
C
C      L1 ,L2 ,L3 ,L4  GROUND, CRANK, COUPLER
C                      AND ROCKER LENGTHES.
C      XLEN1 ,2 ,3 ,4  ARE THE LENGTHES OF JOINTS
C      TH2              CRANK ANGLE IN RADS. WHILE
C      TH21             CRANK ANG. VELOCITY IN RAD/S.
C*****
C
C      SUBROUTINE KIN(RA, TH2 ,TH3 ,TH4 ,TH21 ,STEP,
*                   XLEN1 ,XLEN2 ,AC, XLEN3 ,XLEN4 ,L1 ,L2 ,L3 ,L4 )
REAL L1 ,L2 ,L3 ,L4 ,AC(40) ,RA(36 ,1)
  TH211=0.0
1  A=2.*L3*(L2*COS(TH2)-L1)
  PI=3.1415927
  B=L4**2-L1**2-L2**2-L3**2+2*L1*L2*COS(TH2)
  C=2*L2*L3*SIN(TH2)
  AZ=ABS(A**2+C**2)
  D=SQRT(AZ)
  ABC=ABS((A*B/D**2)**2-(B**2-C**2)/D**2)
  DD=SQRT(ABC)
  DA=SIN(TH2)
  IF(DA.GT.0.)THEN
    TH3=ACOS(A*B/D**2+DD)
  ELSE
    TH3=ACOS(A*B/D**2-DD)
  ENDIF
  TH4=ACOS((L2*COS(TH2)+L3*COS(TH3)-L1)/L4)
  TH31=-TH21*(L2*SIN(TH2-TH4))/(L3*SIN(TH3-TH4))
  THETA2=TH2*180./PI
  THETA3=TH3*180./PI
  THETA4=TH4*180./PI
  TH41=-TH21*(L2*SIN(TH2-TH3))/(L4*SIN(TH3-TH4))
  AA=TH21**2*L2*COS(TH2-TH4)
  BB=TH31**2*L3*COS(TH3-TH4)
  CC=L3*SIN(TH3-TH4)
  TH311=(TH31/TH21)*TH211-(AA+BB-TH41**2*L4)/CC
  EE=TH21**2*L2*COS(TH2-TH3)
  FF=TH41**2*L4*COS(TH3-TH4)

```

```

GG=L4*SIN(TH3-TH4)
TH411=(TH41/TH21)*TH211-(EE-FF+TH31**2*L3)/GC
C=====
C      AC CONTAINS NODAL ACCELERATIONS IN THE
C      GLOBAL FRAME.
C=====
      AC(1)=-L2*(TH21**2*COS(TH2) + TH211*SIN(TH2))
      AC(2)=-L2*(TH21**2*SIN(TH2)-TH211*COS(TH2))
C
      DO 1011 I=3,21,3
      AC(I)=TH311
1011 CONTINUE
C
      DO 1012 I=24,39,3
      AC(I)=TH411
1012 CONTINUE
C
      EL1=(L3-XLEN2-XLEN1)/4.
      DO 1013 I=7,16,3
      II=(I-4)/3
      J=I+1
      AC(I)=AC(1)-(II*EL1+XLEN1)*(TH31**2*COS(TH3)+TH311*SIN(TH3))
      AC(J)=AC(2)-(II*EL1+XLEN1)*(TH31**2*SIN(TH3)-TH311*COS(TH3))
1013 CONTINUE
C
C
      EL2=(L4-XLEN3-XLEN4)/4.
      DO 1014 I=28,37,3
      II=(I-25)/3
      J=I+1
      AC(I)=- (XLEN4+II*EL2)*(TH41**2*COS(TH4)+TH411*SIN(TH4))
      AC(J)=- (XLEN4+II*EL2)*(TH41**2*SIN(TH4)-TH411*COS(TH4))
1014 CONTINUE
C
      AC(4)=AC(1)-XLEN1*(TH31**2*COS(TH3)+TH311*SIN(TH3))
      AC(5)=AC(2)-XLEN1*(TH31**2*SIN(TH3)-TH311*COS(TH3))
C
      AC(19)=-L4*(TH41**2*COS(TH4)+TH411*SIN(TH4))
      AC(20)=-L4*(TH41**2*SIN(TH4)-TH411*COS(TH4))
C
      AC(22)=0.
      AC(23)=0.
C
C
      AC(25)=- (XLEN4)*(TH41**2*COS(TH4)+TH411*SIN(TH4))
      AC(26)=- (XLEN4)*(TH41**2*SIN(TH4)-TH411*COS(TH4))
C
      AC(40)=TH411
C=====
C      TO INCREMENT THE CRANK ANGLE AND HENCE THE MECHANISM
C=====
      11      TH2=TH2+PI/(180.*STEP)
C=====

```

C RA IS DEFINED RELATIVE TO THE FINITE ELEMENT
C PROGRAM WHILE AC IS DEFINED RELATIVE TO THE
C MECHANISM KINEMATICS PROGRAM. WE NOW HAVE THE
C INTERFACE.

C-----

C
DO 1015 I=1,19
J=I+2
RA(I,1)=AC(J)
1015 CONTINUE

C
DO 1016 I=20,36
J=I+4
RA(I,1)=AC(J)
1016 CONTINUE

C
RETURN
END

```
C*****  
C  
C          S T R A I N          *  
C          *                    *  
C      This subroutin is designed to calculate *  
C      the strain of each element          *  
C          *                    *  
C*****  
C  
      SUBROUTINE STRAIN(EBS, BB, UL, EBSE)  
      REAL EBS(1,1), BB(1,6), UL(6,1), EBSE(1,1)  
      CALL MMLT(EBS, BB, UL, 1, 6, 1)  
      RETURN  
      END
```

